Penetration Mechanics: Analytical Modeling

Charles E. Anderson, Jr.
CEA Consulting
San Antonio, TX

CEA
Consulting

Acknowledgements

- *Virtually everything I have learned about penetration and armor mechanics occurred during my 34½ years at Southwest Research Institute*

- *Much of the work was funded by DARPA and/or the Army (TARDEC), although there has been funding by the Navy, Air Force, and Ballistic Missile Defense*

- *There also has been internal funding by SwRI*

The Charge

- *Email from Clive Woodley & Ian Cullis*
  - *Lecture on Terminal Ballistics*
    - *Cover the history*
    - *Key developments*
    - *Main challenges remaining*
- *Decided to narrow the scope and focus on analytical modeling*
  - *Subject to the constraint: the model had to provide considerable insight into the mechanics of penetration*
  - *Major advance and not a modification of an existing model*
    - *Any errors of omission are solely mine (either did not think that it met the selection criteria, or ignorance on my part)*
    - *Any misrepresentation my responsibility*

Outline – 1

- Rigid-body penetration – Poncelet Equation
- Hydrodynamic theory
  - Assumptions
  - Results
- Modifications to hydro theory
  - Shaped-charge jets
  - Allen & Rogers
  - Chistman and Gehring

Outline – 2

- Recht-Ipson
- Projectile deceleration – Tate-Alekseevski theories
  - Target resistance
  - Cavity expansion
- Rigid-body penetration revisted
  - Tate theory
  - Forrestal, et al.'s contribution
    - Dynamic cavity expansion
    - The role of friction & temperature effects
- Transition from rigid-body to eroding penetration

Outline – 3

- Ravid-Bodner
  - Flow fields
  - Failure mechanisms
- Walker-Anderson
  - Flow field
    - Cavity expansion
    - Extent of flow field
  - Effective flow stress
    - Similitude analysis

Outline – 4

- Yarn Impact
- Fabric Modeling and Resin-Impregnated Fabrics
- Ceramics/Glasses
  - Penetration
  - Dwell
  - Dwell-penetration transition
- Summary

Poncelet Equation

- *Jean-Victor Poncelet (1788 – 1867)*
  - *French engineer and mathematician*
  - *Most notable work was in projective geometry*
  - *Commanding General of the École Polytechnique*
- *Poncelet equation describes rigid-body penetration*

$$M\frac{d\mathrm{v}}{dt} = -F = -\left(A + B\mathrm{v}^2\right)$$

Since rigid body, non-deforming: cross-sectional area is a constant

$$\rho_p L\frac{d\mathrm{v}}{dt} = -\left(R_t + b\mathrm{v}^2\right)$$

R_t = static target resistance term

Poncelet Equation

$$\frac{dv}{dt} = -\frac{1}{\rho_p L}\left(R_t + b\,v^2\right)$$

$$\frac{dv}{dt} = \frac{dv}{dx}\frac{dx}{dt} = v\frac{dv}{dx}$$

$$\frac{1}{\rho_p L}\int_0^P dx = -\int_V^0 \frac{v dv}{R_t + b v^2}$$

$$\frac{P}{L} = \frac{\rho_p}{2b}\ln\left(1 + \frac{bV^2}{R_t}\right) \xrightarrow{small\,"x"} \frac{P}{L} = \frac{\rho_p V^2}{2R_t}$$

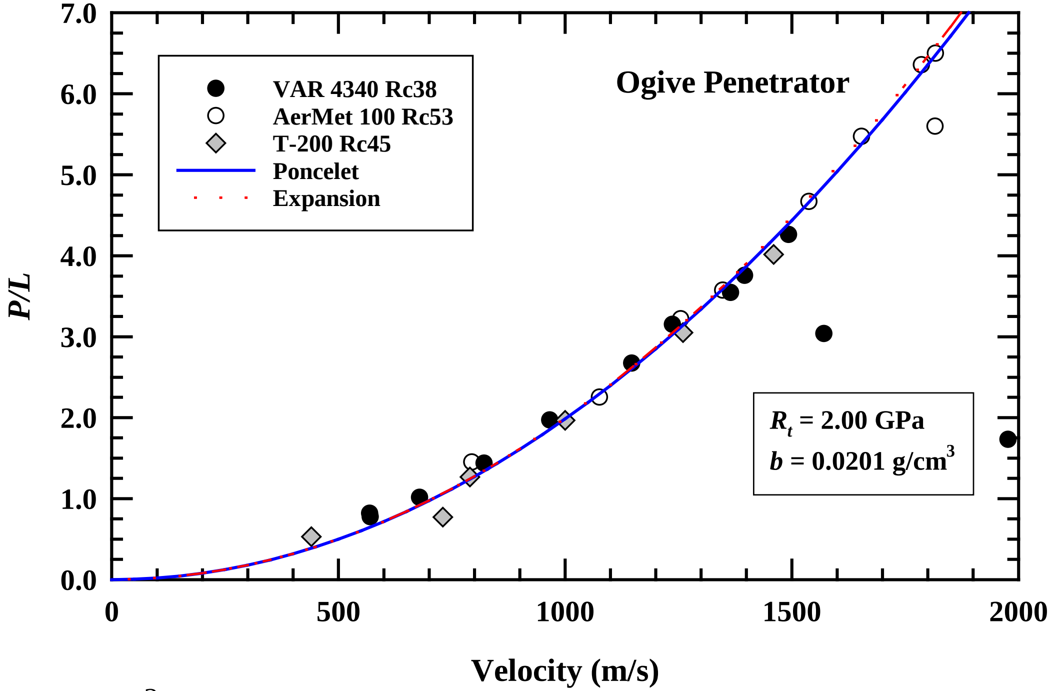

Steel into 6061 aluminum

M. J. Forrestal and A. J. Piekutowski, "Penetration experiments with 6061-T6511 aluminum targets and spherical-nose steel projectiles at striking velocities between 0.5 and 3 km/s," *Int. J. Impact Engng*, **24**: 57-67, 2000.

Tungsten Alloy into Aluminum

- ***Flat-nosed projectiles***

HS: $\rho = 17.0$ g/cm^3
$\sigma_p = 0.985$ GPa

MW: $\rho = 17.6$ g/cm^3
$\sigma_p = 1.37$ GPa

$$\left(\frac{P}{L}\right)_{hydro} = \left(\frac{17.3}{2.8}\right)^{1/2} = 2.48$$

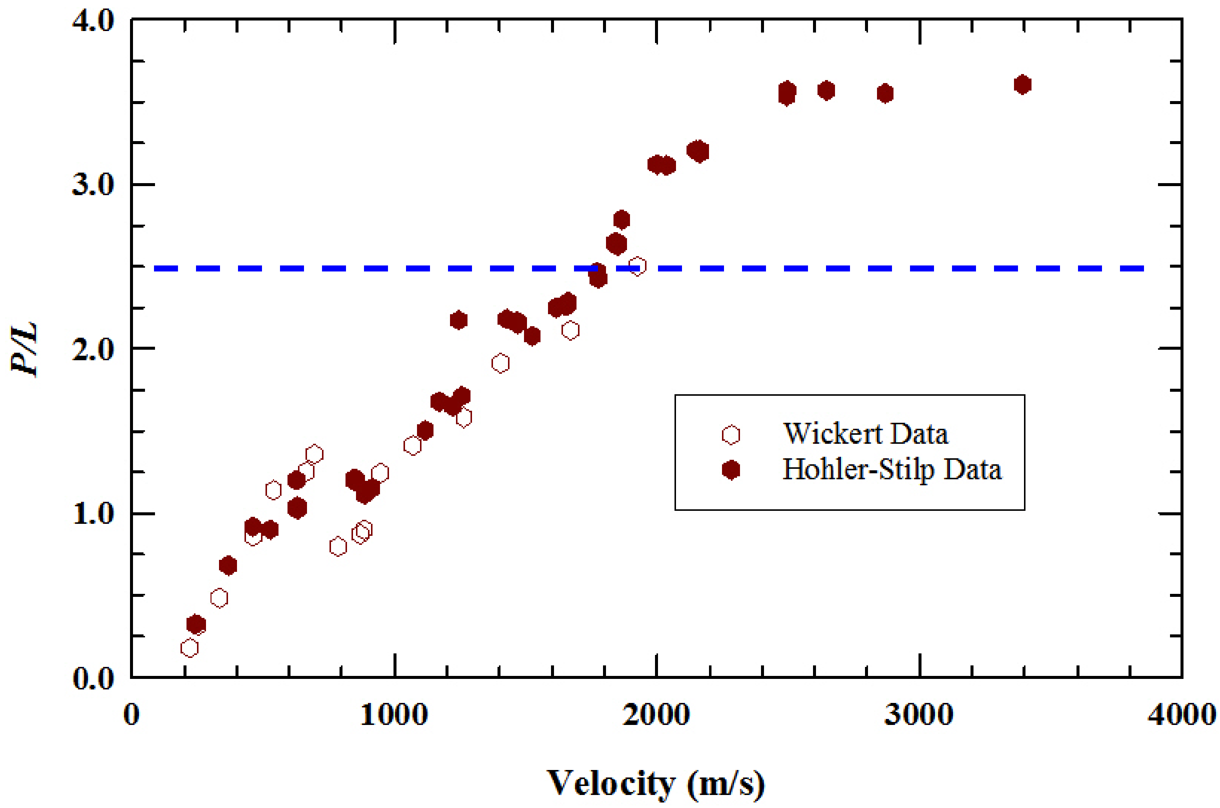

A. J. Stilp and V. Hohler, “Long rod penetration mechanics,” Chapter 5 in ***High Velocity Impact Dynamics*** (J. A. Zukas, ed.), John Wiley & Sons, NY, NY, 1990.

M. Wickert, “Penetration data for a medium caliber tungsten sinter alloy penetrator into aluminum alloy 7020 in the velocity regime from 250 m/s to 1900 m/s,” *Proc. 23rd Int. Symp. Ballistics*, **2**: 1437-1452, (F. Gálvez and V. Sánchez-Gálvez, Eds.), Gráficas Couche, S.L., Madrid, Spain, 2007.

CEA Consulting

Poncelet Equation

$$\frac{d\mathrm{v}}{dt} = -\frac{1}{\rho_p L}\left(R_t + b\,\mathrm{v}^2\right)$$

$$\frac{P}{L} = \frac{\rho_p}{2b}\ln\left(1 + \frac{bV^2}{R_t}\right) \xrightarrow{\text{small "x"}} \frac{P}{L} = \frac{\rho_p V^2}{2R_t}$$

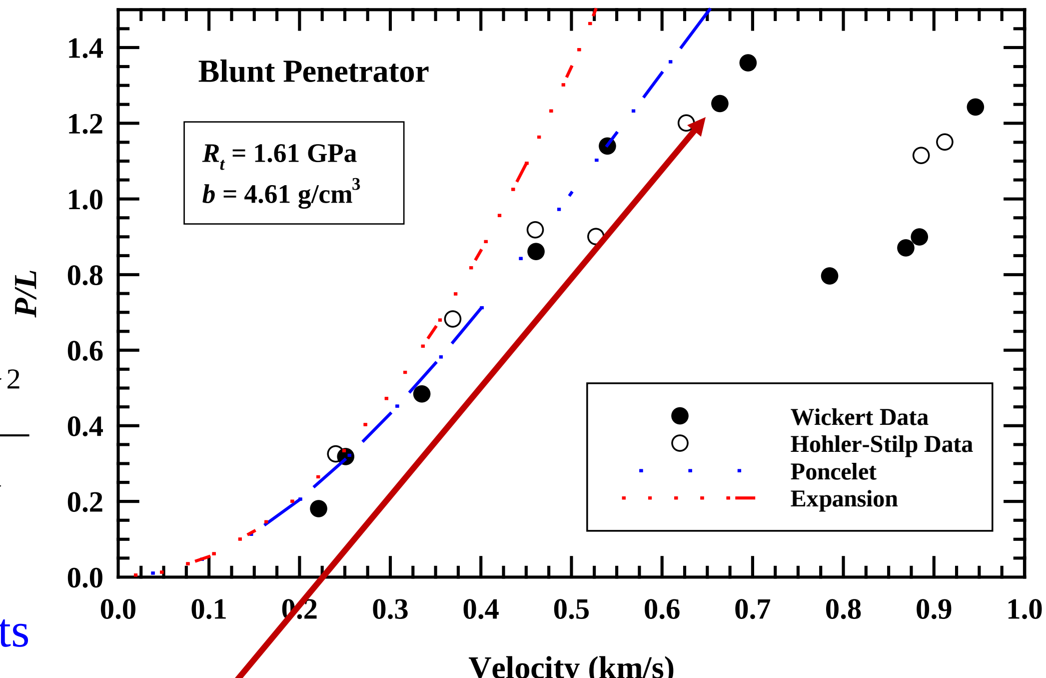

Tungsten alloy into 6061 aluminum

Application of Poncelet solution suggests maybe not rigid-body penetration, i.e., suggestive that projectile is deforming

45% decrease in the fitted standard error by dropping these 3 data points

Hydro Theory

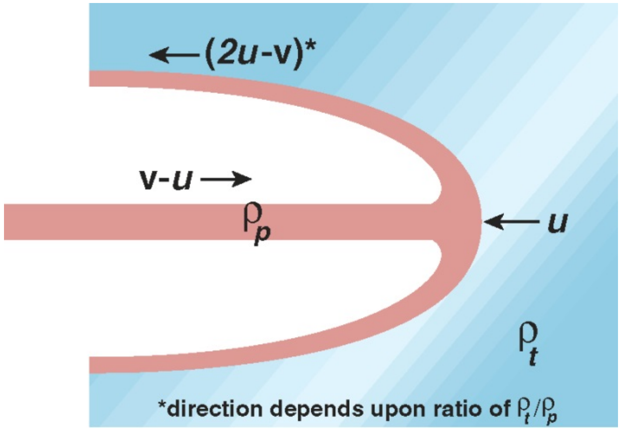

CEA Consulting

Hydrodynamic Theory of Penetration

- *First applied to shaped-charge jet penetration:*
  - *Developed during WWII*
  - *Considered a jet with constant velocity, length, and density*
- *Classic paper by Birkhoff, MacDougall, Pugh, and Taylor: "Explosives with lined cavities," J. Appl. Phys.,* ***19**: 563-582, 1948.*
- *Authors acknowledge the independent work of Hill, Mott and Pack in England that led to the same results*

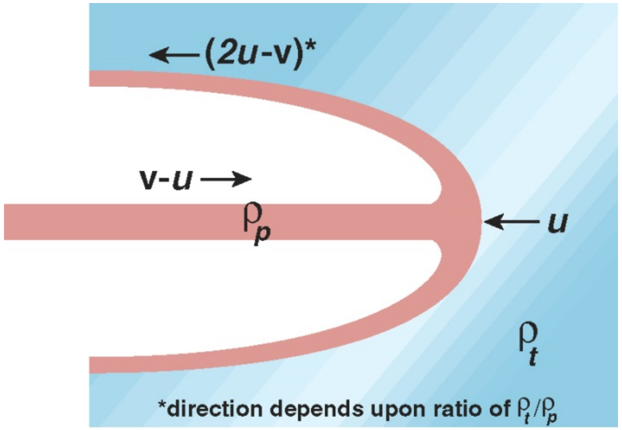

CEA Consulting

Hydrodynamic Theory of Penetration

- *Hydrodynamic: "To a first approximation the strengths and viscosity of target materials can be neglected and the problem can be treated by hydrodynamics."*
- *Incompressible jet material: "…jet with constant length L_o, velocity V, and density ρ_p"*
- *Incompressible target material: "penetrating a semi-infinite target of density ρ_t with a velocity u"*
- *Steady state: "…u has reached a constant value."*

Inviscid Momentum Equation

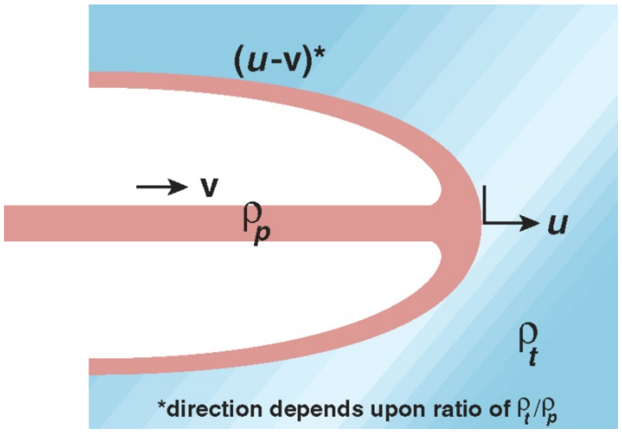

Hydrodynamic

$$\frac{\partial \mathbf{v}}{\partial t} + \frac{1}{2}\nabla\left(\mathbf{v}^2\right) - \mathbf{v}\times\left(\nabla\times\mathbf{v}\right) = -\frac{1}{\rho}\nabla P$$

$$\frac{1}{\rho}\nabla P = \nabla\left(\frac{P}{\rho}\right)$$

Incompressible

Change Coordination System

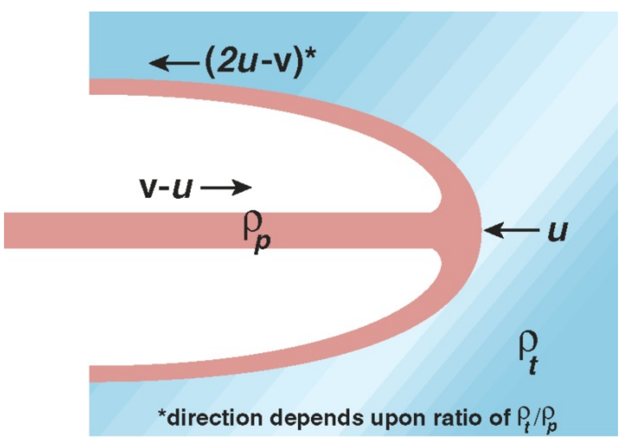

$$\cancelto{0}{\frac{\partial \mathbf{v}}{\partial t}} + \mathbf{v}\times\left(\nabla\times\mathbf{v}\right) = \nabla\left(\frac{1}{2}\mathrm{v}^2 + \frac{P}{\rho}\right)$$

Steady state

Momentum Equation

Take dot product of both sides with **v**

$$\cancel{\mathbf{v}\bullet\left[\mathbf{v}\times\left(\nabla\times\mathbf{v}\right)\right]}^{\,0}=\mathbf{v}\bullet\nabla\left(\frac{1}{2}\mathrm{v}^2+\frac{P}{\rho}\right)$$

$\mathbf{v}\ \mathrm{x}\left(\nabla\ \mathrm{x}\ \mathbf{v}\right)$ is perpendicular to **v**

$\mathbf{v}\bullet\nabla\left(\frac{1}{2}\mathbf{v}^2+\frac{P}{\rho}\right)=0\Rightarrow$ gradient of $\left(\frac{1}{2}\mathbf{v}^2+\frac{P}{\rho}\right)$ is perpendicular to **v**

$$\frac{1}{2}\mathbf{v}^2+\frac{P}{\rho}=\text{constant}$$

hydrodynamic
incompressible
steady state

Very important: although has units of specific energy, this was derived from the momentum equation.

Bernoulli Equation

$$\frac{\partial}{\partial x}\left(\frac{1}{2}\rho \mathrm{v}^{2} + P\right) = 0$$

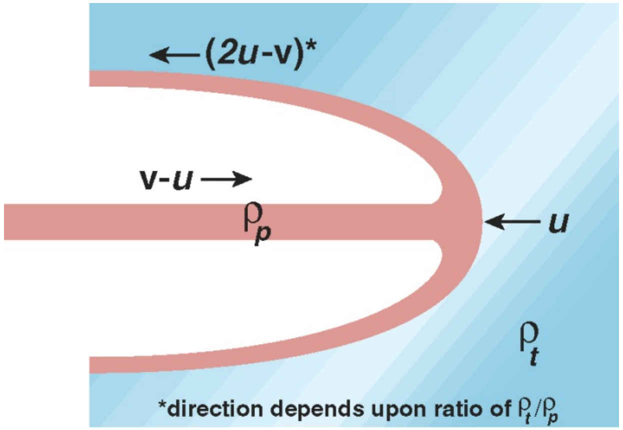

Integrate along the centerline

$$\boxed{\frac{1}{2}\rho_{p}(\mathrm{v}-u)^{2} = \frac{1}{2}\rho_{t} u^{2}}$$

$$\boxed{u = \frac{\mathrm{v}}{1+\sqrt{\rho_{t}/\rho_{p}}}}$$

Predictions of Theory

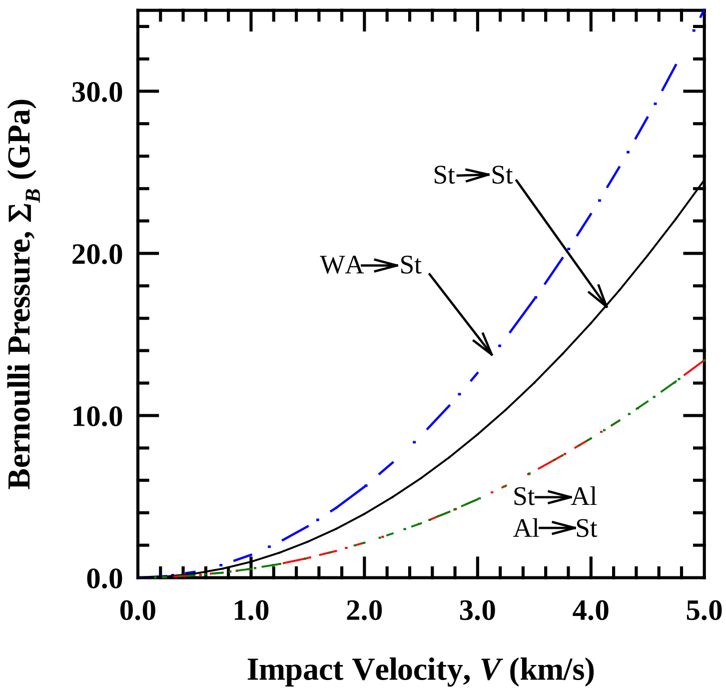

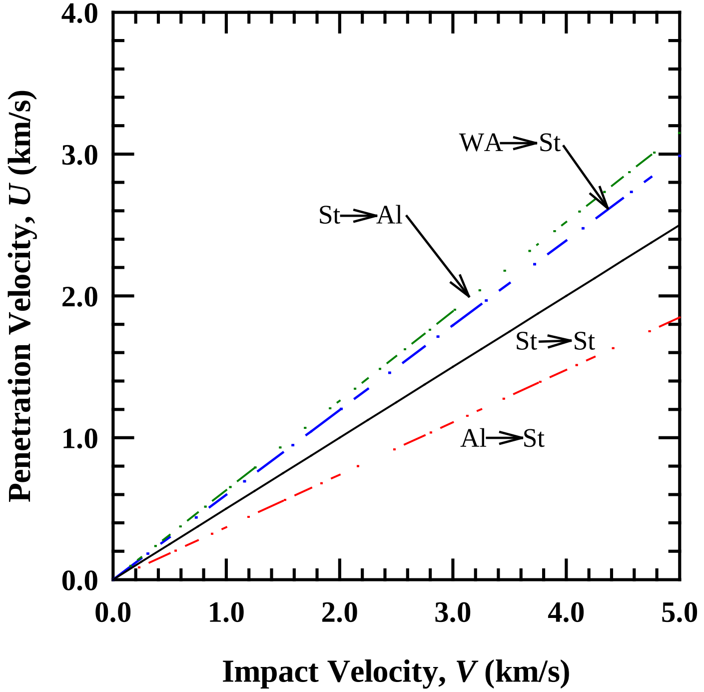

C. E. Anderson, Jr. and D. L. Orphal, "Re-examination of the hydrodynamic theory of penetration," *Int. J. Impact Engng.*, **35**(12): 1386-1392, 2008.

Hydrodynamic Theory of Penetration

- *Additional assumptions required to derive the equation for the penetration depth:*
  - *Shock phase can be neglected: "…steady state is reached instantaneously"*
  - *No terminal phase of penetration: "…penetration stops as soon as the last particle of jet has struck the target"*

- *Since penetration is steady state, time of penetration:*

$$t = \frac{L}{\mathrm{v} - u}$$

- *Penetration depth:* $P = ut$

Hydrodynamic Penetration
Depth of Penetration

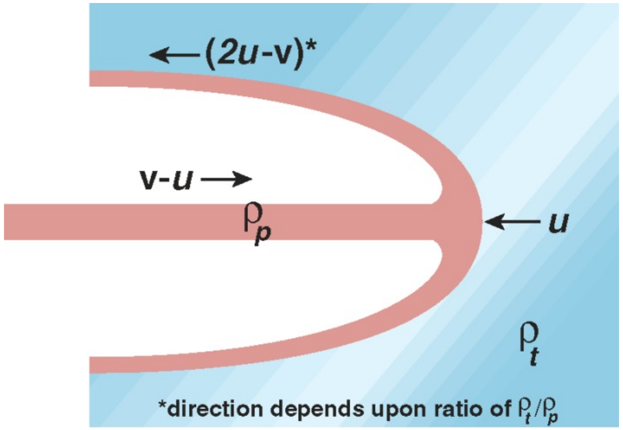

$$\frac{1}{2}\rho_p\,(\mathrm{v}-u)^2 = \frac{1}{2}\rho_t\,u^2$$

$$\boxed{u = \frac{\mathrm{v}}{1+\sqrt{\rho_t / \rho_p}}}$$

$$P = ut \qquad\qquad t = \frac{L}{\mathrm{v}-u}$$

$$P = \frac{u\,L}{\mathrm{v}-u}$$

$$\boxed{\frac{P}{L} = \frac{u}{\mathrm{v}-u} = \sqrt{\rho_p / \rho_t}}$$

CEA Consulting

Bernoulli Equation

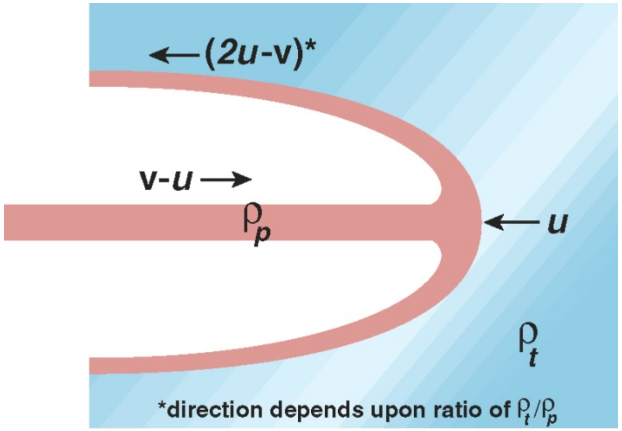

$$\frac{1}{2}\rho_p\,(\mathrm{v}-u)^2 = \frac{1}{2}\rho_t\,u^2$$

$$u = \frac{\mathrm{v}}{1+\sqrt{\rho_t/\rho_p}}$$

$$\frac{P}{L} = \sqrt{\rho_p/\rho_t}$$

Steady state

Incompressible

Hydrodynamic

- *1956 Eichelberger: Need to account for target strength effects*

$$\frac{1}{2}\rho_p\,(\mathrm{v}-u)^2 = \frac{1}{2}\rho_t\,u^2 + \sigma$$

$$\sigma = \sigma_t - \sigma_p$$

σ: resistance to plastic deformation taken to be 1 to 3 times uniaxial yield stress

R. J. Eichelberger, "Experimental test of the theory of penetration by metallic jets," *J. Appl. Phys.*, **27**(1): 63-68, 1956.

Modified Bernoulli Model

$$\frac{1}{2}\rho_p(\mathrm{v}-u)^2 = \frac{1}{2}\rho_t u^2 + \sigma$$

$$\mu = \left(\frac{\rho_t}{\rho_p}\right)^{1/2}$$

$$u = \frac{\mathrm{v} - \mu\left(\mathrm{v}^2 + 2\left(1-\mu^2\right)\sigma/\rho_t\right)^{1/2}}{1-\mu^2} \qquad \rho_p \neq \rho_t$$

$$u = \frac{\mathrm{v}}{2} - \frac{\sigma}{\rho\mathrm{v}} \qquad \rho_p = \rho_t$$

Modified Bernoulli Equation

Allen & Rogers (1961)

$$\frac{1}{2}\rho_p (\mathrm{v}-u)^2 = \frac{1}{2}\rho_t u + \phi_t$$

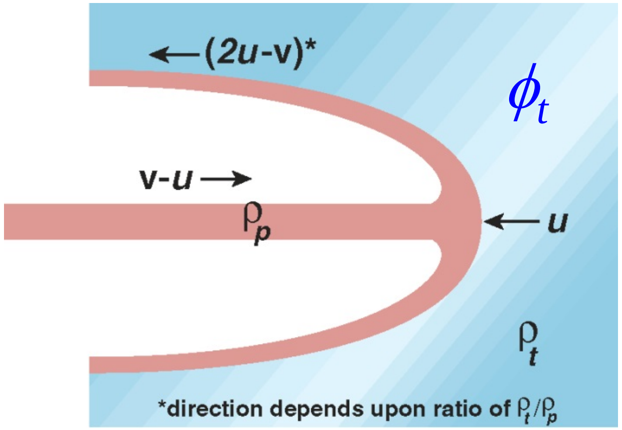

- *Shot 6 different projectile materials into 7075-T6 aluminum Au, Pb, Cu, Sn, Al, Mg*
- *Called ϕ_t a dynamic yield strength of a solid target relative to a fluid jet*
- $\phi_t = 3.9\, Y_t \quad Y_t = 0.48\ \text{GPa}$

  $\phi_t \sim 1.87\ \text{GPa}$
- *Found the ϕ_t had to be written as a function of impact velocity to reproduce final depth of penetration*

W. A. Allen and J. W. Rogers, "Penetration of a rod into a semi-infinite target," *J. Franklin Inst.*, **272**: 275-284, 1961.

Simple Modified Bernoulli Equation

$$\frac{1}{2}\rho_p\left(\mathrm{v}-u\right)^2=\frac{1}{2}\rho_t\,u^2+\sigma$$

- *Applies to relatively weak projectiles*
- *Assumption: projectile is completely consumed, i.e., no projectile remains at bottom of penetration channel*
- *Above assumption true only for very high velocity impacts*

CEA Consulting

Christman and Gehring

- *Christman and Gehring described the phases of penetration for high-velocity impact*
  - *Separated the primary phase from the secondary (transient) phase*

$$P = (L-D)\left(\frac{\rho_p}{\rho_t}\right)^{1/2} + P_c$$

  - *P_c is the crater depth obtained for a rod of L/D = 1*
- *Correlated P_c with experimental data*

$$P_c = 0.13\left(\frac{\rho_p}{\rho_t}\right)^{1/3}\left(\frac{\frac{1}{2}mv^2}{B_{max}}\right)^{1/3}$$

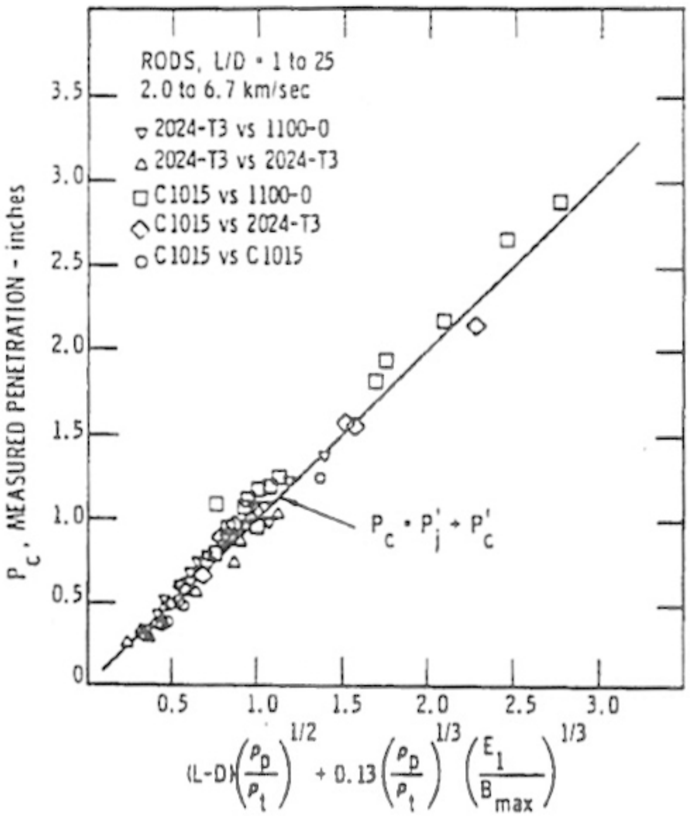

D. R. Christman and J. W. Gehring, "Analysis of high-velocity projectile penetration mechanics," *J. Appl. Phys.*, **37**(4): 1579-1587, 1966.

CEA Consulting

Recht-Ipson

- *Perforation of plates by blunt projectiles (fragments)*
  - *Normal and oblique impact*
- *Assumptions*
  - *Relatively chunky projectiles*
  - *Relatively thin plates*
    $$\left[\frac{T}{L}<\frac{1}{2};\frac{T}{d}<\frac{1}{2}\right]$$
  - *Projectiles do not deform excessively (no erosion)*

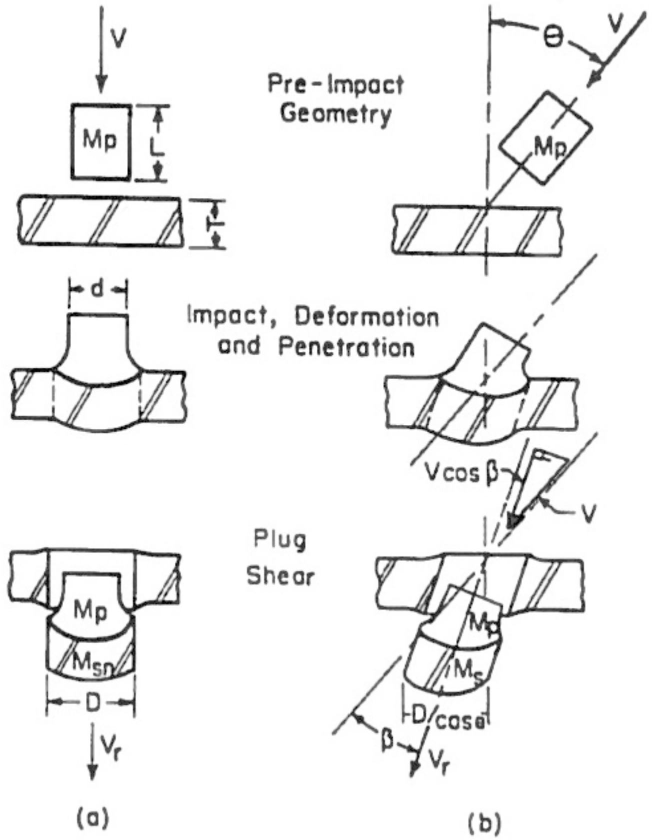

R. F. Recht and T. W. Ipson, “Ballistic perforation dynamics,” *J. Appl. Mech.*, Sept.: 384-390, 1963.

CEA Consulting

Recht-Ipson

- *Observation: a plate plug is ejected*
- *Conservation of momentum and energy*
  - *Work required to shear the plug from the target is related to V_{50}*

$$V_r = \frac{M_p}{M_p + M_{sn}} \left(V^2 - V_{50}^2\right)^{1/2}$$

$$V_r = \frac{1}{1 + \frac{\rho_t}{\rho_p}\left(\frac{D}{d}\right)^2 \frac{T}{L}} \left(V^2 - V_{50}^2\right)^{1/2}$$

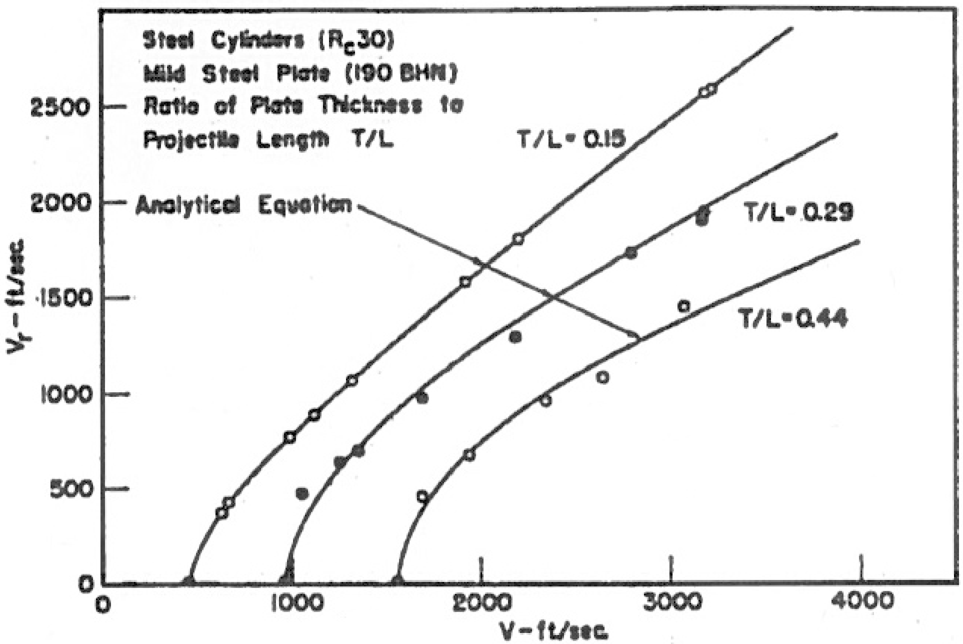

R. F. Recht and T. W. Ipson, "Ballistic perforation dynamics," *J. Appl. Mech.*, Sept.: 384-390, 1963.

Recht-Ipson

- Made engineering estimates for V_{50}
- Oblique impact
  - Line-of-sight thickness
  - Angular change in fragment direction
- Thick plates perforated by cylinders
  - Problem is the plug mass; experimentally determined
- Plates perforated by AP projectiles (no plug)

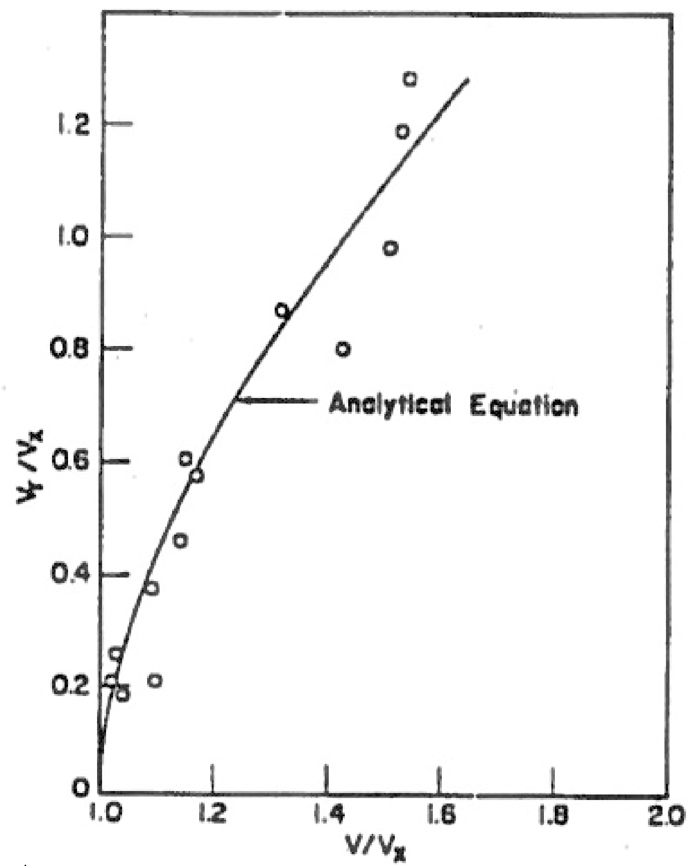

$$\frac{V_r}{V_{50}} = \left(\frac{V^2}{V_{50}^2} - 1\right)^{\frac{1}{2}}$$

Note on Conservation of Energy

- Energy is conserved, but:
  - It is difficult to account for all the various mechanisms that dissipate energy
  - The proportion of energy dissipation (energy transfer mechanisms) changes with impact velocity
  - In particular, as the impact velocity increases, the projectile kinetic energy is transferred to the target in terms of target kinetic energy and elastic compression energy; this compression energy is dissipated by plastic work at later times*
    - Walker demonstrated** that it is the transfer of this energy at the time of penetration that defines the forces on the projectile
    - For energy rate balance to be successful, must include transfer of energy stored in the target as elastic compression
- Conservation of energy can be useful in analytical modeling, but generally over a limited velocity range and/or target-projectile configuration

*C. E. Anderson, Jr., D. L. Littlefield, and J. D. Walker, "Long-rod penetration, target resistance, and hypervelocity impact," *Int. J. Impact Engng.*, **14**: 1-14, 1993.

J. D. Walker, "Hypervelocity penetration modeling: momentum vs. energy and energy transfer mechanisms," *Int. J. Impact Engng.*, **26: 809-822, 2001.

Residual Velocity vs. Impact Velocity

- *Large set of experimental data*
  - *Tungsten alloy and 6 different steels with different heat treats*
  - *17 different projectiles*
  - *Two different target (armor steel) hardnesses*

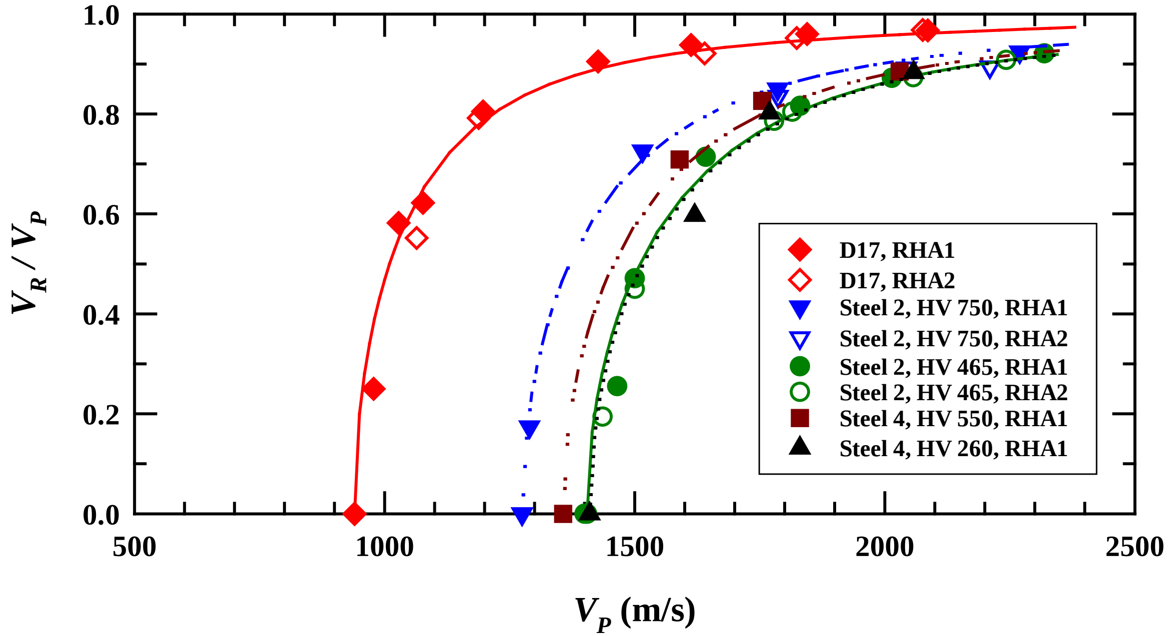

C. E. Anderson, Jr., V. Hohler, J. D. Walker, and A. J. Stilp, "The influence of projectile harness on ballistic performance," *Int. J. Impact Engng.*, **22**(6): 619-632, 1999.

Scaling of Residual Velocity

$$V_R = \begin{cases} a\left(V_p^m - V_{BL}^m\right)^{1/m} & V_P > V_{BL} \\ 0 & V_P \le V_{BL} \end{cases}$$

$$\frac{V_R}{V_{BL}} = a\left[\left(\frac{V_P}{V_{BL}}\right)^m - 1\right]^{1/m}$$

CEA Consulting

Normalized Residual Velocity

- *Similitude modeling, with correct choice of parameters, permits collapse of data*
- *Demonstrates that a lot of basic information about projectile and target material response is contained in V_{BL} or V_{50})*
- *However, similitude analysis does not explicitly allow us to determine these relationships*

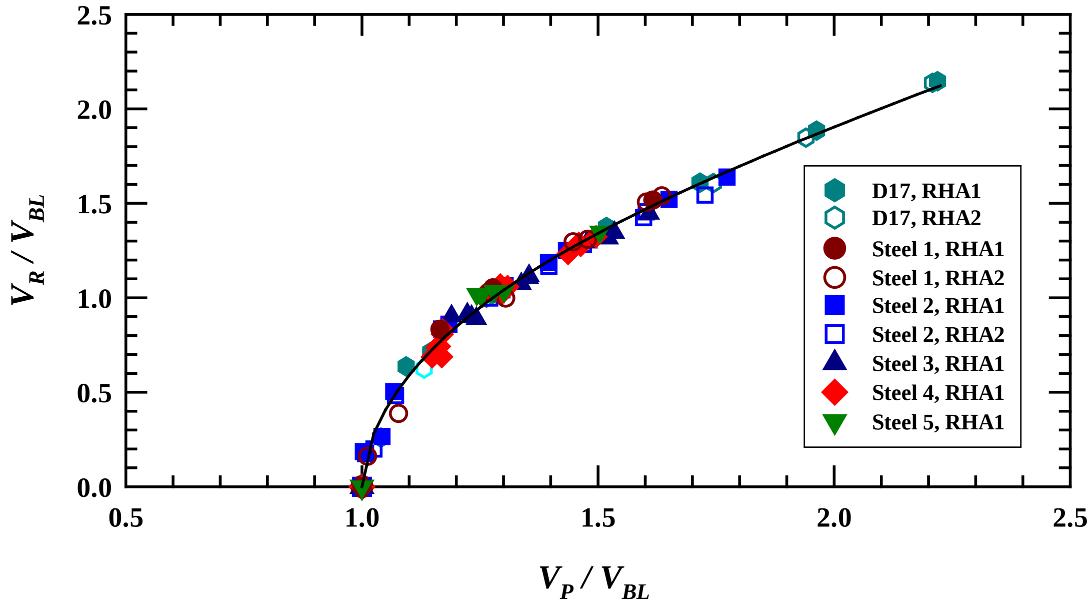

$$\frac{V_R}{V_{BL}} = \frac{\left(0.90x^2 + 1.3x + 1.6x^{1/2}\right)}{(x+1)} \qquad x = \frac{V_P}{V_{BL}} - 1$$

C. E. Anderson, Jr., V. Hohler, J. D. Walker, and A. J. Stilp, "The influence of projectile harness on ballistic performance," *Int. J. Impact Engng.*, **22**(6): 619-632, 1999.

Tate Model

A. Tate, "A theory for the deceleration of long rods after impact," *J. Mech. Phys. Solids*, **15**: 387-399,1967

A. Tate, "Further results in the theory of long rod penetration," *J. Mech. Phys. Solids*, **17**: 141-150, 1969.

A. Tate, K. E. B. Green, P. C. Chamberlain, and R. G. Baker, "Model scale experiments on long rod penetration, *Proc. 4th Int. Symp. Ballistics*, 1978.

A. Tate, "Long rod penetration models—Part I. A flow field model for high speed long rod penetration," *Int. J. Mech. Sci.*, **28**(8): 535-548, 1986.

A. Tate, "Long rod penetration models—Part II. Extensions to the hydrodynamic theory of penetration," *Int. J. Mech. Sci.*, **28**(9): 599-612, 1986.

A. Tate, "A theoretical estimate of temperature effects during rod penetration," *Proc. 9th Int. Symp. Ballistics*, **2**: 307-314, Shriverhem, UK, 1986.

Tate Model

- *Real rods decelerate while penetrating*
- *Tate (1967, 1969), and Alekseevski (1966) independently postulated a different modified Bernoulli equation*

$$\frac{1}{2}\rho_p\left(\mathrm{v}-u\right)^2+Y_p=\frac{1}{2}=\rho_t\,u^2+R_t$$

- *Y_p: dynamic flow stress of projectile material*
- *R_t: target resistance*

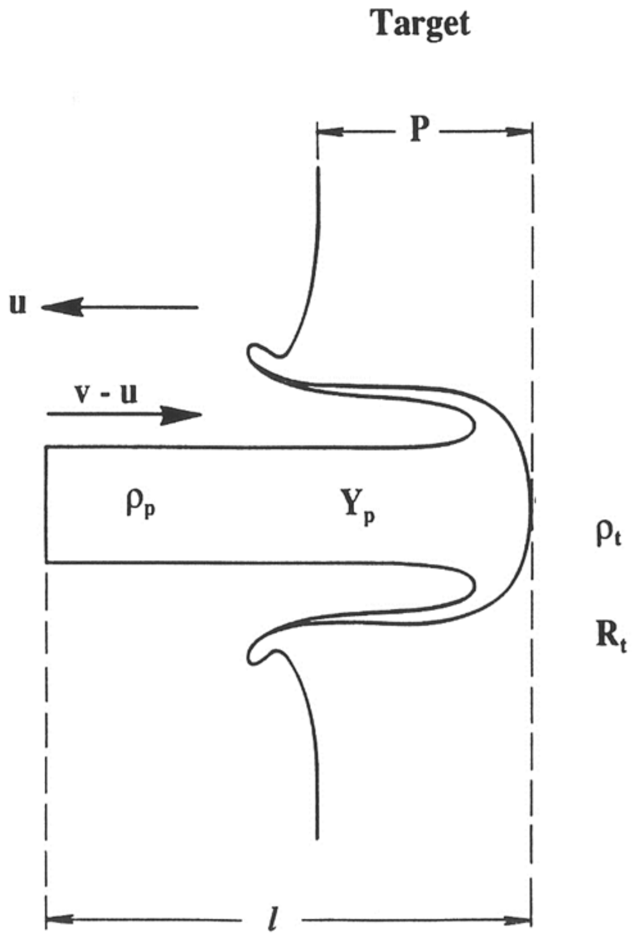

Rod Deceleration

- *Force acting to decelerate residual rod ℓ :*

$$\rho_p \ell \pi R^2 \frac{d\mathrm{v}}{dt} = -\pi R^2 Y_p$$

$$\rho_p \ell \frac{d\mathrm{v}}{dt} = -Y_p$$

- *Rod is getting shorter as it erodes*

$$\frac{d\ell}{dt} = -(\mathrm{v} - u)$$

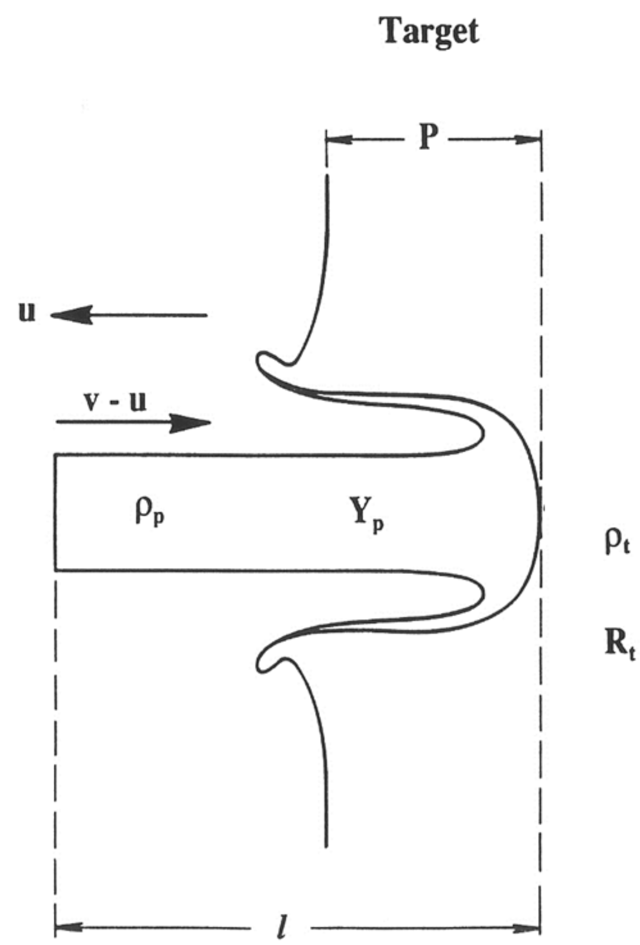

Tate Model

$$\frac{1}{2}\rho_p (\mathrm{v}-u)^2 + Y_p = \frac{1}{2}\rho_t u^2 + R_t$$

$$\rho_p \ell \frac{d\mathrm{v}}{dt} = -Y_p$$

$$\frac{d\ell}{dt} = -(\mathrm{v}-u)$$

Simultaneous solution of three equations

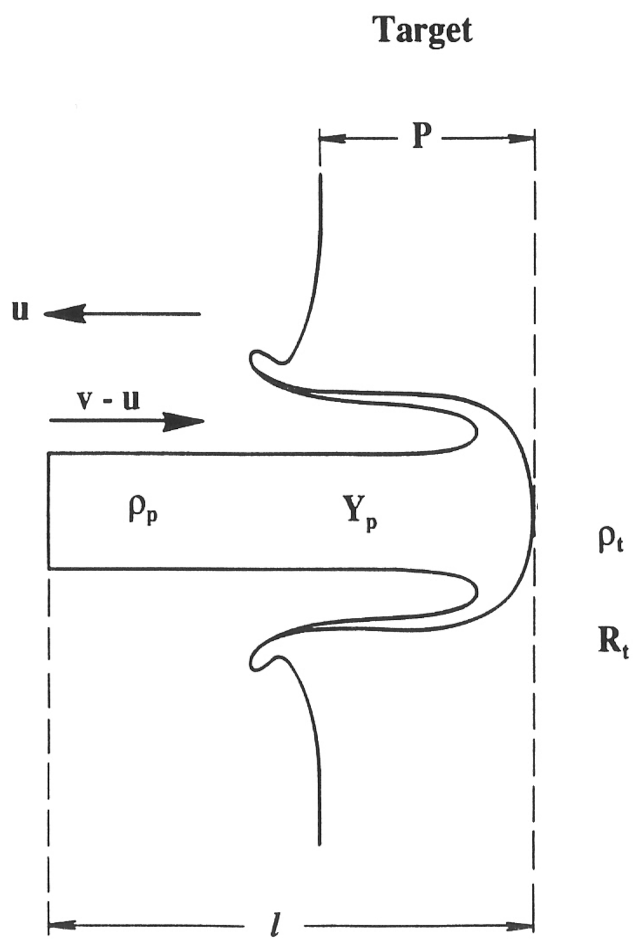

Tate Model

$$\frac{1}{2}\rho_p\,(\mathrm{v}-u)^2 + Y_p = \frac{1}{2}\rho_t\,u^2 + R_t$$

$$u = \frac{\mathrm{v}-\mu\left(\mathrm{v}^2 + A\right)^{1/2}}{1-\mu^2} \qquad \rho_p \neq \rho_t$$

$$\mu = \left(\frac{\rho_t}{\rho_p}\right)^{1/2} \qquad A = \frac{2\left(R_t - Y_p\right)\left(1-\mu^2\right)}{\rho_t}$$

$$u = \frac{\mathrm{v}}{2} - \frac{\left(R_t - Y_p\right)}{\mathrm{v}\,\rho} \qquad \rho_p = \rho_t$$

Critical Velocity (when $u = 0$):

$$\mathrm{v}_c = \left[\frac{2\left(R_t - Y_p\right)}{\rho_p}\right]^{1/2}$$

No penetration below v_c

How to Estimate Y_p and R_t?

$$\frac{1}{2}\rho_p\left(\mathrm{v}-u\right)^2+Y_p=\frac{1}{2}\rho_t\,u^2+R_t$$

- $Y_p=\left(1+\lambda\right)\sigma_p \qquad \sigma_p=3.92\bullet\mathrm{BHN}\quad\left[\mathrm{N/mm^2}\right]$
- *$\lambda \equiv$ a factor to account for dynamic effects*
- *Use quasistatic cavity expansion to estimate the target resistance R_t*

Cavity Expansion Theory

- *Assume an incompressible or compressible plastic region and an elastic region.*
- *Opening up a cavity from zero radius to R quasi-statically.*
- *Find a similarity solution.*
- *Solution leads to elastic region - plastic region and allows calculation of stress at interface.*

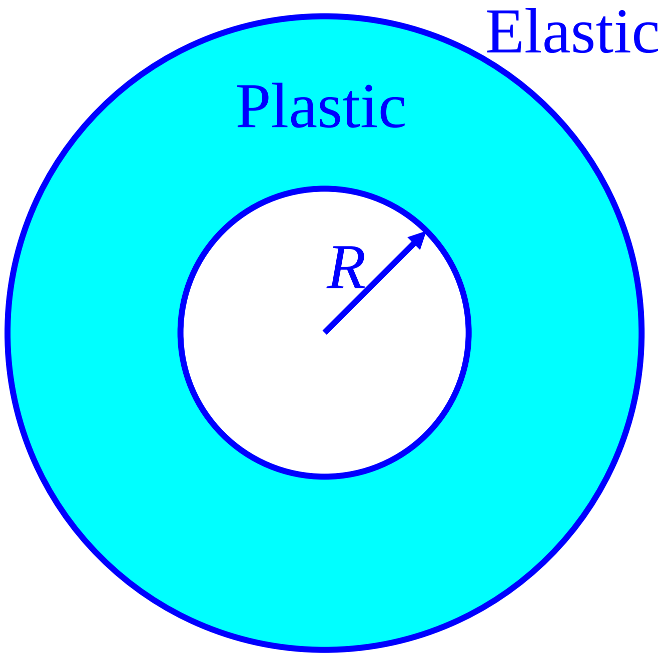

R. F. Bishop, R. Hill, and N. F. Mott, "The Theory of Indentation and Hardness," *Proc. Royal Soc.*, **57**(3): 147-159, 1945.

Cavity Expansion Theory

- Spherical Expansion (incompressible)

$$P_{\mathrm{sph}} = \frac{2Y_t}{3}\left[1+\ln\left(\frac{E_t}{(1+\nu_t)Y_t}\right)\right] \rightarrow \frac{2Y_t}{3}\left[1+\ln\left(\frac{2E_t}{3Y_t}\right)\right]$$

- Cylindrical Expansion (incompressible)

$$P_{\mathrm{cyl}} = \frac{Y_t}{\sqrt{3}}\left[1+\ln\left(\frac{\sqrt{3}\,E_t}{2(1+\nu_t)Y_t}\right)\right] \rightarrow \frac{Y_t}{\sqrt{3}}\left[1+\ln\left(\frac{\sqrt{3}\,E_t}{3\,Y_t}\right)\right]$$

- Spherical Expansion (compressible)

$$P_{\mathrm{sph}} = \frac{2Y_t}{3}\left[1+\ln\left(\frac{E_t}{3(1-\nu_t)Y_t}\right)\right]$$

- Cylindrical Expansion (compressible)

$$P_{\mathrm{cyl}} = \frac{Y_t}{\sqrt{3}}\left[1+\ln\left(\frac{\sqrt{3}\,E_t}{6(1-\nu_t)Y_t}\right)\right]$$

Cavity Expansion Theory

- Tate – Solenoidal model
  - Inspired by the magnetic flow lines in a solenoid
  - Material is incompressible
  - The von Mises yield criterion applies
  - J_2 flow law applies
  - When yielding, the materials are perfectly plastic
  - No attempt to account for rate effects, microstructural features, etc.

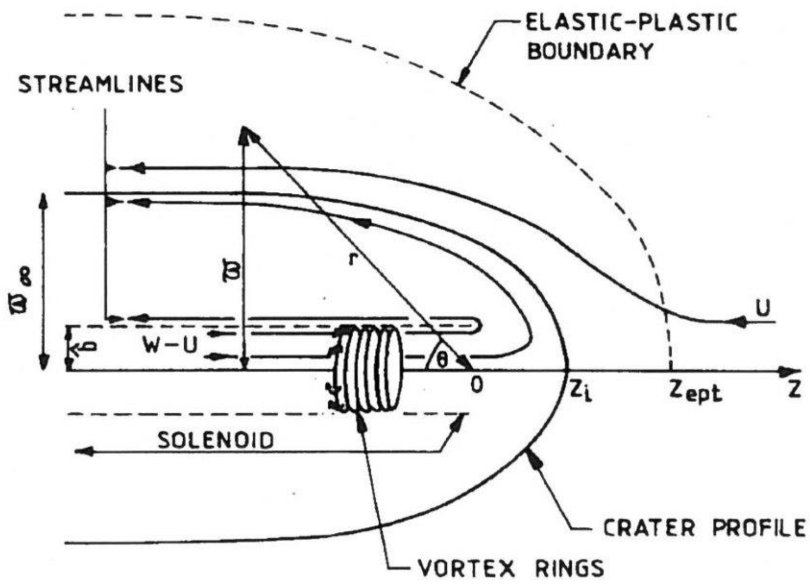

$$P_{Tate} = Y_t\left[\frac{2}{3} + \ln\left(\frac{2E_t}{\left(4-e^{-\lambda}\right)Y_t}\right)\right] \xrightarrow{\lambda = 0.7} Y_t\left[\frac{2}{3} + \ln\left(\frac{0.59\,E_t}{Y_t}\right)\right]$$

CEA Consulting

Determination of Y_p and R_t

- Y_p: dynamic yield strength of projectile ($Y_p = 1.7\sigma_p$)
- R_t: target resistance; assumed constant for a given material

$$R_t = \frac{2Y_t}{3}\left[1 + \ln\left(\frac{2E_t}{3Y_t}\right)\right]$$

$$R_t = \frac{Y_t}{\sqrt{3}}\left[1 + \ln\left(\frac{\sqrt{3}\,E_t}{3\,Y_t}\right)\right]$$

$$R_t = \frac{2\,Y_t}{3}\left[1 + \ln\left(\frac{E_t}{3(1-\nu_t)Y_t}\right)\right]$$

$$R_t = \frac{Y_t}{\sqrt{3}}\left[1 + \ln\left(\frac{\sqrt{3}E_t}{6(1-\nu_t)Y_t}\right)\right]$$

$$R_t = Y_t\left[\frac{2}{3} + \ln\left(\frac{0.59\,E_t}{Y_t}\right)\right]$$

- R_t is the resistance to plastic deformation

Estimates for R_t

- Compute R_t for an armor-like steel
  - E_t = 200 GPa
  - Y_t = 1.0 GPa

$$R_t = \frac{2Y_t}{3}\left[1 + \ln\left(\frac{2E_t}{3Y_t}\right)\right] \quad = 3.93 \text{ GPa}$$

$$R_t = \frac{Y_t}{\sqrt{3}}\left[1 + \ln\left(\frac{\sqrt{3}\,E_t}{3\,Y_t}\right)\right] \quad = 3.32 \text{ GPa}$$

$$R_t = \frac{2\,Y_t}{3}\left[1 + \ln\left(\frac{E_t}{3(1-\nu_t)Y_t}\right)\right] \quad = 3.74 \text{ GPa}$$

$$R_t = \frac{Y_t}{\sqrt{3}}\left[1 + \ln\left(\frac{\sqrt{3}E_t}{6(1-\nu_t)\,Y_t}\right)\right] \quad = 3.15 \text{ GPa}$$

$$R_t = Y_t\left[\frac{2}{3} + \ln\left(\frac{0.59\,E_t}{Y_t}\right)\right] \quad = 5.44 \text{ GPa}$$

- R_t: 3-5 times dynamic yield strength of target material
- Problem: R_t is **not** a material constant; R_t changes with impact velocity

Critical Velocities

$$\frac{1}{2}\rho_p (\mathrm{v}-u)^2 + Y_p = \frac{1}{2}\rho_t u^2 + R_t$$

- $R_t > Y_p$ and $u = 0$
- Critical velocity

$$\mathrm{v}_c = \left[\frac{2(R_t - Y_p)}{\rho_p}\right]^{1/2}$$

- No penetration below v_c

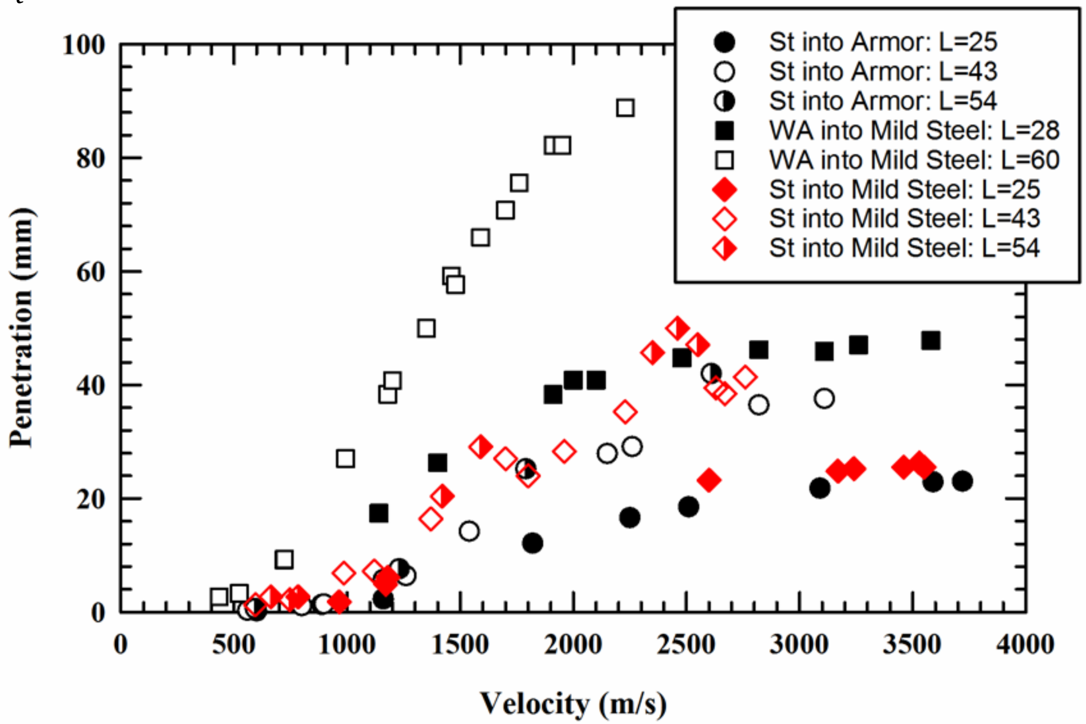

WA into armor steel: v_c = 642 m/s

Steel into armor steel: v_c = 1050 m/s

Rigid-Body Penetration

$$\frac{1}{2}\rho_p\left(\mathrm{v}-u\right)^2+Y_p=\frac{1}{2}\rho_t\,u^2+R_t$$

- $Y_p > R_t$ and $u \equiv v$
- Rigid-body penetration
- Crater diameter = projectile diameter

Rigid & Eroding Penetration

- *Threshold velocity*

$$\mathrm{v}_{th} = \left[\frac{2\left(Y_p - R_t\right)}{\rho_t} \right]^{1/2}$$

- *$V_p < v_{th}$, rigid*
- *$V_p > v_{th}$, eroding*
- *Deceleration of projectile*

$$\frac{d\mathrm{v}}{dt} = -\frac{\tilde{\sigma}}{\rho_p L} = -\frac{1}{\rho_p L}\left(\frac{1}{2}\rho_t \mathrm{v}^2 + R_t\right)$$

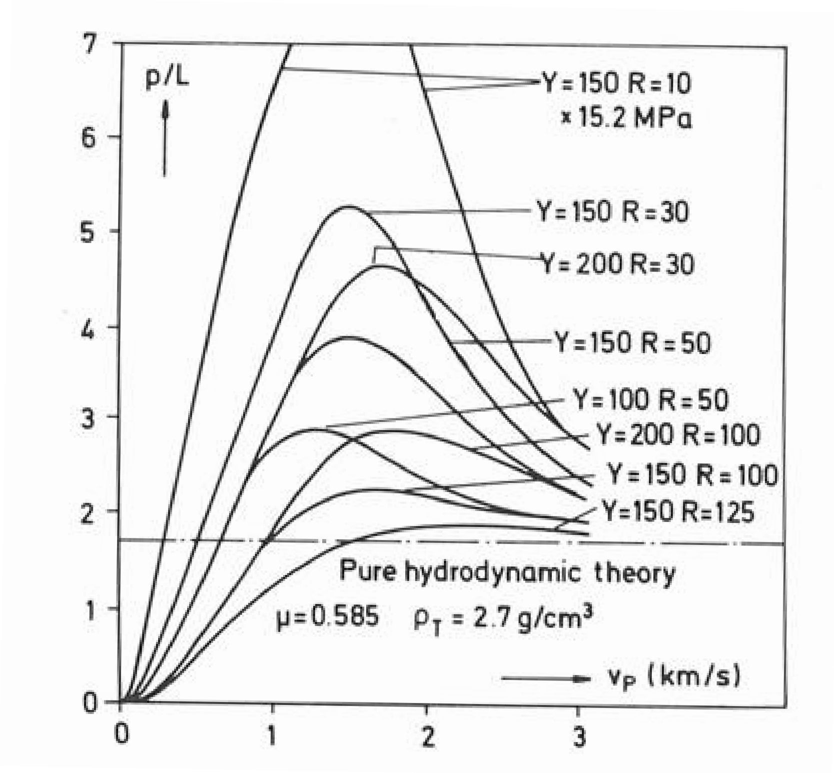

- *Tate model demonstrates the mechanics, but complications in trying to determine “accurate” Y_p and R_t*

Poncelet Equation

$$M\frac{dv}{dt} = -F = -\left(A + Bv^2\right)$$

$$\rho_p L\frac{dv}{dt} = -\left(a' + b' v^2\right)$$

$$a' = R_t \qquad b' = \frac{1}{2}\rho_t$$

Tate

$$\frac{dv}{dt} = -\frac{1}{\rho_p L}\left(R_t + \frac{1}{2}\rho_t v^2\right)$$

"Tate" Poncelet Equation

CEA Consulting

"Tate" Poncelet

- *Ogive steel penetrator into 6061-T6 aluminum*
- *Poncelet with 2-parameter fit; can use expansion*
  - $$\frac{P}{L}=\frac{1}{2}\frac{\rho_p}{R_t}V^2$$
  - $R_t = 2.10$ *GPa*
- *Tate: one-parameter fit*
  - $R_t = 1.260$ *GPa*

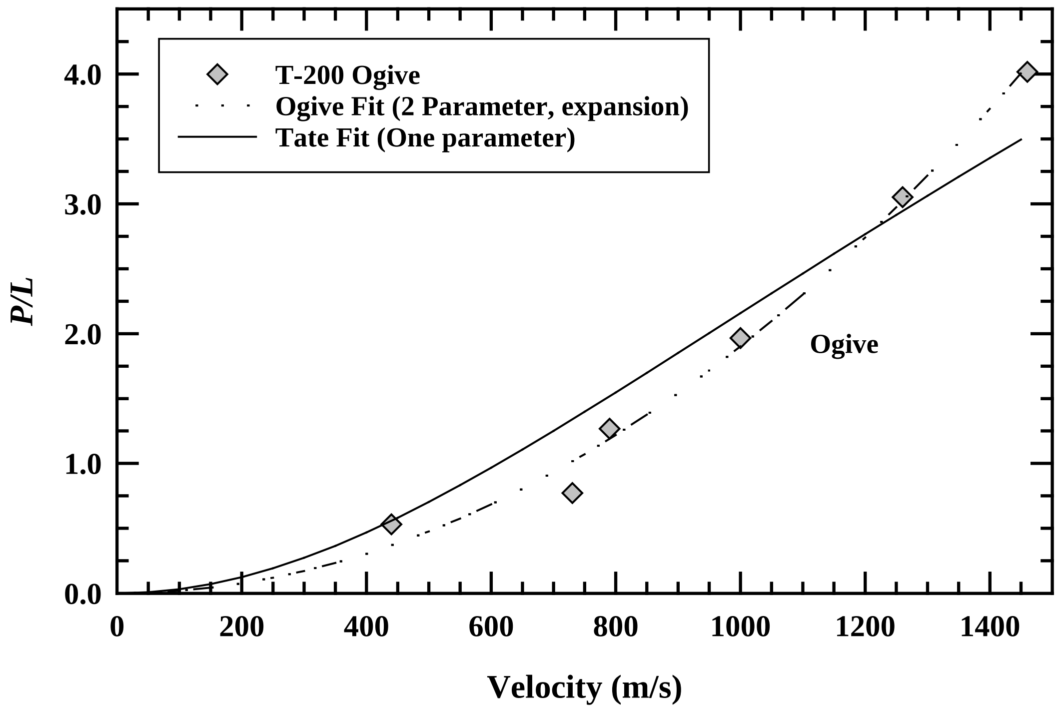

M. J. Forrestal, J. K. Okajima, and V. K. Luk, "Penetration of 6061-T651 aluminum targets with rigid long rods," *J. Appl. Mech*. **55**: 755-760, 1988.

Tate Model: Summary

- *A one-dimensional model that predicts time history of penetration, including projectile deceleration*
- *Target resistance, R_t, is not a constant, but depends upon material and impact velocity—although not a material property, a useful metric for comparison of different target performance*
- *Provides insights into dependence of penetration on material properties (e.g., density, strength)*
- *Predicts a critical velocity ($u = 0$)*
- *Predicts rigid-body penetration and threshold velocity for transition from rigid-body to eroding penetration*

CEA Consulting

Rigid-Body Penetration

- *Vascomax steel into 6061-T6 aluminum*
- *Hydro limit =* $\left(\dfrac{8.0}{2.71}\right)^{1/2}$ *=1.72*
- $$\frac{P}{L} = \frac{1}{2}\frac{\rho_p}{R_t}V^2$$
- $R_t = 2.34$ *GPa (conical)*
- $R_t = 2.10$ *GPa (ogive)*
- $\sigma_t = 0.414$ *GPa;* $\sigma_p = 1.5$ *GPa*

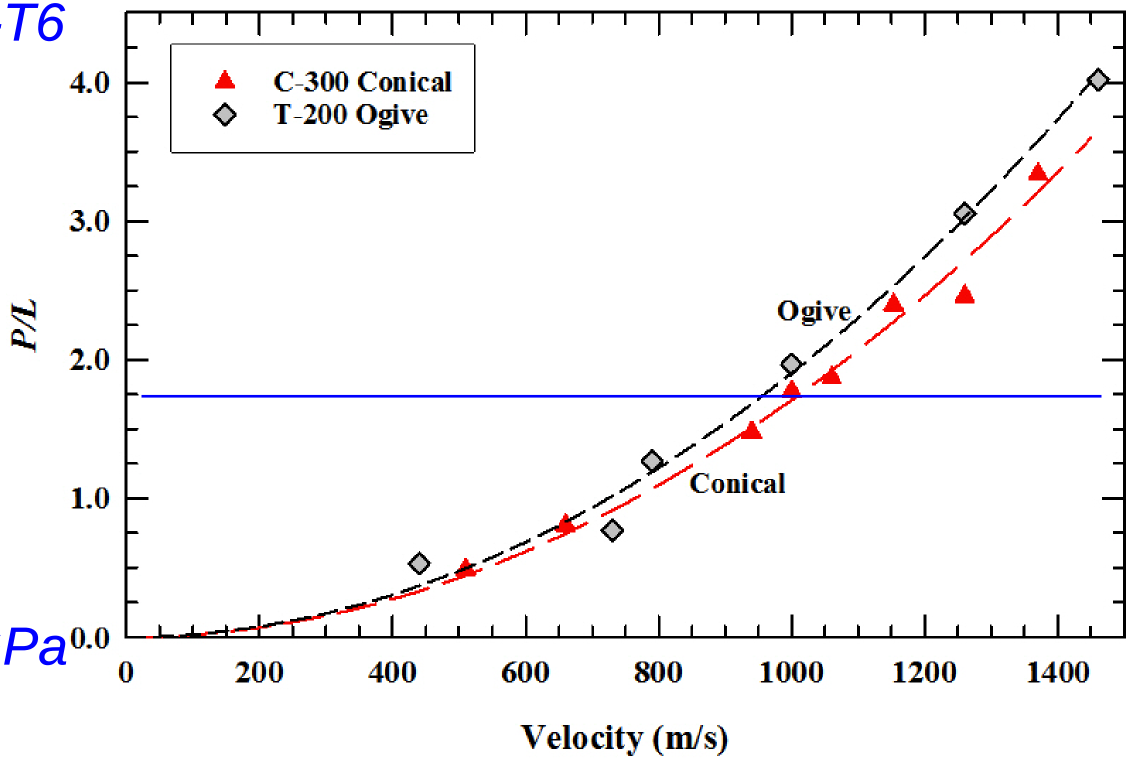

M. J. Forrestal, J. K. Okajima, and V. K. Luk, "Penetration of 6061-T651 aluminum targets with rigid long rods," *J. Appl. Mech*. **55**: 755-760, 1988.

Forrestal & Colleagues

- Modeled rigid-body penetration
- Calculated the force on the projectile nose
  - Different nose shapes
  - Dynamic cavity expansion
  - Accurate constitutive model
    - Strain hardening
    - Rate effects

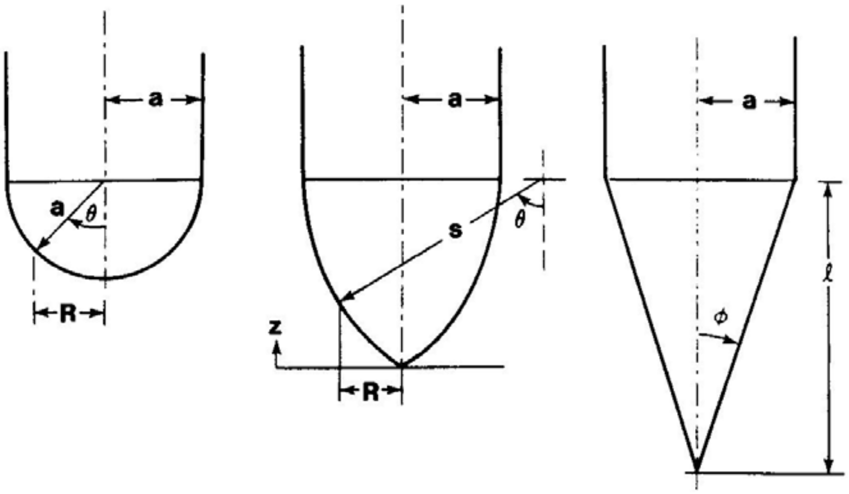

M. J. Forrestal, J. K. Okajima, and V. K. Luk, "Penetration of 6061-T651 aluminum targets with rigid long rods," *J. Appl. Mech*. **55**: 755-760, 1988.

Decelerating Force

For the hemispherical nose:

$$dF_z = 2\pi Ra\cos\theta\,\sigma_n(V_z,\theta)\,d\theta \qquad R = a\sin\theta$$

$$F_z = \pi a^2 \int_0^{\pi/2} \sigma_n(V_z,\theta)\sin 2\theta\, d\theta$$

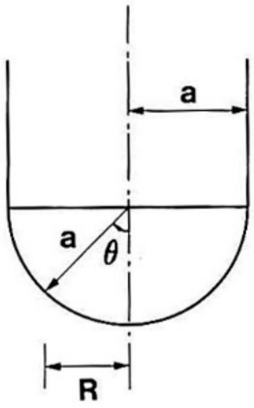

Now need to calculate $\sigma_n(V_z,\theta)$

Dynamic Cavity Expansion Theory

- *Assume an incompressible or compressible plastic region and an elastic region.*
- *Cavity opened at constant velocity.*
- *Find similarity solution.*
- *Solution leads to elastic region - plastic region and interface velocity.*
- *Solution allows calculation of stress at interface.*

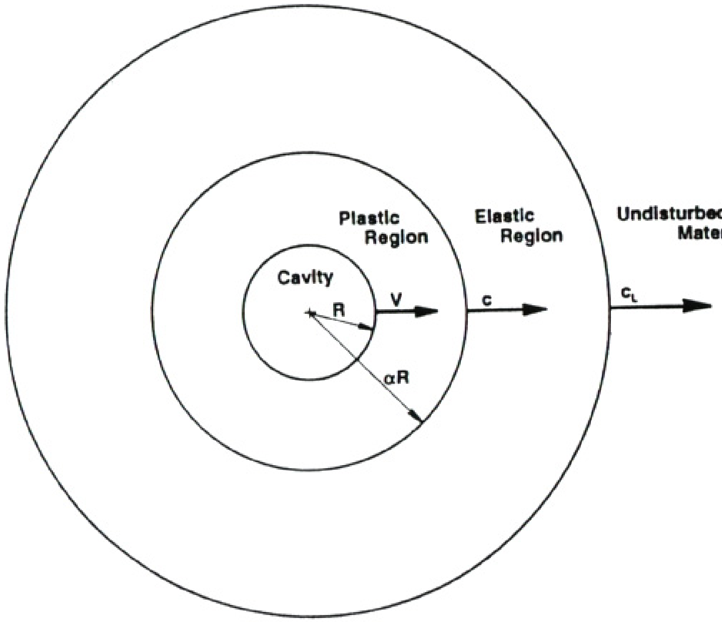

H. G. Hopkins, “Dynamic expansion of spherical cavities in Metals,” Progress in Solid Mechanics, Vol. 1 (I. Sneddon and R. Hill, Eds.), North-Holland, NY, pp. 85-164, 1960.

CEA Consulting

Dynamic Spherical Cavity Expansion

Conservation of momentum

$$\frac{\partial \sigma_r}{\partial r}+\frac{2(\sigma_r-\sigma_\theta)}{r}=-\rho\left(\frac{\partial v}{\partial t}+v\frac{\partial v}{\partial r}\right)$$

Conservation of mass

$$\rho_o\frac{\partial}{\partial r}\left[(r-u)^3\right]=3\rho r^2$$

Particle displacement – particle velocity

$$\frac{\partial u}{\partial t}=v\left(1-\frac{\partial u}{\partial r}\right)$$

True strain rates $\dot{\varepsilon}_r=-\frac{\partial v}{\partial r}$ $\dot{\varepsilon}_\theta=-\frac{v}{r}$

True strain-displacement

$$\varepsilon_r=\ln\left(1-\frac{\partial u}{\partial r}\right) \qquad \varepsilon_\theta=\ln\left(1-\frac{u}{r}\right)$$

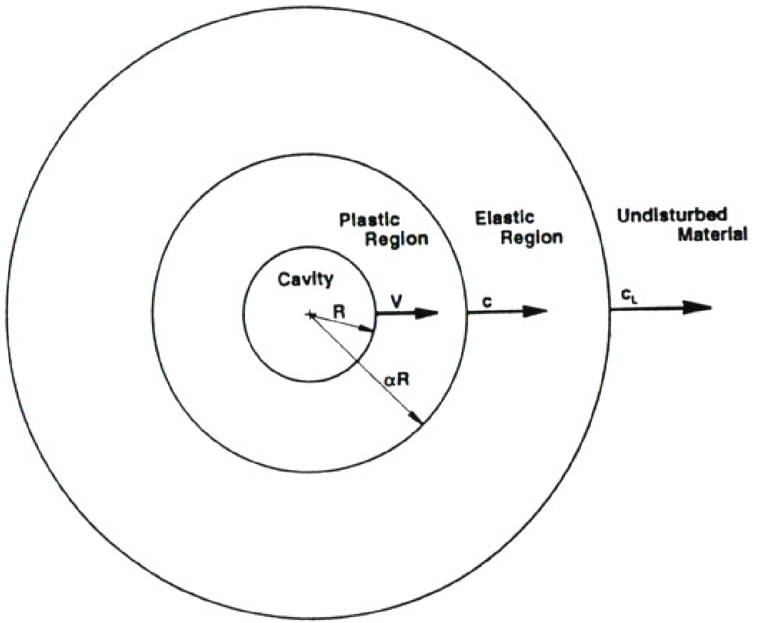

And now a lot of math

Dynamic Spherical Cavity Expansion

$$\frac{\partial \sigma_r}{\partial r} + \frac{2(\sigma_r - \sigma_\theta)}{r} = -\rho\left(\frac{\partial v}{\partial t} + v\frac{\partial v}{\partial r}\right)$$

$$\rho_o \frac{\partial}{\partial r}\left[(r-u)^3\right] = 3\rho r^2$$

If incompressible: $\rho = \rho_o$

$$\sigma_r = \frac{2Y_t}{3}\left[1 + \ln\left(\frac{2E_t}{3Y_t}\right)\right] + \frac{3}{2}\rho_t V^2 \;= A + BV^2$$

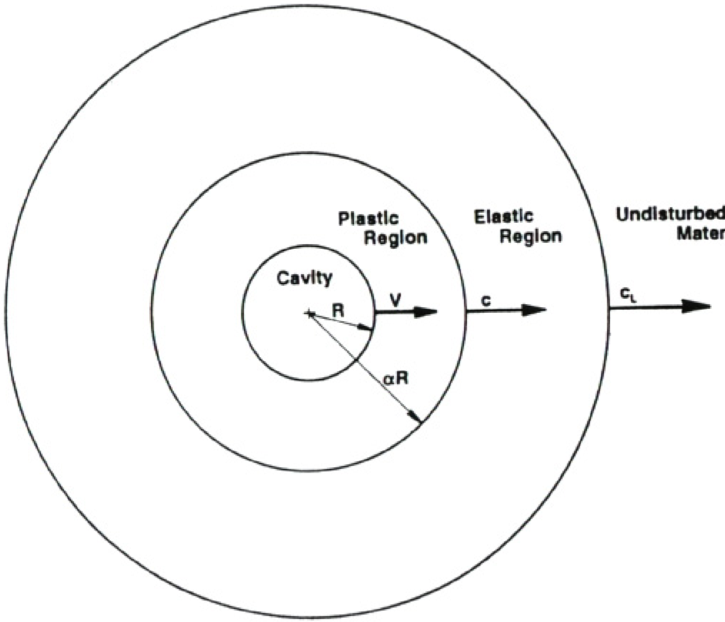

Now have a resistance term that includes strength and inertial effects

Also note that the “resistance” is proportional to the square of the cavity velocity

Note: in virtually all the work of Forrestal and colleagues, they used spherical cavity expansion

Decelerating Force

For the hemispherical nose:

$$F_z = \pi a^2 \int_0^{\pi/2} \sigma_n(V_z,\theta)\sin 2\theta d\theta \qquad \sigma_n(V_z,\theta) = A + BV^2 = A + BV_z^2\cos^2\theta$$

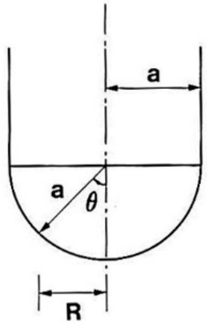

$$F_z = \pi a^2\left[A + \frac{B}{2}V_z^2\right] \qquad M\frac{d\mathrm{v}}{dt} = M\mathrm{v}_z\frac{d\mathrm{v}_z}{dx} = -F_z$$

$$\int_{V_0}^{0}\left[\frac{M\mathrm{v}_z d\mathrm{v}_z}{A + B\mathrm{v}_z^2/2}\right] = -\pi a^2\int_0^P dx \qquad M = \pi a^2\rho_p\left(L + \frac{2a}{3}\right)$$

$$\frac{P}{L + 2a/3} = \frac{\rho_p}{B}\ln\left(1 + \frac{BV_0^2}{2A}\right) = \frac{2\rho_p}{3\rho_t}\ln\left(1 + \frac{\frac{3}{2}\rho_t V_0^2}{\frac{4}{3}Y_t\left[1 + \ln\left(\frac{2E}{3Y_t}\right)\right]}\right)$$

Accurate Constitutive Modeling

$$\frac{\partial \sigma_r}{\partial r} + \frac{2(\sigma_r - \sigma_\theta)}{r} = -\rho\left(\frac{\partial v}{\partial t} + v\frac{\partial v}{\partial r}\right)$$

$$\sigma = \begin{cases} E\varepsilon & \sigma \le Y_d \\ Y\left(\dfrac{E\varepsilon}{Y_d}\right)^n + \alpha\left(\dfrac{\dot{\varepsilon}}{\dot{\varepsilon}_o}\right)^m & \sigma > Y_d \end{cases}$$

$$Y_d = Y + \alpha\left(\frac{\dot{\varepsilon}}{\dot{\varepsilon}_o}\right)^m$$

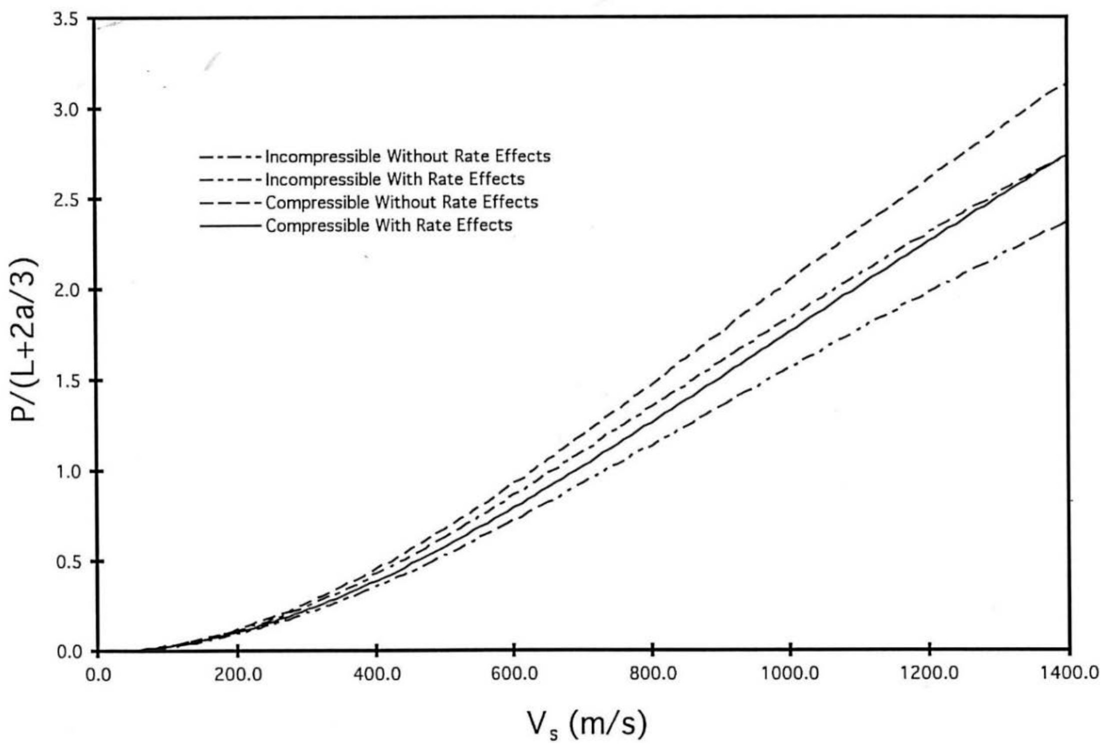

And now a whole lot of math

T. L. Warren and M. J. Forrestal, "Effects of strain hardening and strain-rate sensitivity on the penetration of aluminum targets with spherical-nosed rods," *Int. J. Solids Structures* **35**(28-29): 3737-3753, 1998.

CEA Consulting

Accurate Constitutive Modeling

$$\sigma = \begin{cases} E\varepsilon & \sigma \le Y_d \\ Y\left(\dfrac{E\varepsilon}{Y_d}\right)^n + \alpha\left(\dfrac{\dot{\varepsilon}}{\dot{\varepsilon}_o}\right)^m & \sigma > Y_d \end{cases}$$

$$Y_d = Y + \alpha\left(\frac{\dot{\varepsilon}}{\dot{\varepsilon}_o}\right)^m$$

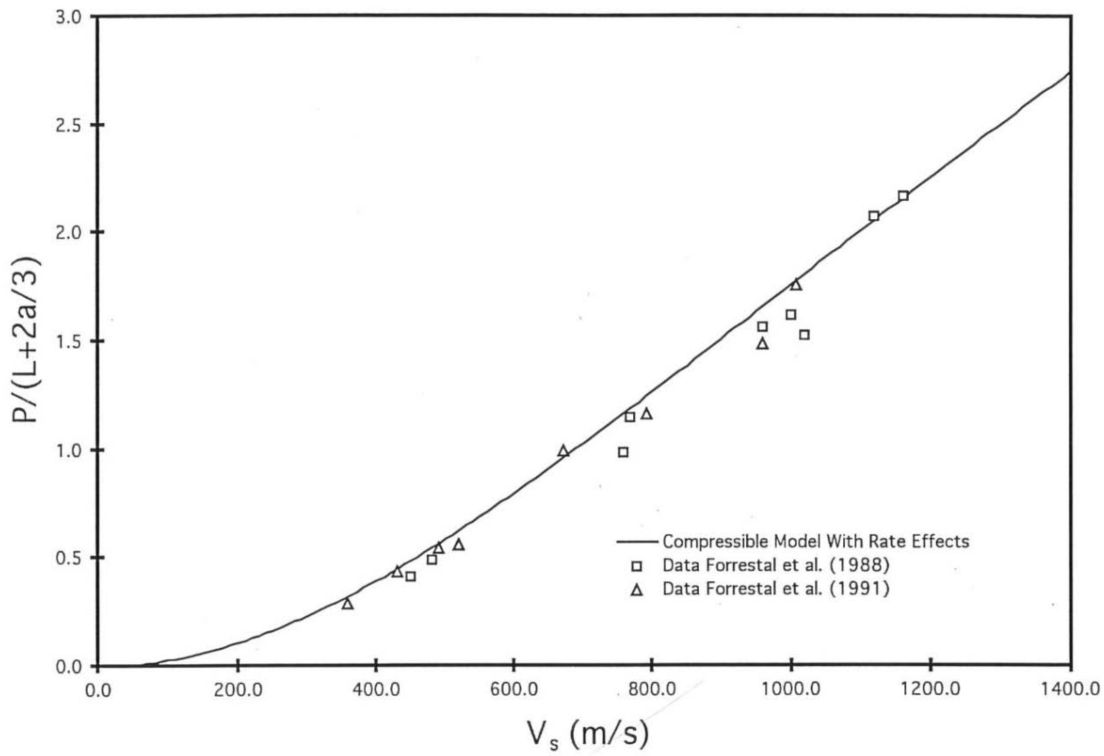

T. L. Warren and M. J. Forrestal, “Effects of strain hardening and strain-rate sensitivity on the penetration of aluminum targets with spherical-nosed rods,” *Int. J. Solids Structures* **35**(28-29): 3737-3753, 1998.

Friction

- *Initially, Forrestal and colleagues were concerned about friction effects between the projectile and penetration cavity wall—included frictional forces in their model*
- *Later, determined that when used accurate constitutive model, there was no need to include friction*

CEA Consulting

Camacho and Ortiz

- *Performed detailed finite element simulations of some of the experiments, using a new adaptive meshing technique and a constitutive material law*
  - *strain hardening*
  - *rate-dependent plasticity*
  - *heat conduction*
  - *thermal-mechanical coupling*
- *Simulations showed a very thin melted layer in the target next to the projectile that resulted in a nearly frictionless interface*

G.T. Camacho and M. Ortiz, "Adaptive Lagrangian modeling of ballistic penetration of metallic targets," *Comput. Methods Appl. Mech. Eng.*, 142:269-301, 1997.

Temperature Effects

- *Tate made an estimate of temperature effects during rod penetration*
  - *Thermal conduction is significant only very close to the interface*
  - *When distances are scaled relative to the crater diameter:*
    - *Temperature distribution is independent of the impact velocity*
    - *Temperature approaches the melting temperature in a small region which is of the same order of size as the conduction dominated zone*

A. Tate, "A theoretical estimate of temperature effects during rod penetration," *Proc. 9th Int. Symp. Ballistics*, 2-307-314, Shriverham, UK, 1996.

Friction Effects

- *Mark Wilkins initially did not have friction forces in Lagrangian hydrocode HEMP, but had good agreement with experiments*
- *Added friction, and calculated results got worse*
- *Friction in penetration mechanics: that quantity added to an analytic model to improve agreement with experiment, whose sole justification is that the friction coefficient is on the order of 0.1 – 0.2 and thus appears reasonable*

Rigid-Body to Eroding Penetration

CEA Consulting

High-Velocity Ogive Data

- Projectile strength
  - T-200: σ_p = 1.38 GPa
  - 4340 VAR: σ_p = 1.50 GPa
  - AerMet100: σ_p = 1.93 GPa
- Transition occurs over very narrow velocity interval

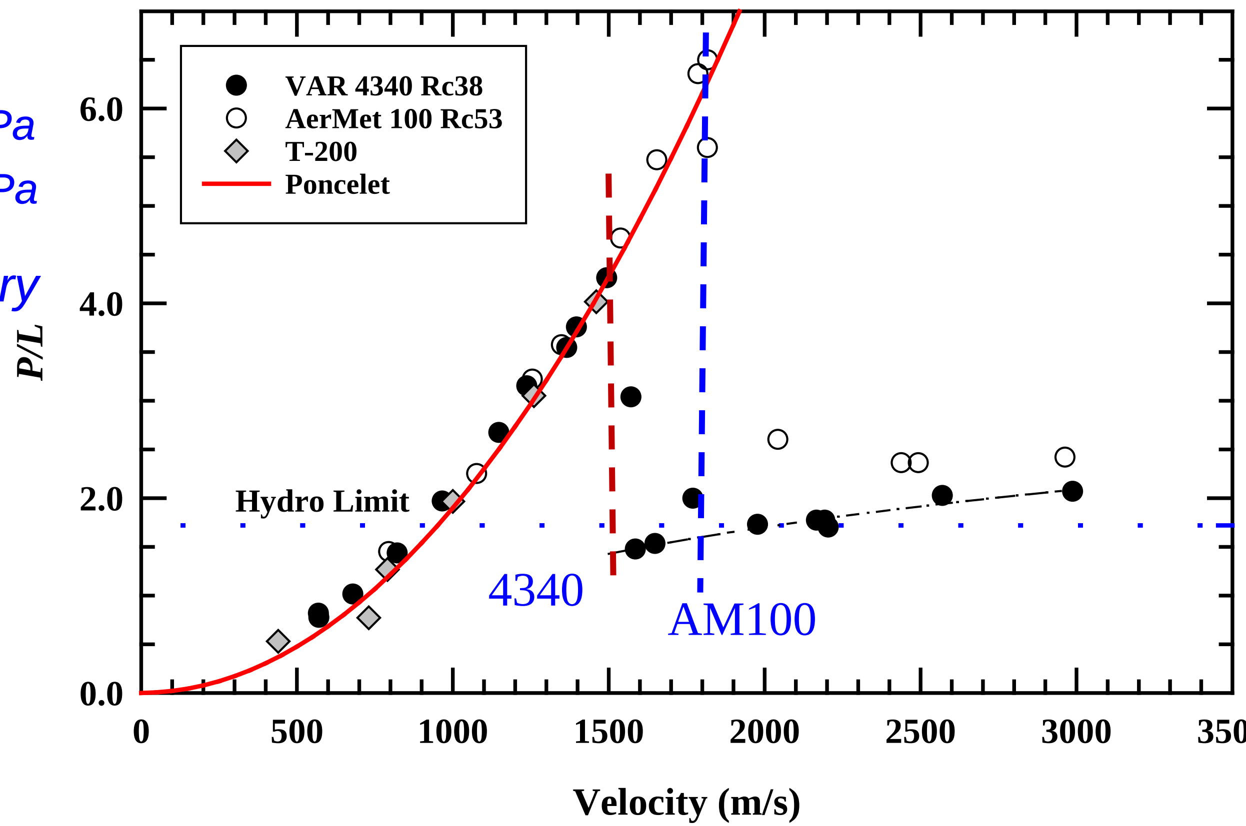

A. J. Piekutowski, M. J. Forrestal, K. L. Poormon, and T. L. Warren, "Penetration of 6061-T6511 aluminum targets by ogive-nose steel projectiles with striking velocities between 0.5 and 3.0 km/s," *Int. J. Impact Engng*., **23**: 723-734, 1999.

CEA Consulting

Tungsten Alloy into Aluminum

- *Flat-nosed projectiles*

HS: $\rho = 17.0$ g/cm^3
$\sigma_p = 0.985$ GPa

MW: $\rho = 17.6$ g/cm^3
$\sigma_p = 1.37$ GPa

$$\left(\frac{P}{L}\right)_{hydro} = \left(\frac{17.3}{2.8}\right)^{1/2} = 2.48$$

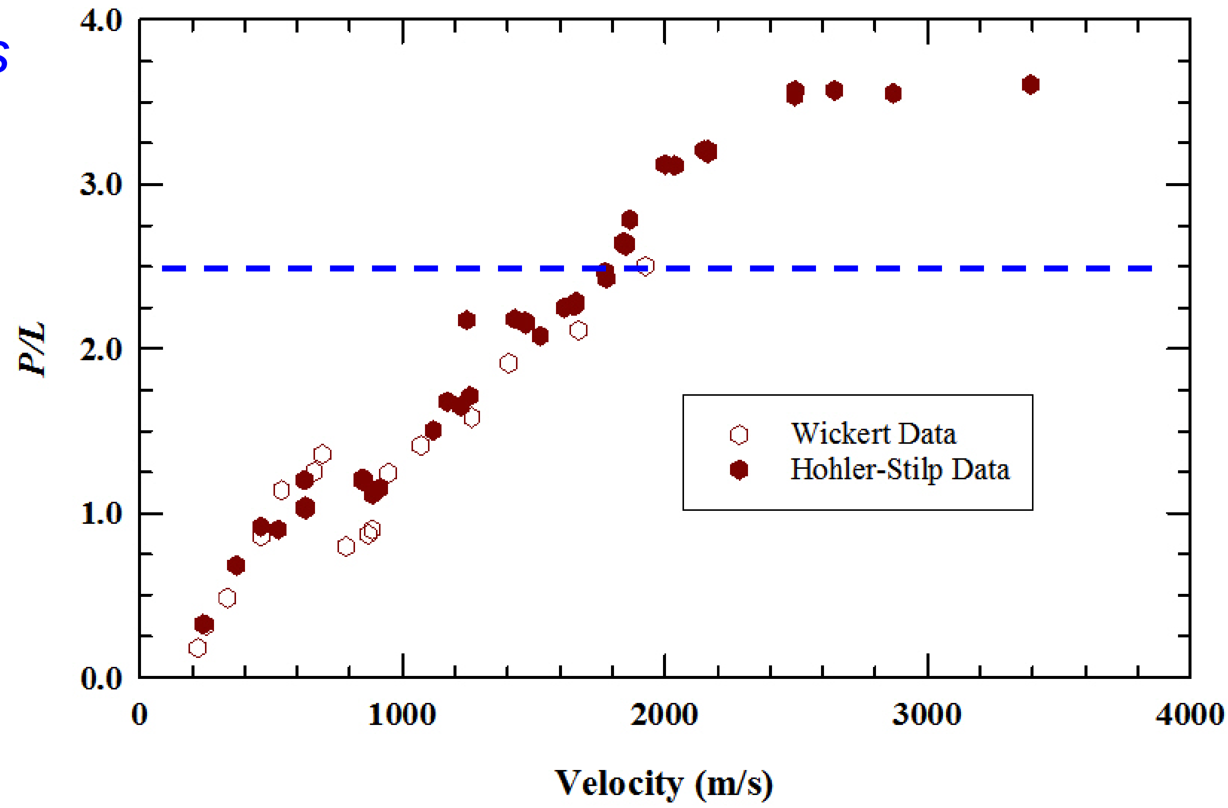

A. J. Stilp and V. Hohler, "Long rod penetration mechanics," Chapter 5 in ***High Velocity Impact Dynamics*** (J. A. Zukas, ed.), John Wiley & Sons, NY, NY, 1990.

M. Wickert, "Penetration data for a medium caliber tungsten sinter alloy penetrator into aluminum alloy 7020 in the velocity regime from 250 m/s to 1900 m/s," *Proc. 23rd Int. Symp. Ballistics*, **2**: 1437-1452, (F. Gálvez and V. Sánchez-Gálvez, Eds.), Gráficas Couche, S.L., Madrid, Spain, 2007.

CEA
Consulting

Poncelet Equation

$$\frac{d\mathrm{v}}{dt} = -\frac{1}{\rho_p L}\left(R_t + b\,\mathrm{v}^2\right)$$

$$\frac{P}{L} = \frac{\rho_p}{2b}\ln\left(1 + \frac{bV^2}{R_t}\right) \xrightarrow{\text{small "x"}} \frac{P}{L} = \frac{\rho_p V^2}{2R_t}$$

Tungsten alloy more ductile than the very hard steels, allowing mushrooming before eroding

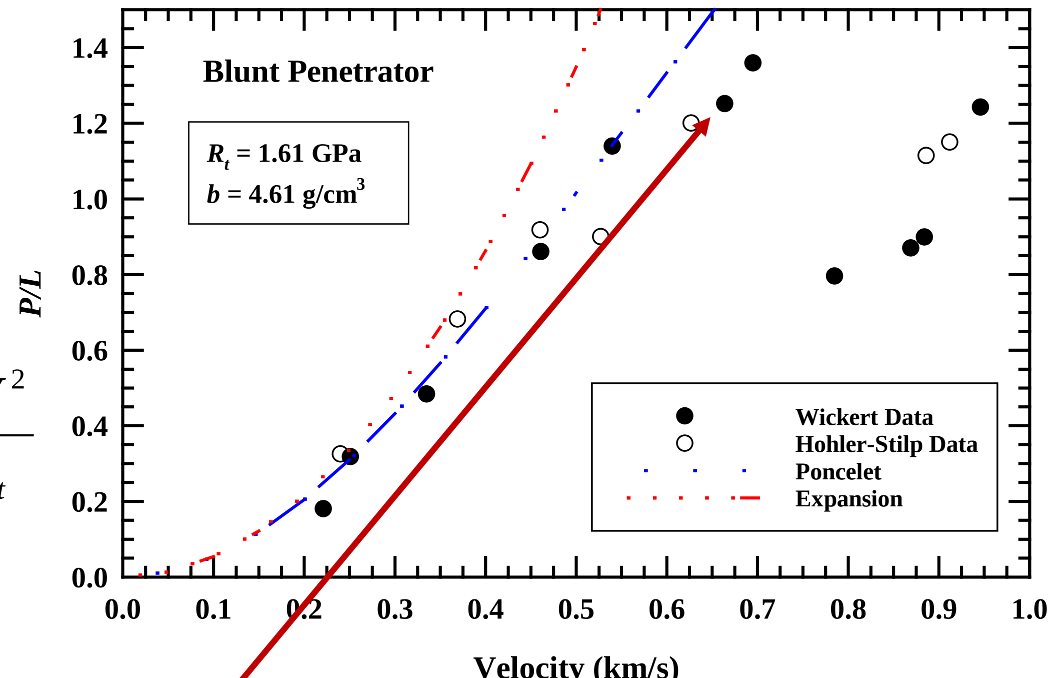

Tungsten alloy into 6061 aluminum

45% decrease in the fitted standard error by dropping these 3 data points

Tungsten Alloy into Aluminum Secondary Penetration

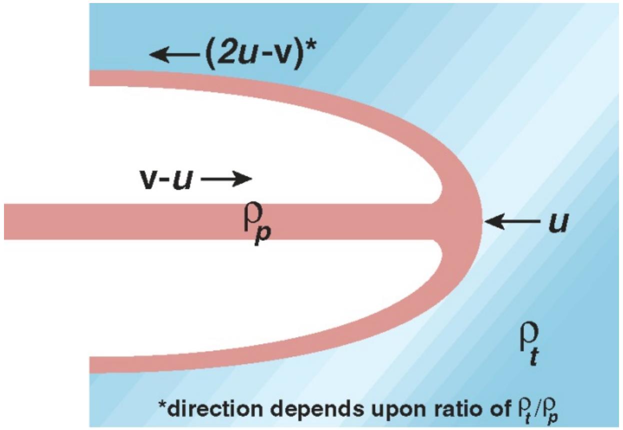

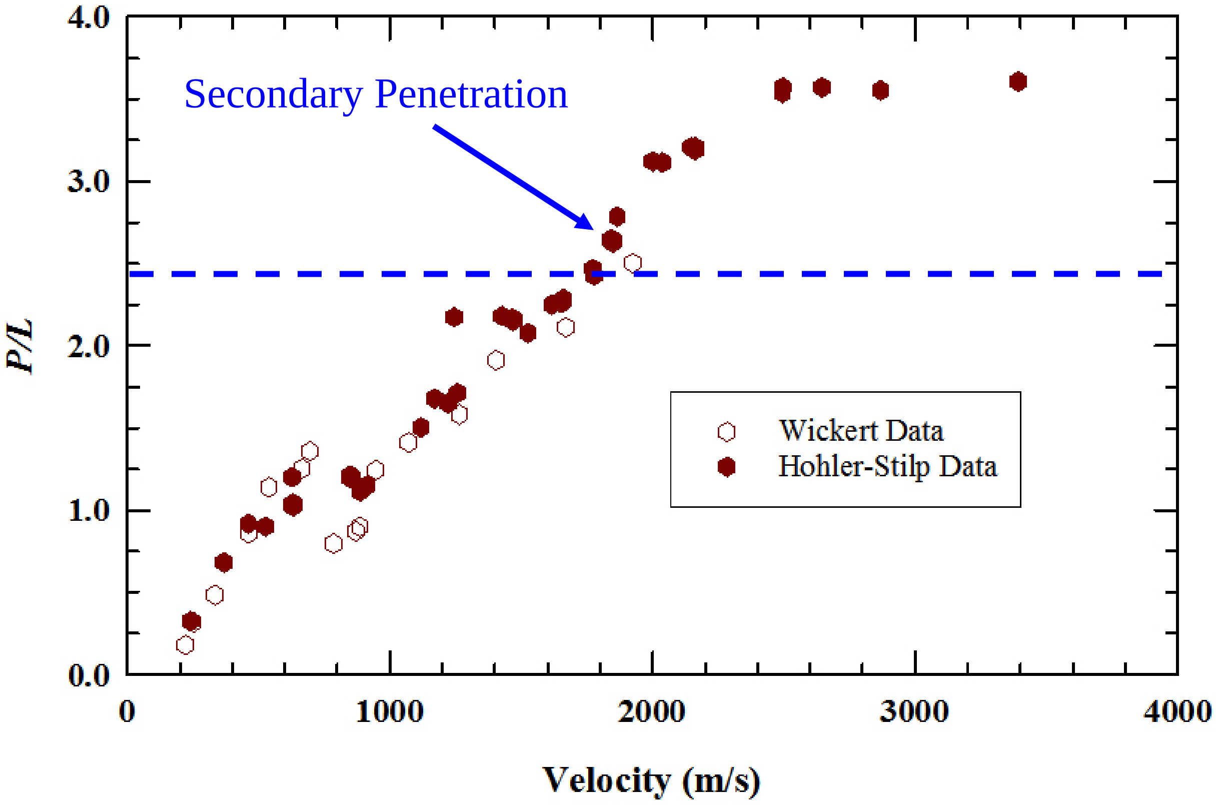

- $u_{debris} = (2u\text{-}v)$
- $\rho_p << \rho_t$, $u \approx 0$, $u_{debris} \sim -v$
- $\rho_p = \rho_t$, $u_{debris} = 0$
- $\rho_p > \rho_t$, u_{debris} *into target*
- $\frac{1}{2}\rho_p u_{debris}^2 > R_t$ *additional penetration*

Rigid-Body Penetration

- *Can obtain deep penetration when projectile remains rigid, particularly compared to eroding penetration*
- *Diameter of penetration channel is the diameter of the projectile*
- *At sufficiently high velocities, projectile begins to deform and then begins to erode*
  - *Deformation occurs over a relatively small range of impact velocities*
  - *Projectile material strength and ductility important near/at transition velocity*
  - *Nose shape is important*
- *Projectile typically does not want to penetrate straight*

Dynamic Plasticity

Plastic Deformation Flow Fields

Ravid-Bodner Model

- *Multi-stage penetration/perforation model by a rigid projectile*
  - *Penetration*
  - *Bulge formation*
  - *Bulge advancement*
  - *Plug formation and exit*
  - *Projectile exit*

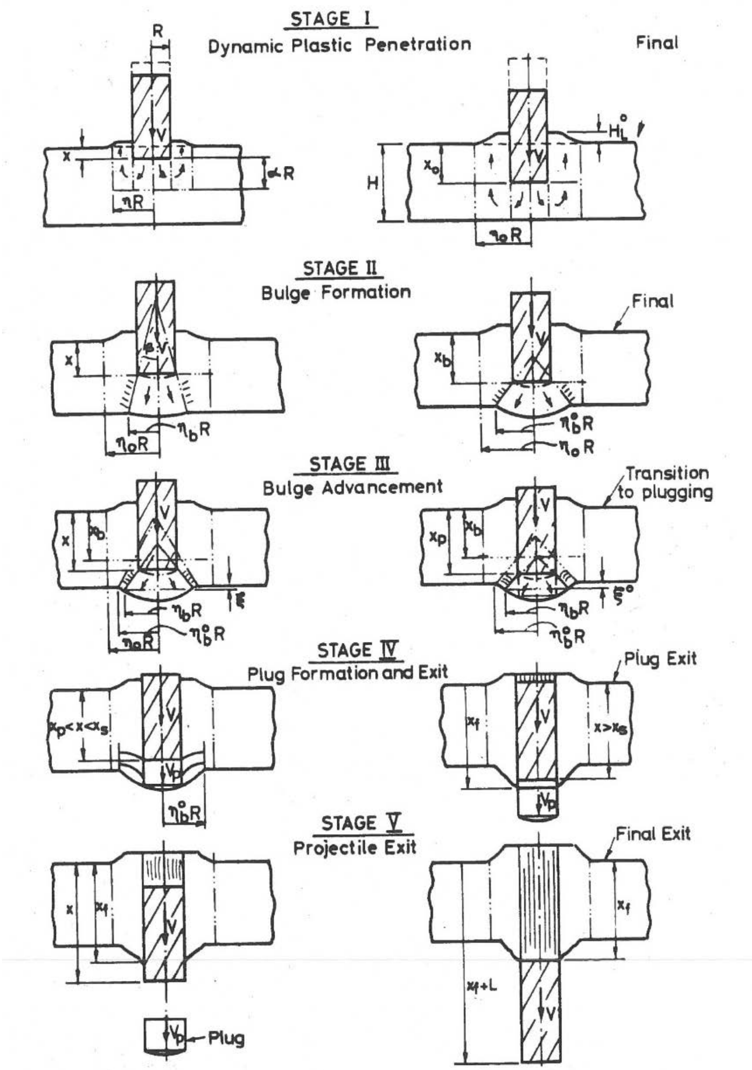

M. Ravid and S. R. Bodner, Dynamic perforation of viscoplastic plates by rigid projectiles," *Int. J. Engng. Sci.*, **21**(6): 577-591, 1983.

Ravid-Bodner Model

- *Established plastic flow fields within the target*
  - *Specified velocity distributions subject to compatibility and continuity conditions*
  - *Computed plastic work rates (including strain-rate effects)*
- *Solved for the radial and axial extent of the plastic zone fields (ηR and αR, where R is the projectile radius)*
- *Deceleration of projectile computed from an energy rate balance*

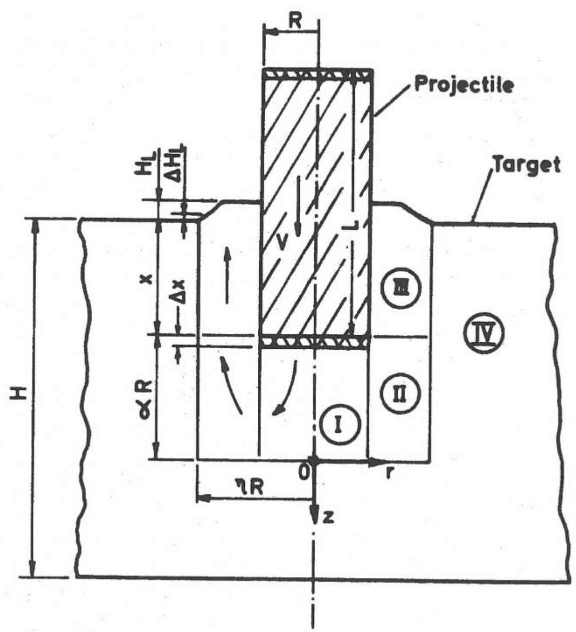

M. Ravid and S. R. Bodner, Dynamic perforation of viscoplastic plates by rigid projectiles," *Int. J. Engng. Sci.*, **21**(6): 577-591, 1983.

Ravid-Bodner Model

- When plastic zone reaches rear of target, bulging begins
- At some point, the bulge no longer expands radially, and instead, the bulge advances in direction of penetration
- When a failure criterion is met (variety of failure modes), target material fails and the plug is ejected
- Projectile exits the target

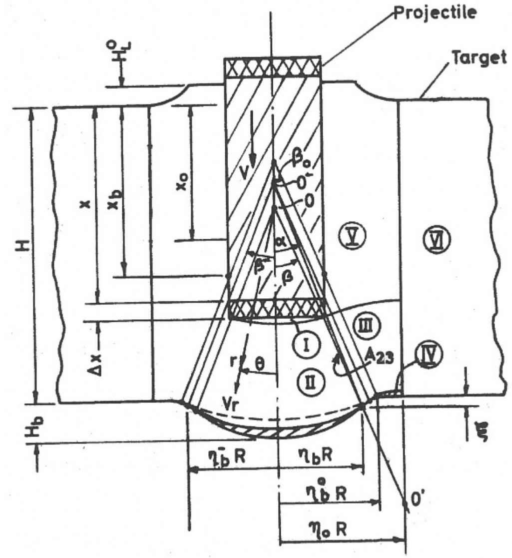

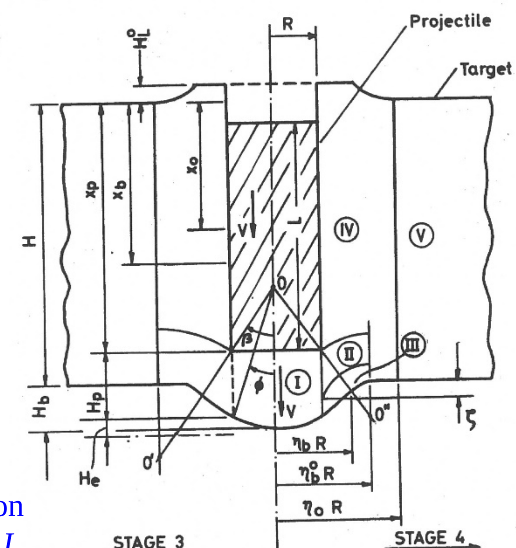

M. Ravid and S. R. Bodner, Dynamic perforation of viscoplastic plates by rigid projectiles," *Int. J. Engng. Sci.*, **21**(6): 577-591, 1983.

Ravid-Bodner Model

- Steel plate: 12-mm thick
- 7.62-mm AP bullet
- Impact velocity: 855 m/s
- Exit velocity: 300-390 m/s
- Model
  - Plug velocity: 424 m/s
  - Bullet velocity: 364 m/s

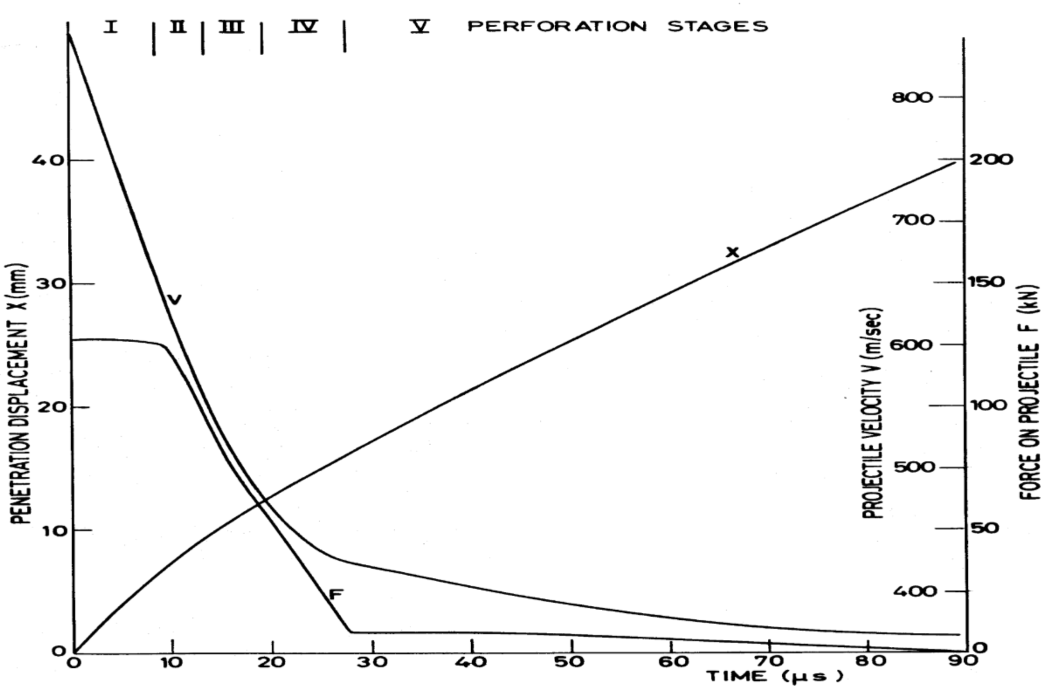

M. Ravid and S. R. Bodner, Dynamic perforation of viscoplastic plates by rigid projectiles," *Int. J. Engng. Sci.*, **21**(6): 577-591, 1983.

CEA Consulting

Walker-Anderson Model

$$\rho_p \int_{z_p}^{z_1} \frac{\partial u_z}{\partial t} dz + \rho_t \int_{z_i}^{+\infty} \frac{\partial u_z}{\partial t} dz + \frac{1}{2}\rho_p u_z^2 \Big|_{z_p}^{z_i} + \frac{1}{2}\rho_t u_z^2 \Big|_{z_i}^{+\infty} - \sigma_{zz}\Big|_{z_p}^{+\infty} - 2\int_{z_p}^{+\infty} \frac{\partial \sigma_{xz}}{\partial x} dz = 0$$

$\longrightarrow$ **z**

$$\rho_p \int_{z_p}^{z_i} \frac{\partial u_z}{\partial t} dz + \rho_t \int_{z_i}^{+\infty} \frac{\partial u_z}{\partial t} dz + \frac{1}{2}\rho_p \left(u^2 - \mathrm{v}^2\right) - \frac{1}{2}\rho_t u^2 - \int_{z_p}^{+\infty} \frac{\partial \sigma_{xz}}{\partial x} dz = 0$$

- *Integrate momentum equation along the centerline over the projectile and target*
- *Three assumptions*
  - *Velocity profile along the centerline in projectile and target specified*
  - *The rear of the projectile is decelerated by elastic waves*
  - *Shear behavior of the target material is specified*

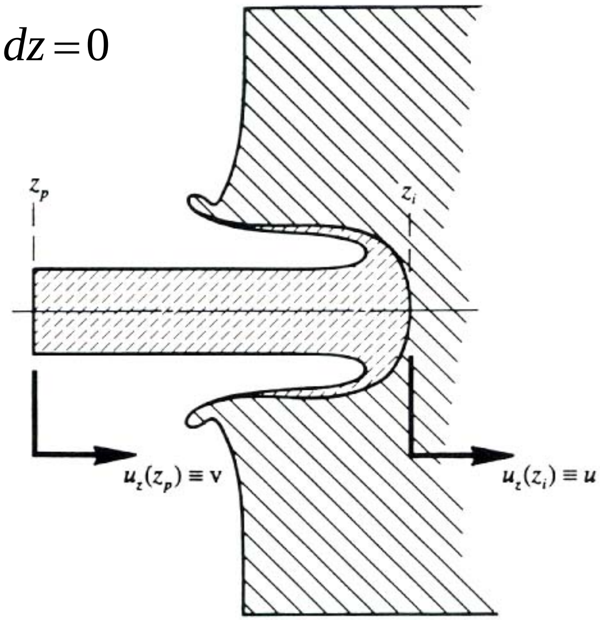

J. D. Walker and C. E. Anderson, Jr., “A time-dependent model for long-rod penetration,” *Int. J. Impact Engng.*, **16**(1): 19-48, 1995.

CEA Consulting

Velocity Profile Along the Centerline

Projectile

$$u_z(z)=\begin{cases} u-\dfrac{\mathrm{v}-u}{s}(z-z_i) & (z_i-s)\le z<z_i \\ \mathrm{v} & z_p\le z<(z_i-s) \end{cases}$$

Target

$$u_z(z)=\begin{cases} \dfrac{u}{\alpha^2-1}\left[\left(\dfrac{\alpha R}{r(z)}\right)^2-1\right] & R\le r(z)<\alpha R \\ 0 & r(z)\ge \alpha R \end{cases}$$

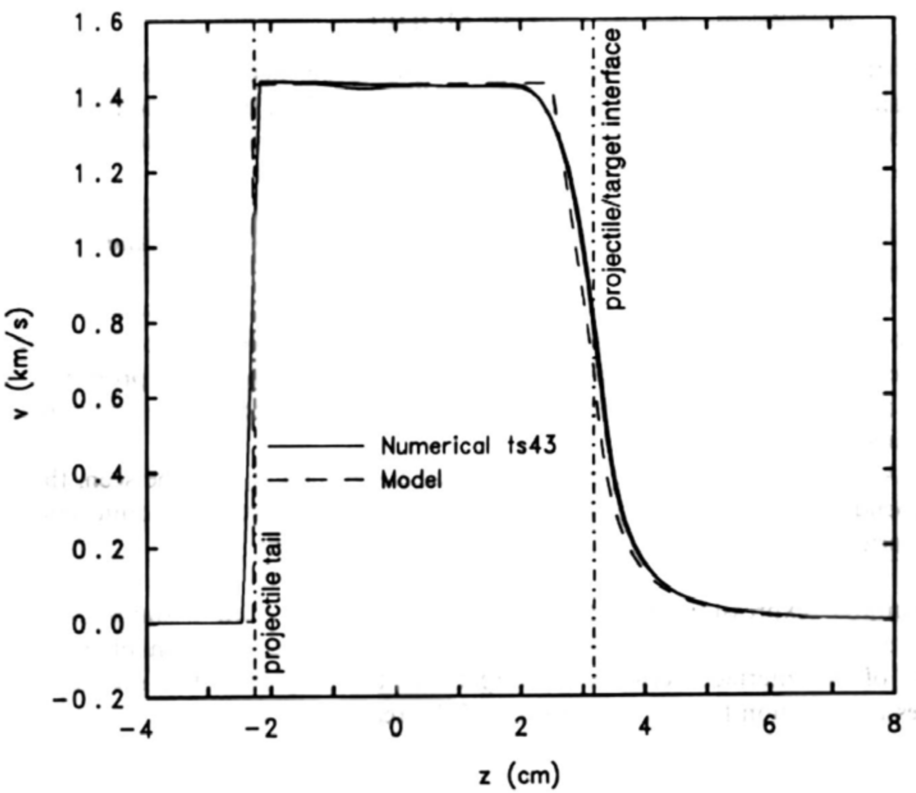

Velocity field derived from a vector potential

Extent of flow field in target = αR
R = crater radius

J. D. Walker and C. E. Anderson, Jr., “A time-dependent model for long-rod penetration,” *Int. J. Impact Engng*., **16**(1): 19-48, 1995.

Projectile Deceleration

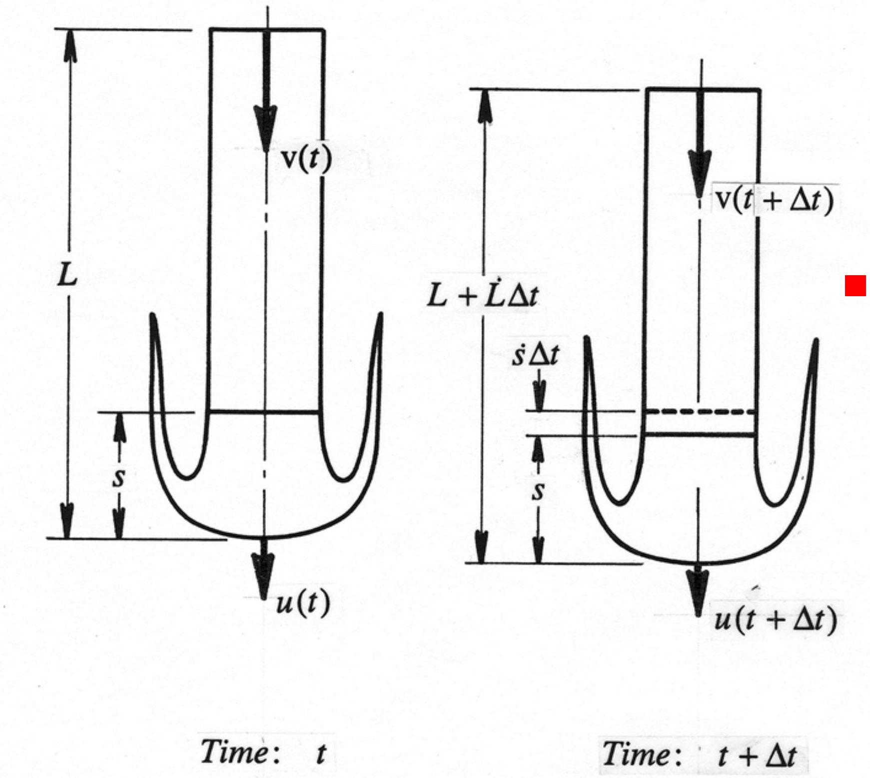

J. D. Walker and C. E. Anderson, Jr., "A time-dependent model for long-rod penetration," *Int. J. Impact Engng.*, **16**(1): 19-48, 1995.

- *Front end and back end of projectile have different velocities - thus projectile erodes during penetration event.*

$$\dot{L} = -(\mathrm{v} - u)$$

- *Back of projectile is decelerated by elastic waves that travel up and down the length of the projectile, reflecting off the free surface at the back and at the elastic-plastic interface at the front.*

$$\Delta \mathrm{v} = -2c\frac{\sigma_p}{E_p}$$

$$\dot{\mathrm{v}} = -\frac{\sigma_p}{\rho_p (L - s)}\left\{1 + \frac{\mathrm{v} - u}{c} + \frac{\dot{s}}{c}\right\}$$

Shear Behavior of Target

$$s_{ij} = \lambda D_{ij}$$

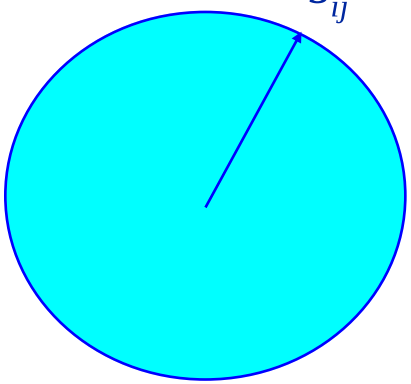

$$Y_t = \sqrt{3J_2}$$

- *Shear stress is directly proportional to rate of deformation (rigid plasticity)* $s_{ij} = \lambda D_{ij}$
- *A von Mises yield surface is assumed*

$$s_{ij}s_{ij} = 2J_2 = \frac{2}{3}Y_t^2 \quad or \quad Y_t = \sqrt{3J_2}$$

$$s_{ij} = \lambda D_{ij} = \frac{\sqrt{\frac{2}{3}}Y_t}{\sqrt{D_{ij}D_{ij}}}D_{ij}$$

- *Assumed target flow field gives*

$$\alpha = \frac{Extent\,of\,Plastic\,Zone}{Crater\,Radius}$$

$$\int_R^{\alpha R} \left.\frac{\partial s_{xz}}{\partial x}\right|_{x=0} dz = -\frac{7Y_t}{6}\ln(\alpha)$$

J. D. Walker and C. E. Anderson, Jr., “A time-dependent model for long-rod penetration,” *Int. J. Impact Engng*., **16**(1): 19-48, 1995.

Walker-Anderson Model

$$\rho_p \dot{\mathrm{v}}(L-s)+\dot{u}\left\{\rho_p s+\rho_t R\frac{\alpha-1}{\alpha+1}\right\}+\rho_p\frac{d}{dt}\left(\frac{\mathrm{v}-u}{s}\right)\frac{s^2}{2}+\rho_t\dot{\alpha}\frac{2Ru}{(\alpha+1)^2}$$

$$=\frac{1}{2}\rho_p(\mathrm{v}-u)^2-\left\{\frac{1}{2}\rho_t u^2+\frac{7}{3}Y_t\ln\alpha\right\}$$

(Centerline momentum balance)

$$\dot{\mathrm{v}}=-\frac{\sigma_p}{\rho_p(L-s)}\left\{1+\frac{\mathrm{v}-u}{c}+\frac{\dot{s}}{c}\right\}$$

(Projectile rear deceleration)

$$\dot{L}=-(\mathrm{v}-u)$$

(Erosion)

J. D. Walker and C. E. Anderson, Jr., "A time-dependent model for long-rod penetration," *Int. J. Impact Engng*., **16**(1): 19-48, 1995.

Target Resistance

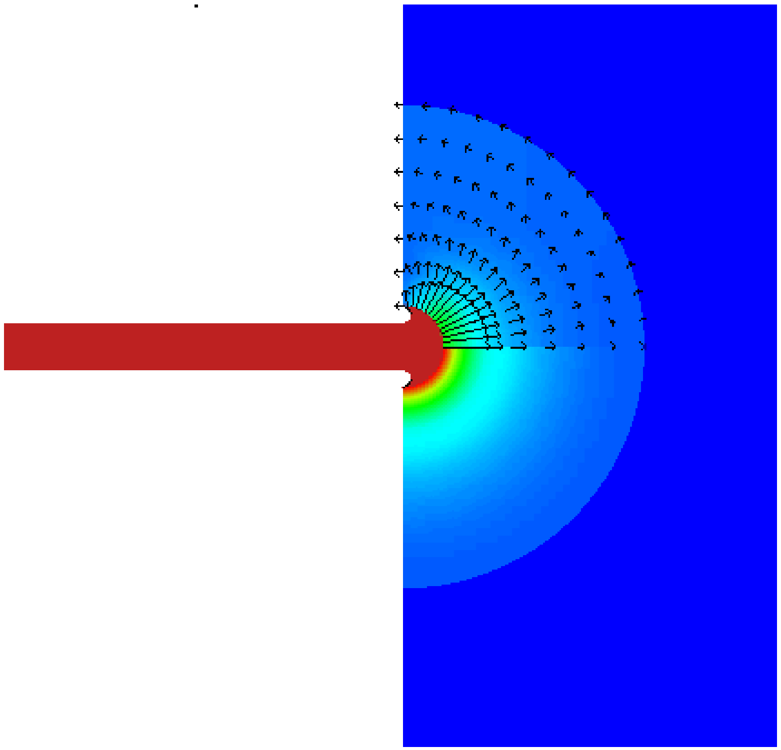

- *Ignoring transient terms, the target resistance is*

$$target\ resistance \sim -\left\{\frac{1}{2}\rho_t u^2 + \frac{7Y_t}{3}\ln(\alpha)\right\}$$

the first term is due to inertial terms, moving target material out of the way, and the second term is due to plastic flow in the target.

J. D. Walker and C. E. Anderson, Jr., "A time-dependent model for long-rod penetration," *Int. J. Impact Engng.*, **16**(1): 19-48, 1995.

CEA Consulting

Estimating the Extent of Plastic Flow

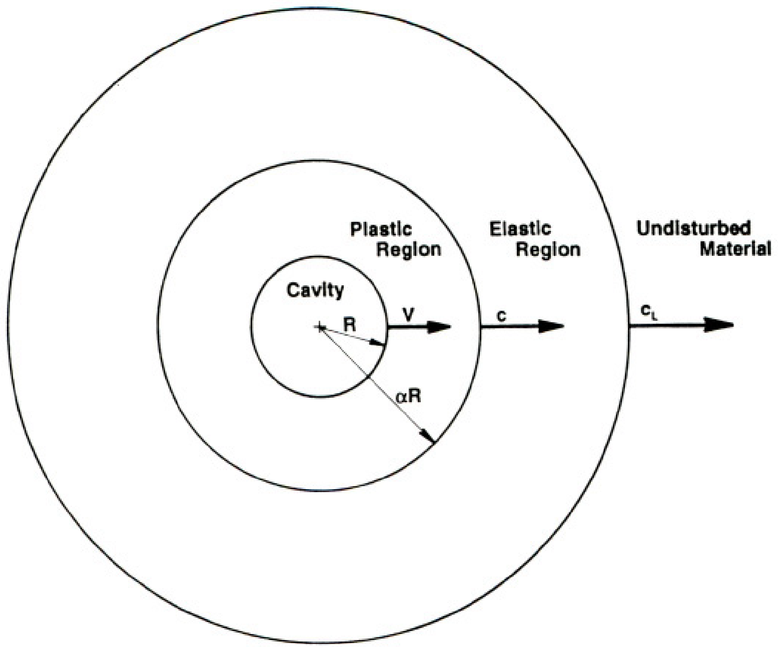

2-D Cylindrical Cavity Expansion

S. Chocron, C. E. Anderson, Jr., and J. D. Walker, "Long-rod penetration: Cylindrical vs. spherical cavity expansion for the extent of plastic flow," *Proc 17th Symp. Ballistics*, 1998.

- *Cylindrical compressible cavity expansion*
- *Two regions identified, separated by three boundaries with appropriate B.C.:*
  - *elastic*
  - *elastic-plastic (compressible)*
- *The inner cavity is driven at a constant velocity V*
- *Important approximate assumption: the velocity is assumed continuous between the elastic and elastic-plastic region*
- *Cylindrical cavity expansion considerably more accurate than spherical cavity expansion*

2-D Cylindrical Cavity Expansion

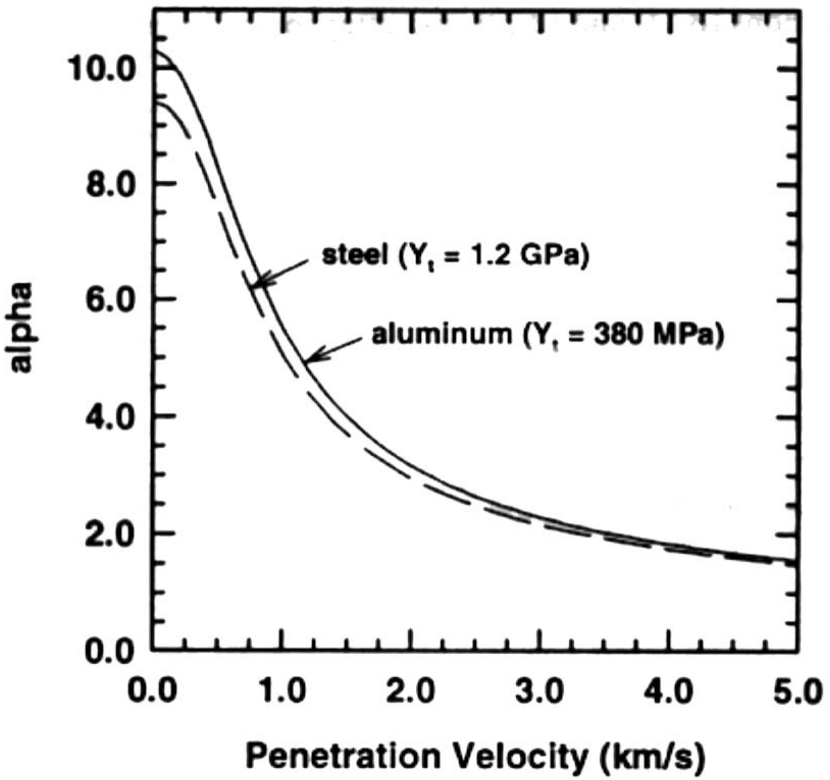

α is a function of impact velocity

- *Interface between elastic-plastic and elastic region moves at a constant velocity c.*
- *The extent of the plastic flow field within the target is defined as*

$$\alpha(u) = c(u)/u$$

- *The cavity expansion provides an expression for this extent:*

$$\left(1+\frac{\rho_t u^2}{Y_t}\right)\sqrt{K_t - \rho_t u^2 \alpha} = \left(1+\frac{\rho_t u^2 \alpha^2}{2G_t}\right)\sqrt{K_t - \rho_t u^2}$$

- *Compressibility of the target is reflected in α.*
- *High pressure stiffness adjustment*

$$K_t \sim K_0\left(1+k\frac{u_p}{c_0}\right)$$

Crater Radius

- *Curve fit based on experimental data: depends on projectile and target material properties and penetration velocity*

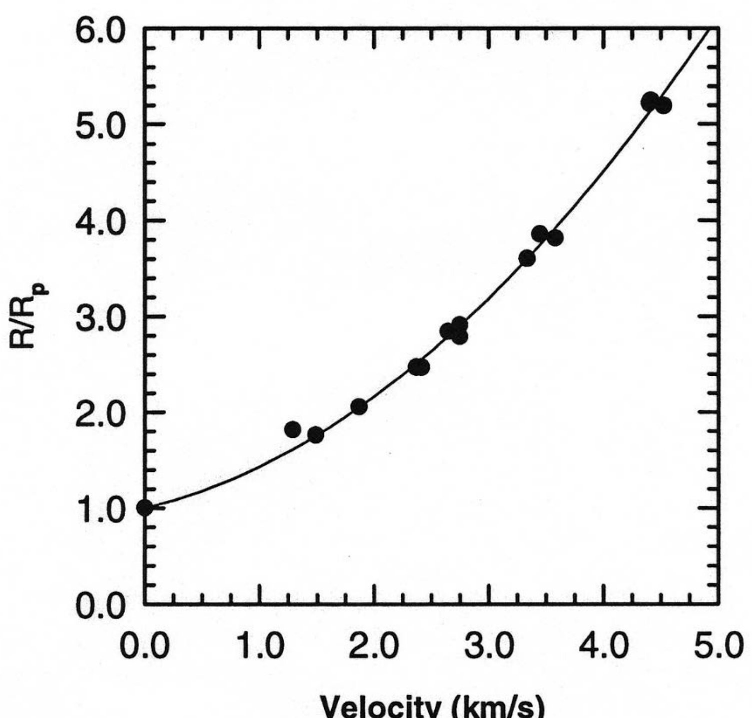

$$R = R_p\left(1 + 0.287\text{v}_o + 0.148\text{v}_o^2\right)$$

$[\text{v}_o] = \text{km/s}$

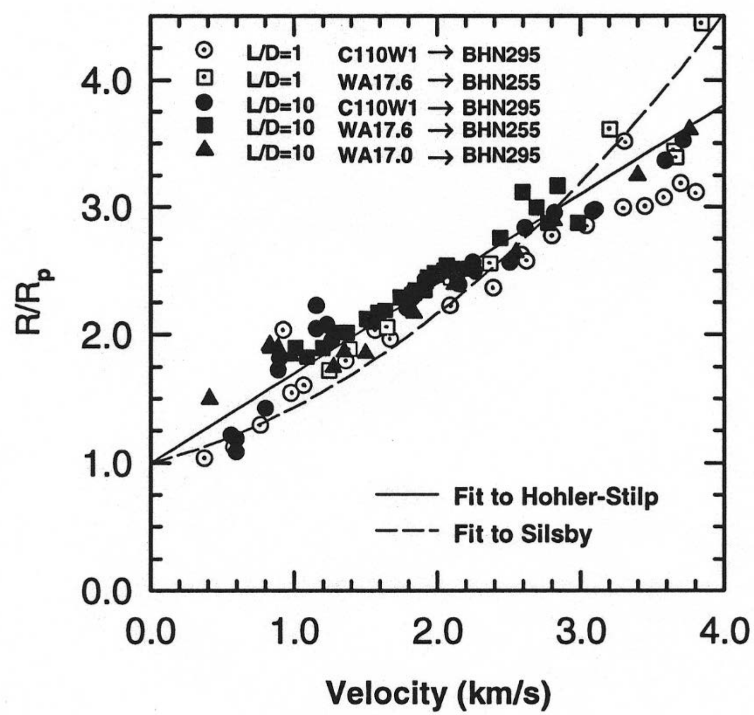

$$R = R_p\left(1 + 0.70\text{v}_o\right)$$

Walker-Anderson Model Results

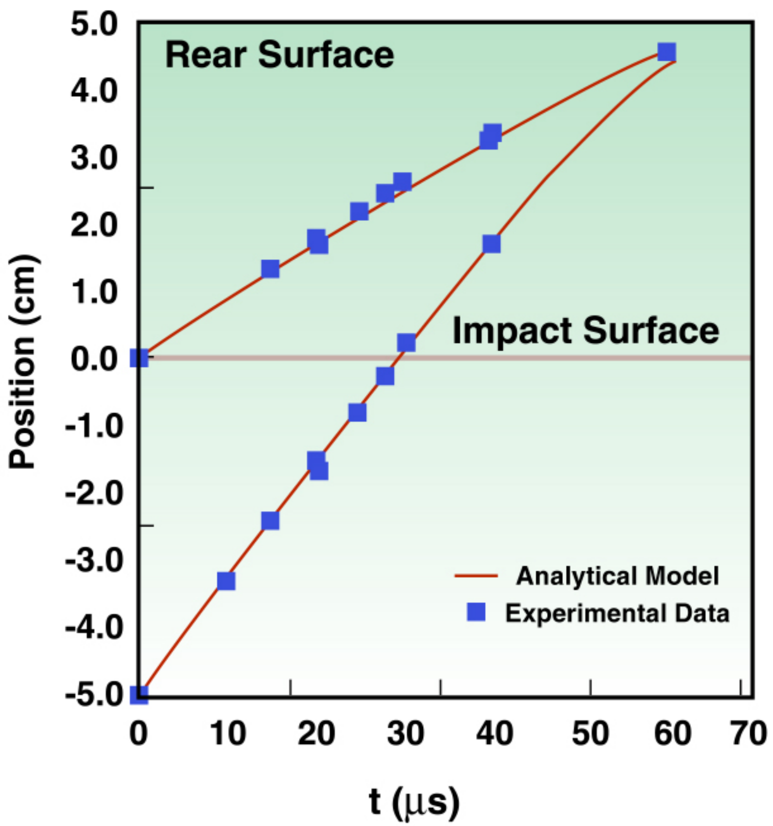

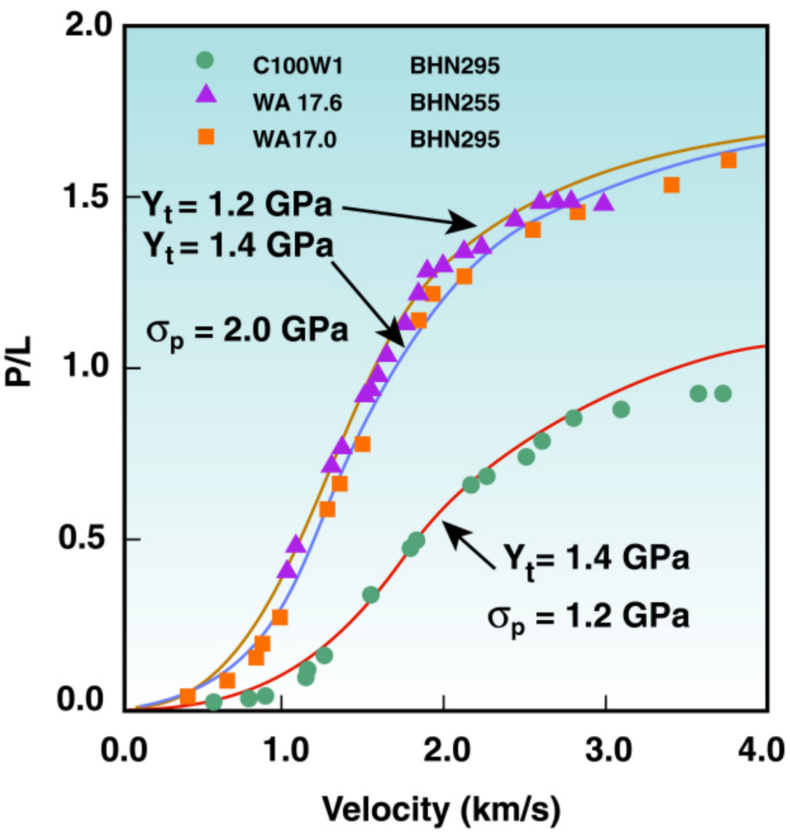

J. D. Walker and C. E. Anderson, Jr., "A time-dependent model for long-rod penetration," *Int. J. Impact Engng*., **16**(1): 19-48, 1995.

Walker-Anderson Model ⇒ Tate Model

$$\rho_p \dot{\mathrm{v}}(L-s) + \dot{u}\left\{\rho_p s + \rho_t R\frac{\alpha-1}{\alpha+1}\right\} + \rho_p \frac{d}{dt}\left(\frac{\mathrm{v}-u}{s}\right)\frac{s^2}{2} + \rho_t \dot{\alpha}\frac{2Ru}{(\alpha+1)^2}$$
$$= \frac{1}{2}\rho_p(\mathrm{v}-u)^2 - \left\{\frac{1}{2}\rho_t u^2 + \frac{7}{3}Y_t \ln\alpha\right\}$$

- *In the limit where the three dimensional terms are removed, the Walker-Anderson penetration model reduces to the Tate model:*
  $R \to 0$ and $s \to 0$

  Also let the Young's modulus in the projectile become large: $c \to \infty$

- *Then* $$-\rho_p \dot{\mathrm{v}} L + \frac{1}{2}\rho_p(\mathrm{v}-u)^2 = \frac{1}{2}\rho_t u^2 + \frac{7Y_t}{3}\ln(\alpha)$$

$$\dot{\mathrm{v}} = -\frac{\sigma_p}{\rho_p L} \qquad \dot{L} = -(\mathrm{v}-u)$$

Tate: $$Y_p = 1.7\sigma_p$$
$$R_t = \frac{7Y_t}{3}\ln(\alpha)$$

Walker-Anderson Model Results

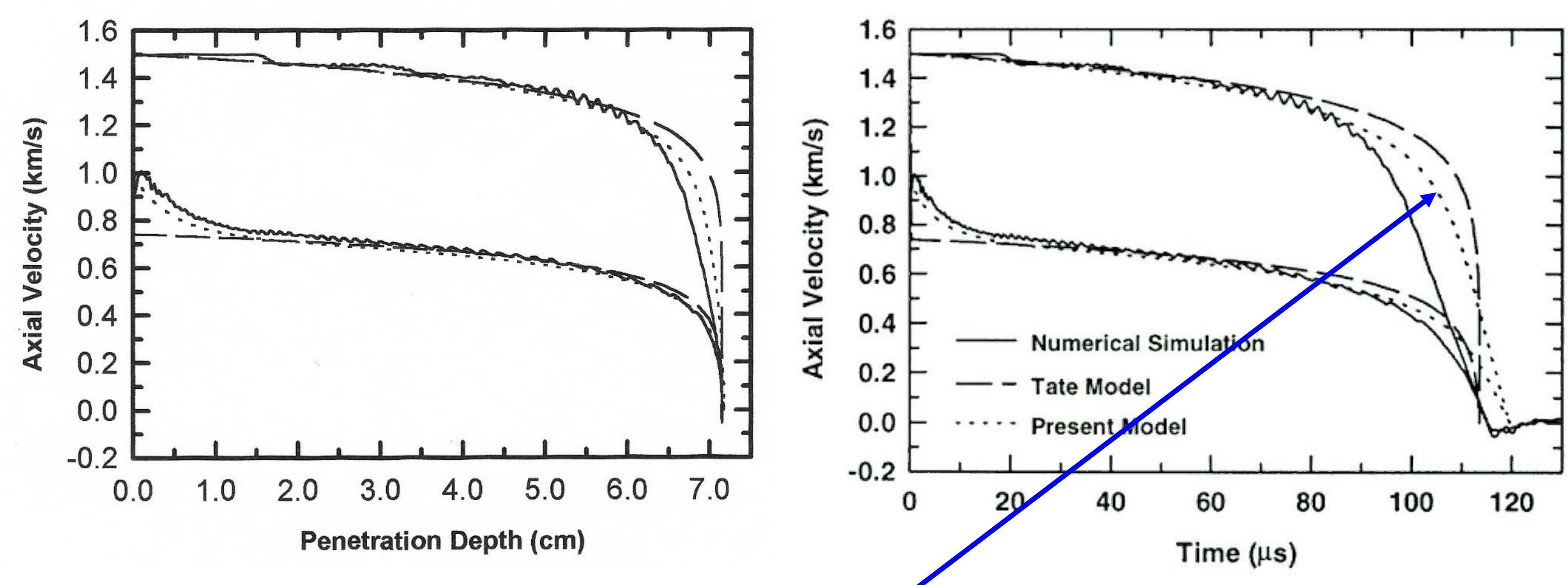

When rod is short (*L/D* ~ 1), tail of rod does not decelerate quite as rapidly as should; tail "sees" the high-pressures at projectile-target interface, not just elastic deceleration waves

Walker-Anderson Model Results

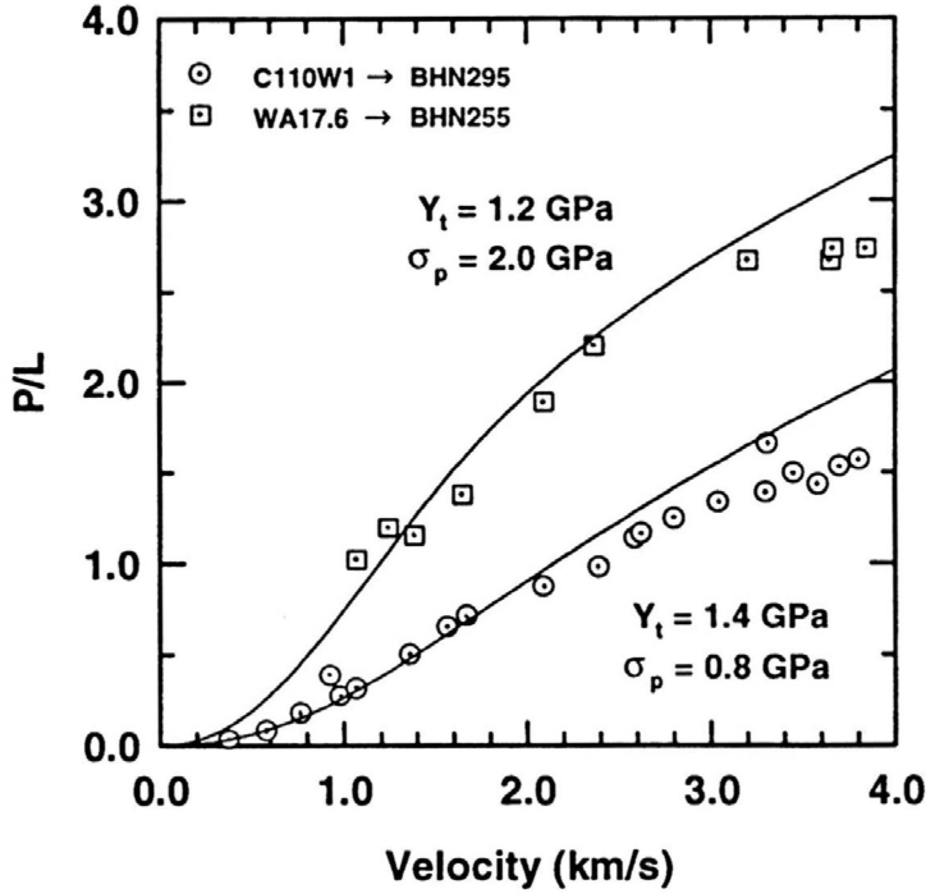

$L/D = 1$

CEA Consulting

Bulging: Shear Flow Field

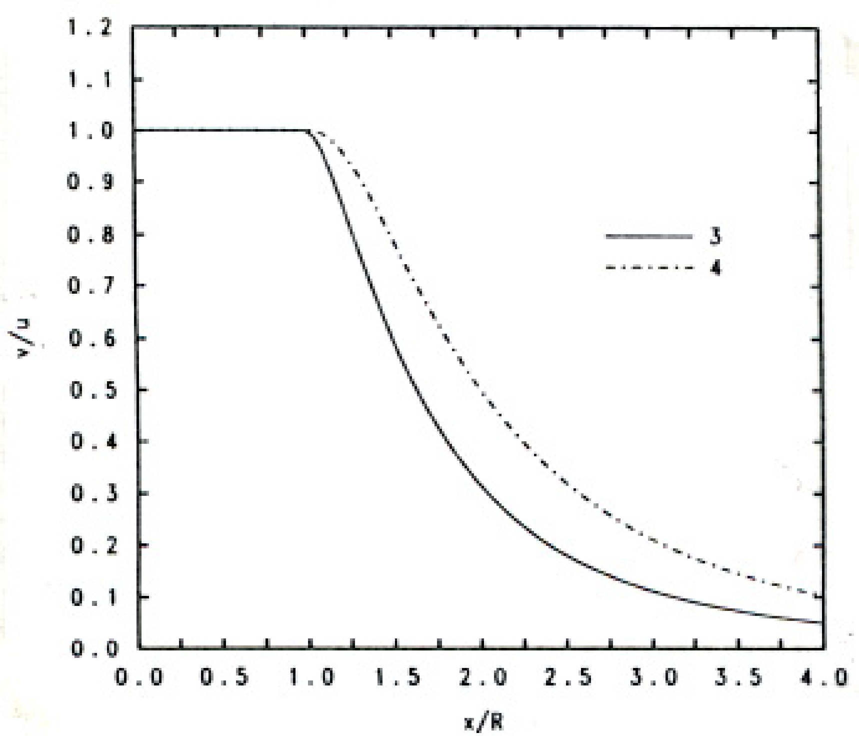

J. D. Walker, "An analytic velocity field for back surface bulging," *Proc. Int. Symp. Ballistics*, **2**: 1239-1246, Technomic Publishing Company, Lancaster, PA, 1999.

- *For back surface bulge, a flow field is achieved through a multiplicative blending of the potentials for hemispherical flow and a shear flow*

$$\vec{A}(r,\theta) = A_{deep}^{\lambda} \, A_{shear}^{1-\lambda} \, \hat{e}_{\phi}$$

- *Velocity is obtained from curl*

$$\vec{\mathrm{v}} = curl\left(A(r,\theta)\hat{e}_{\phi}\right)$$

- *Two shear flows are*

$$(\mathrm{v}_z)_3 = u\left(\frac{R}{x}\right)^3 \left\{4 - 3\frac{R}{x}\right\}$$

$$(\mathrm{v}_z)_4 = u\left(\frac{R}{x}\right)^3 \left\{10 - 15\frac{R}{x} + 6\left(\frac{R}{x}\right)^2\right\}$$

CEA Consulting

Modifications for Back Surface Bulge

- *Amount of material with shear vs. deep penetration potential is based on the hemisphere volume (radius $\tilde{R}$) overlapping the remaining thickness cylinder volume (thickness T)*

$$\lambda = \frac{3}{2}\frac{T}{\tilde{R}} - \frac{1}{2}\left(\frac{T}{\tilde{R}}\right)^3$$

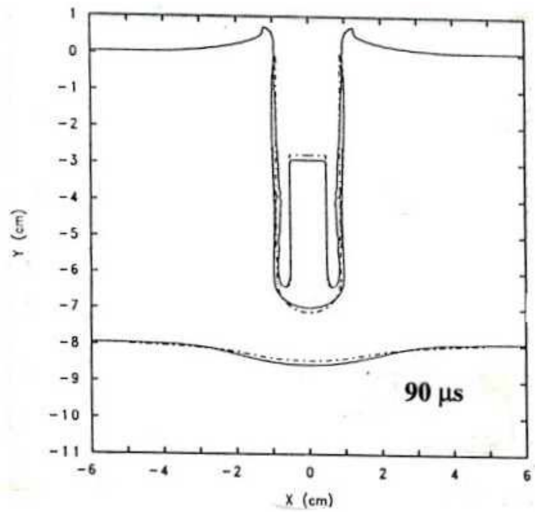

- *Target resistance term is replaced by*

$$-\left\{\frac{1}{2}\rho_t u^2 + \frac{7}{3}Y_t \ln(\alpha)\right\} \quad \text{by} \quad -\frac{1}{2}\rho_t (u - u_{back})^2 + \frac{7}{3}Y_t \ln(\tilde{\alpha})$$

- *Back surface location can be computed since the velocity is known.*

CEA Consulting

Analytical Model Compared to Numerical Simulations

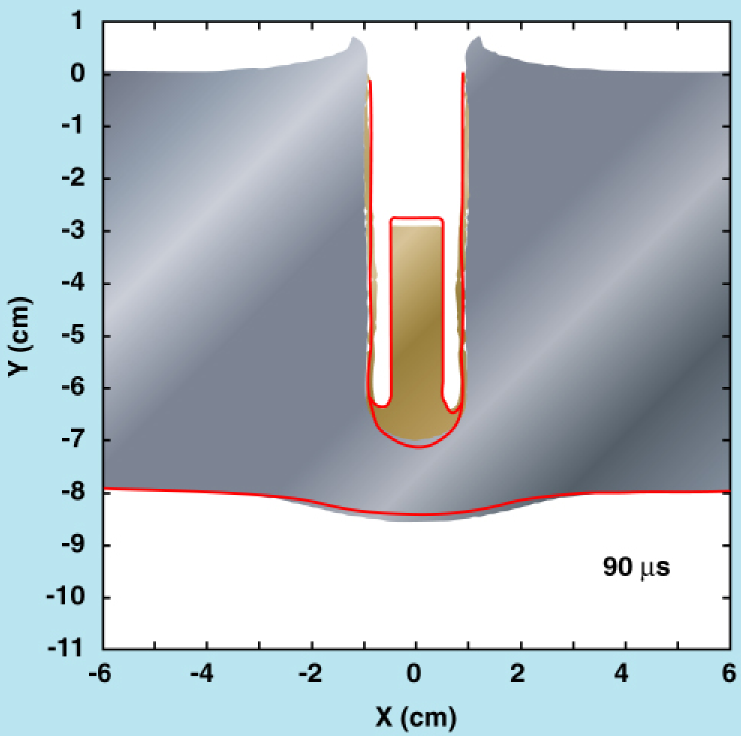

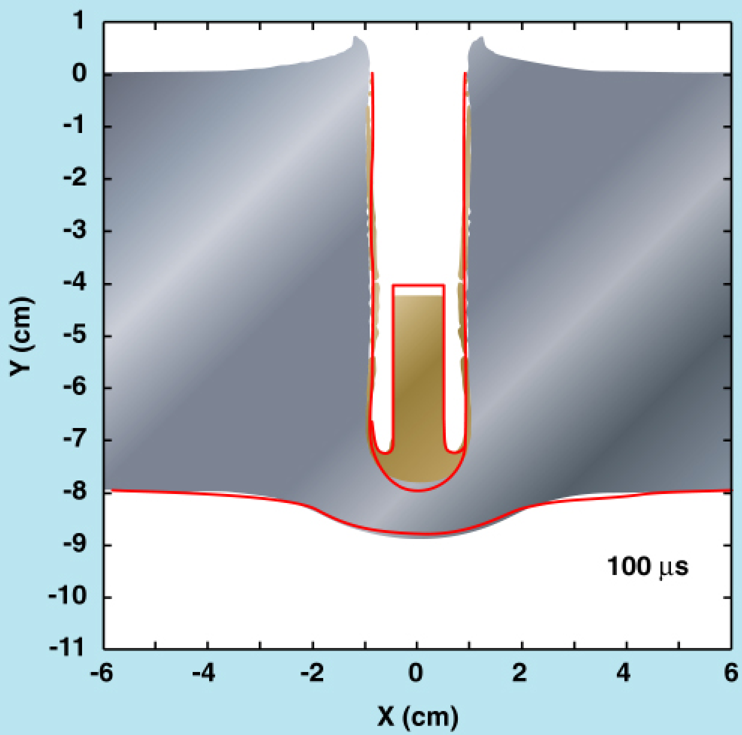

Tungsten into Steel, L/D=10, 1.5 km/s

CEA Consulting

Analytical Model Compared to Numerical Simulations

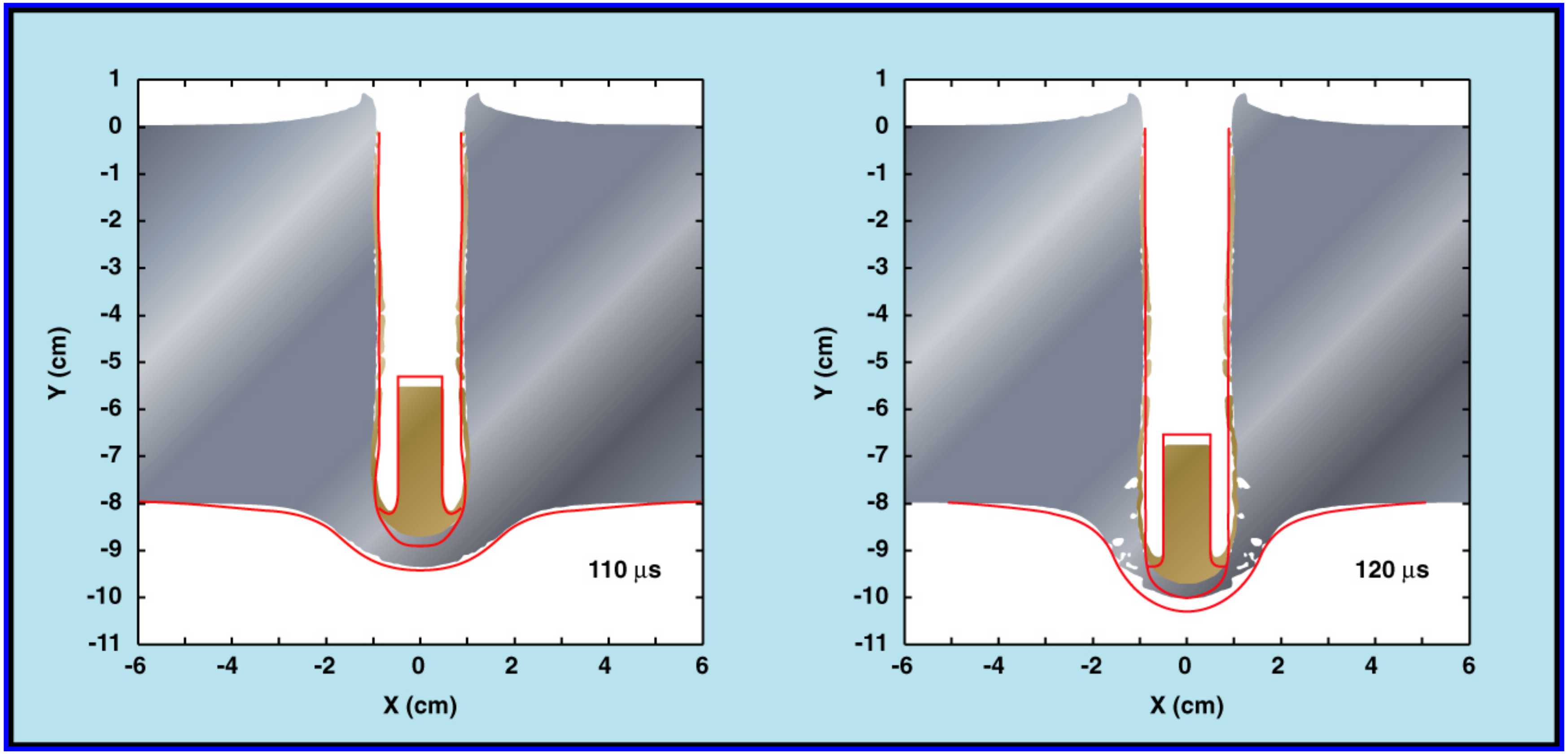

Tungsten into Steel, L/D=10, 1.5 km/s

Back Surface Strains

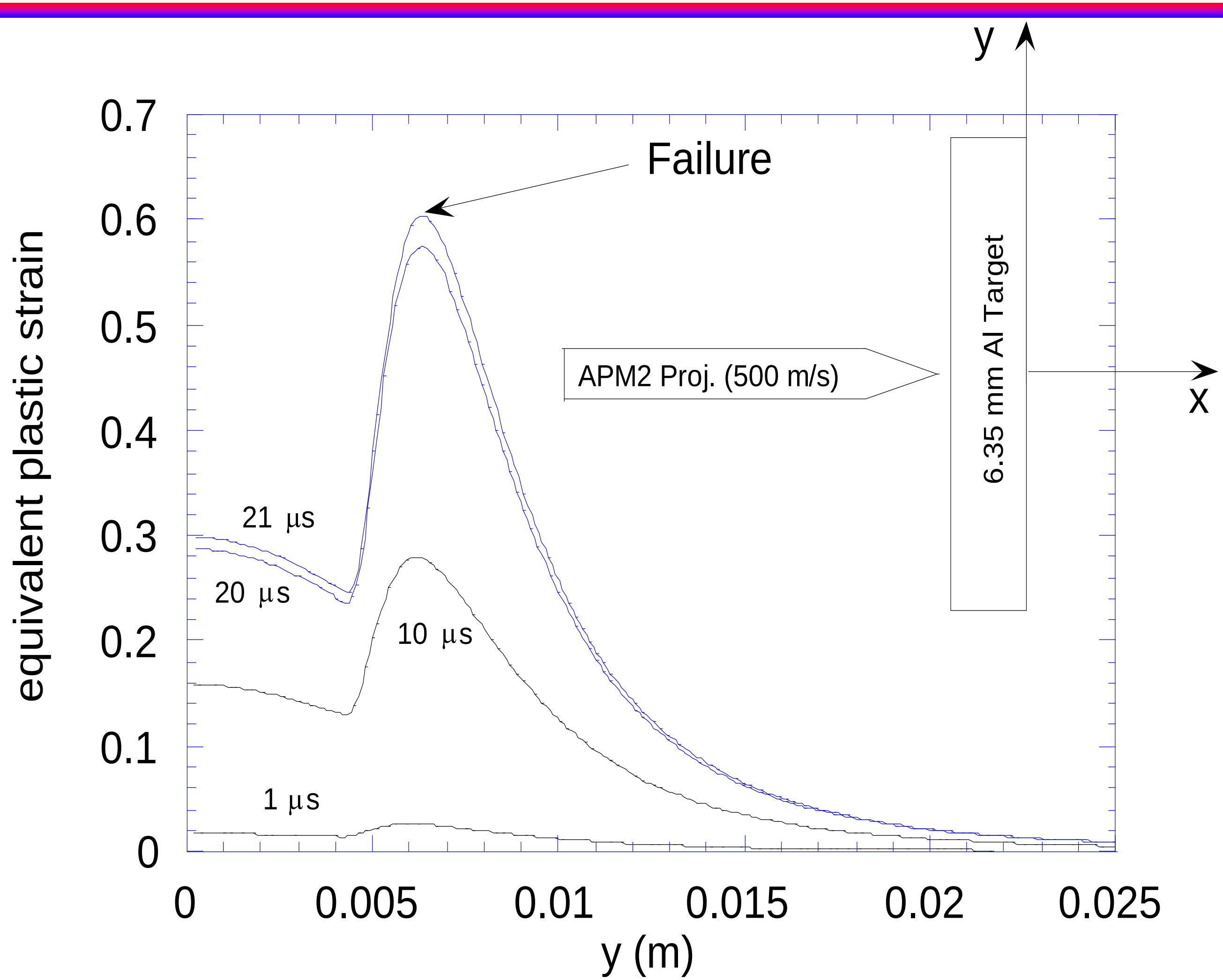

Analytical Model Compared to Experiment

T = 2.90 cm

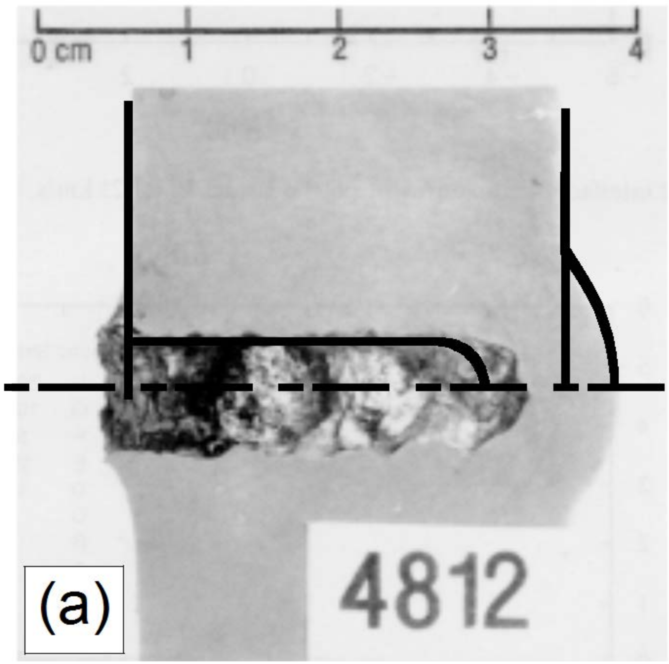

V_o = 1241 m/s

T = 4.95 cm

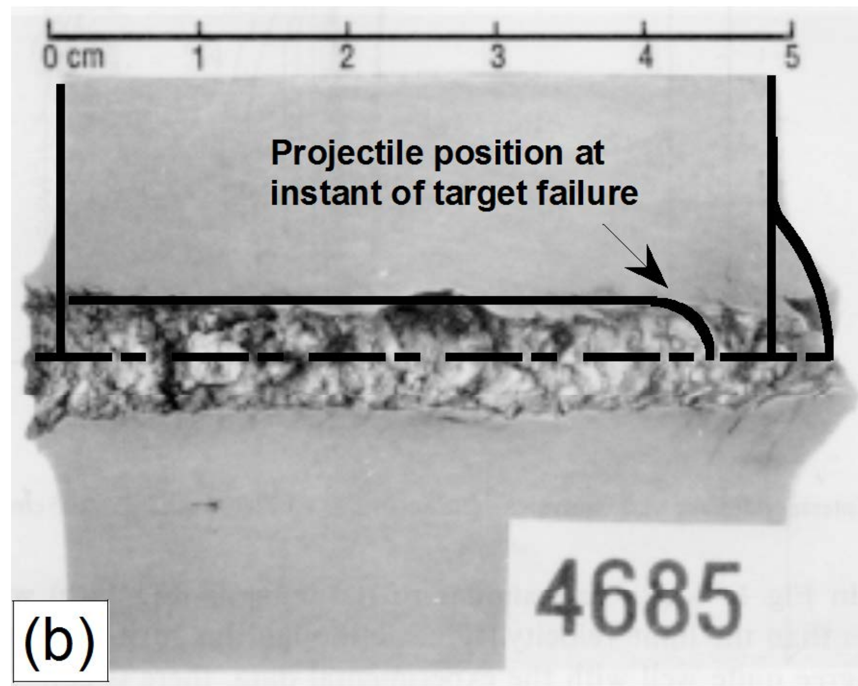

V_o = 1700 m/s

J. D. Walker, "An analytic velocity field for back surface bulging," *Proc. Int. Symp. Ballistics*, **2**: 1239-1246, Technomic Publishing Company, Lancaster, PA, 1999.

Model Results

Similitude Analysis

P/L vs. Impact Velocity

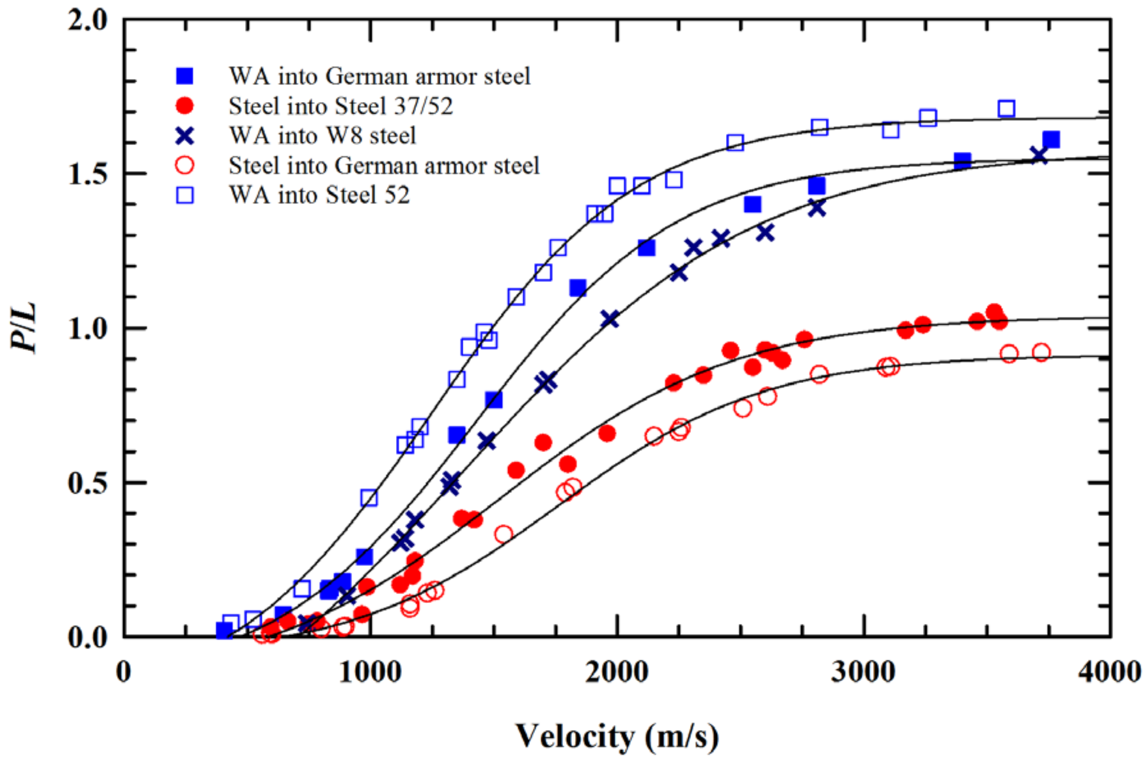

Data from Hohler and Stilp, compiled in: C. E. Anderson, Jr., B. L. Morris, and D. L. Littlefield, “A penetration mechanics database,” SwRI Report 3593/001, San Antonio TX, 1992, prepared for DARPA.

Effective Flow Stress

	ρ (g/cm^3)	σ_t (GPa-)
tungsten alloy	17.0	-
W8 steel	7.85	1.57
St 52 steel	7.85	0.858
St37/52 steel	7.85	1.09
German armor steel	7.85	1.41

- *Non-dimensionalization*
  - $P/\alpha L \quad \alpha = \sqrt{\rho_p/\rho_t}$
  - $\left(\dfrac{\rho_p V^2}{\sigma_t}\right)^{0.2} \alpha^{-0.14}$

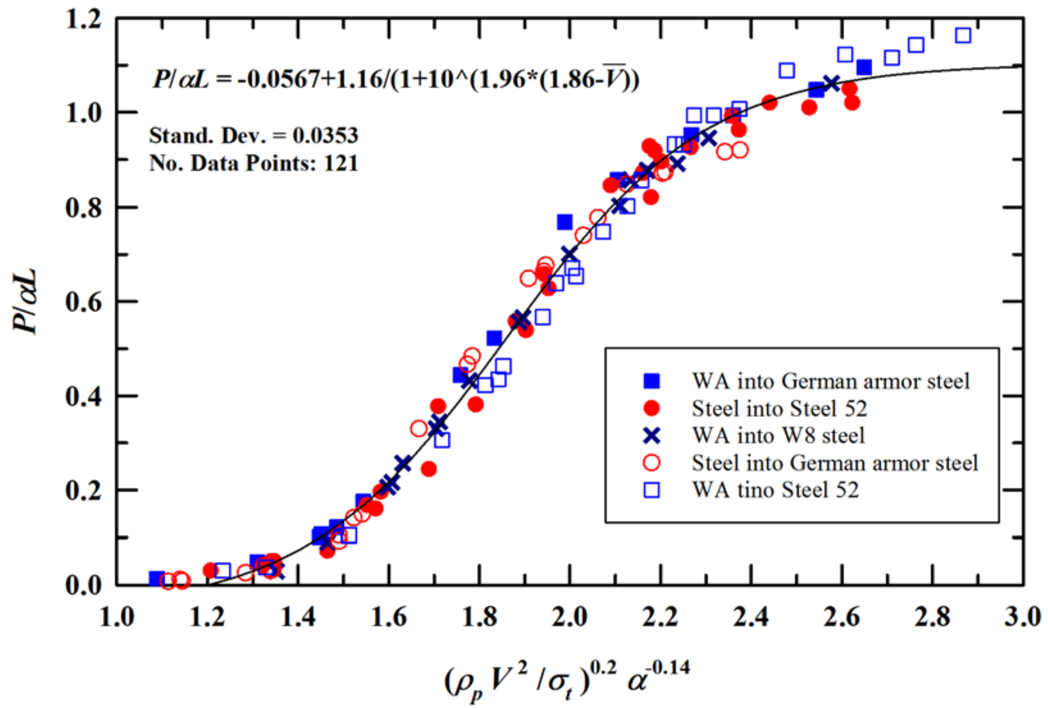

C. E. Anderson, Jr. and J.P. Riegel III, “A penetration model based on experimental data,” *Int. J. Impact Engng.*, **80**: 24-35, 2015.

CEA Consulting

Effective Flow Stress

- Use Walker-Anderson model
  - Parametric study on P/L as a function of velocity for various values of σ_t
  - Select value of σ_t that minimized the root mean square error on P/L

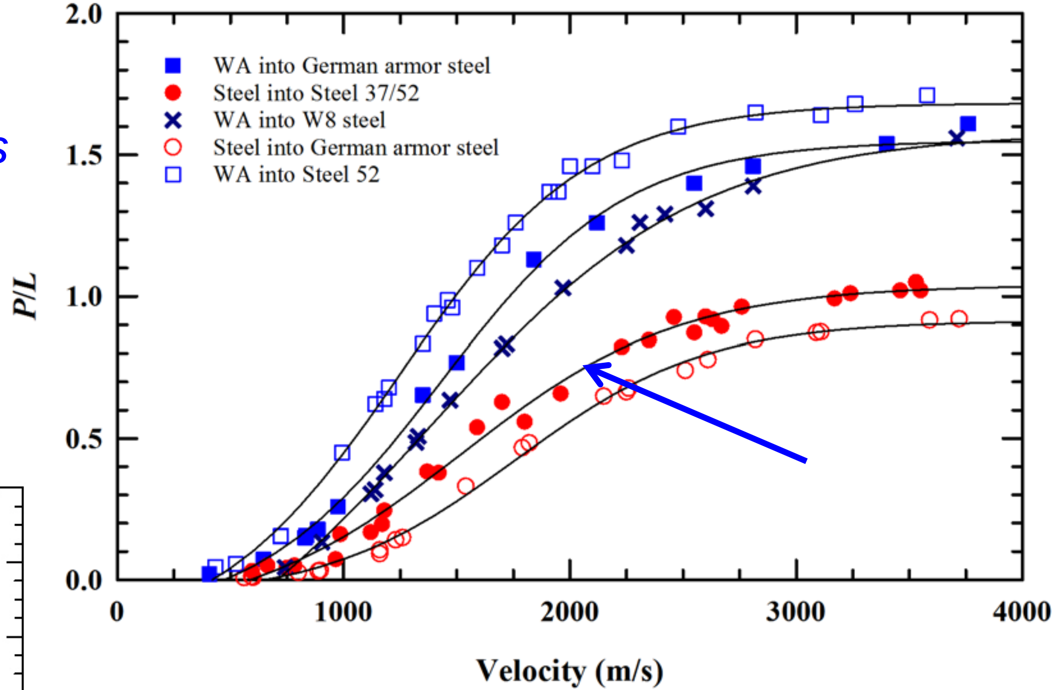

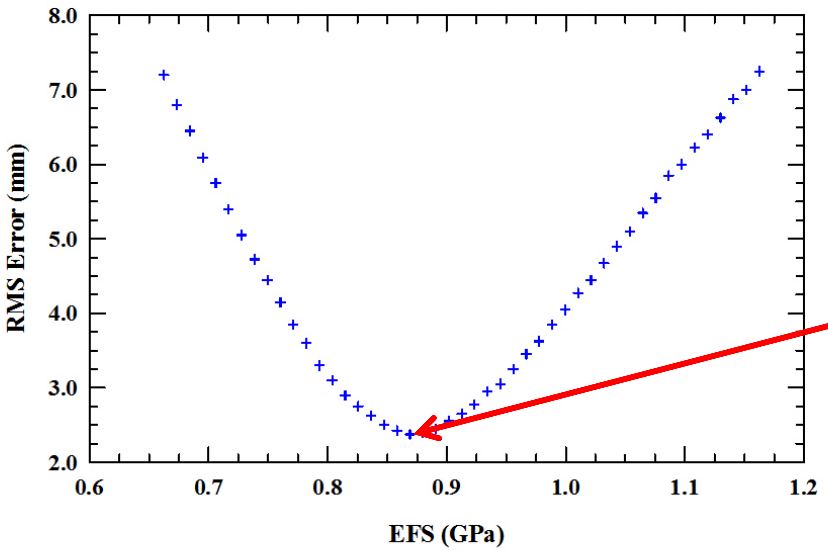

σ_t = 0.858 GPa

$$R_t = \frac{7Y_t}{3}\ln(\alpha)$$

J.P. Riegel, III and C. E. Anderson, Jr., "Target effective flow stress calibrated using the Walker-Anderson penetration model," *Proc. 28th Int. Symp. Ballistics*, DESTech Publications, Inc., **2**: 1242-1253, 2014.

Effective Flow Stress

Do these values of σ_t have any relationship to reality?

	ρ (g/cm^3)	σ_t (GPa-)
tungsten alloy	17.0	-
W8 steel	7.85	1.57
St 52 steel	7.85	0.858
St37/52 steel	7.85	1.09
German armor steel	7.85	1.41

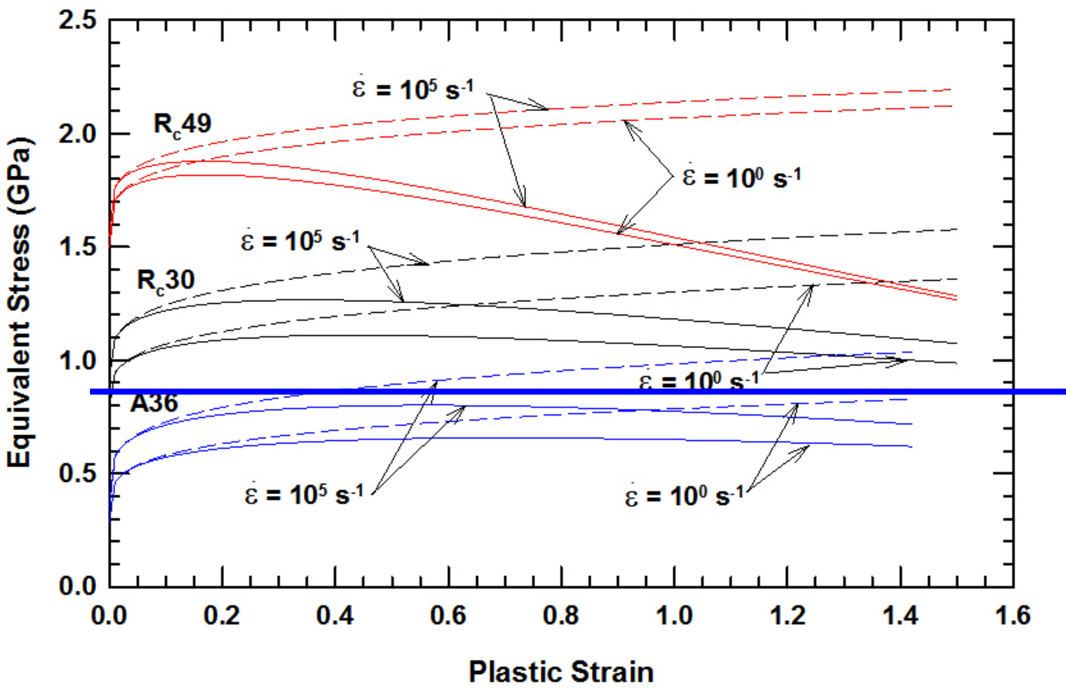

Interpretation: $\sigma_t \equiv Y_t$ is the average flow stress over the volume of the plastic zone including strain-hardening and strain-rate effects

Ceramics & Glasses

Ceramic and Glass Penetration

- Drucker-Prager yield surface

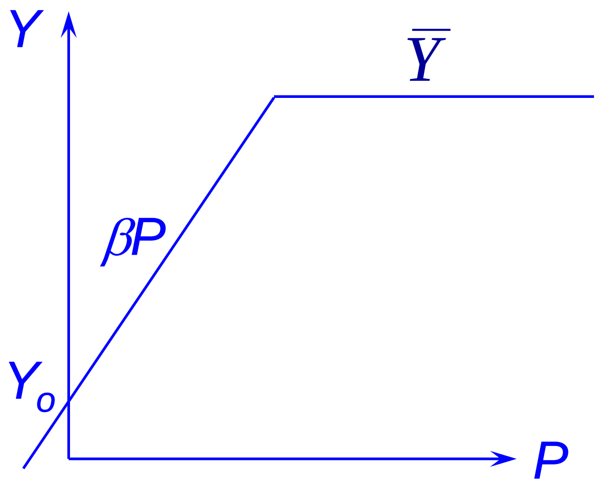

- Requires solving for an interior boundary

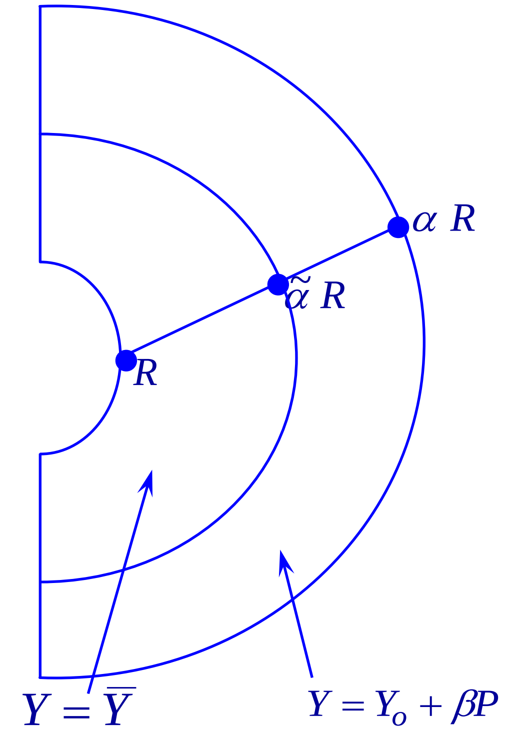

J. D. Walker, “Analytic model for penetration of thick ceramic targets,” *Ceramic Transactions*, **134**: 337-348 (2002)

Modeled Orphal-Franzen Experiments

- *Tungsten long rods into SiC*
- *Assumption: penetrating failed material*
- *Determined Y_o (0.1 GPa), β (2.5), and Y_{cap} (3.7 GPa)*
- *Used same parameters in numerical simulations*

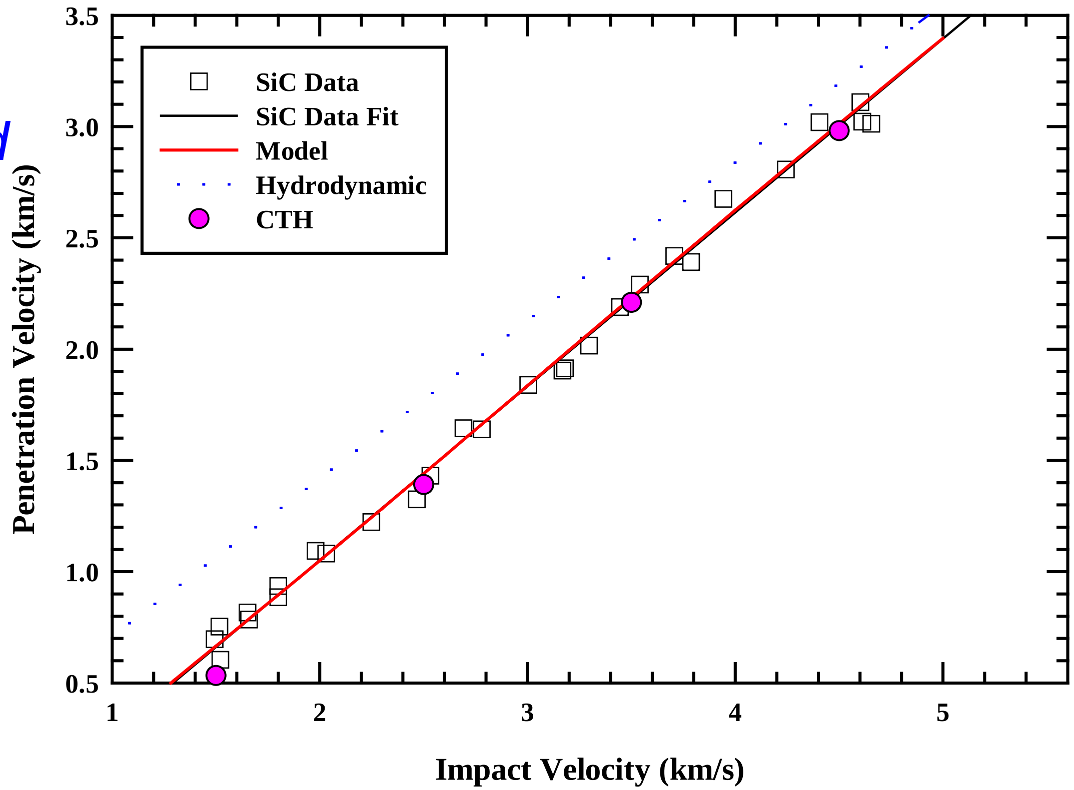

J. D. Walker, "Analytic model for penetration of thick ceramic targets," *Ceramic Transactions*, **134**: 337-348 (2002)

D. L. Orphal and R. R. Franzen, "Penetration of confined silicon carbide targets by tungsten long rods at impact velocities from 1.5 to 4.6 km/s," *Int. J. Impact Engng*., **19**(1): 1-13 (1997).

CEA Consulting

Modeled Orphal-Franzen Experiments

SwRI

- *Tungsten long rods into SiC*
- *Assumption: penetrating failed material*
- *Determined Y_o (0.1 GPa), β (2.5), and Y_{cap} (3.7 GPa)*

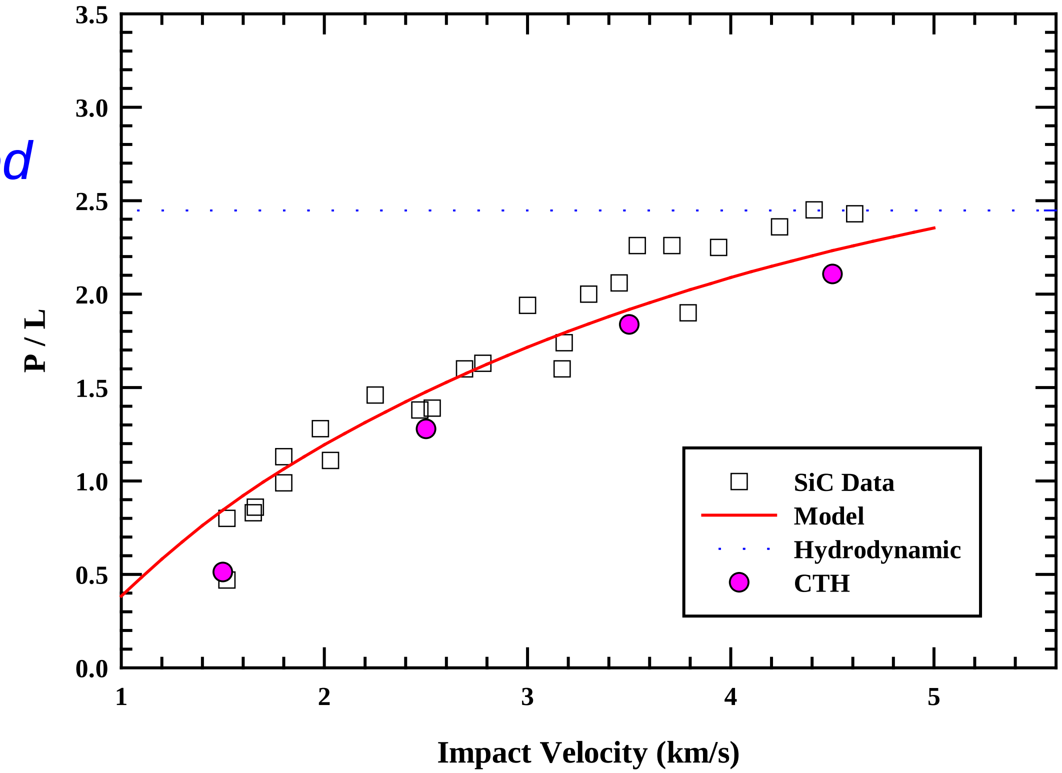

J. D. Walker, "Analytic model for penetration of thick ceramic targets," *Ceramic Transactions*, **134**: 337-348 (2002)

D. L. Orphal and R. R. Franzen, "Penetration of confined silicon carbide targets by tungsten long rods at impact velocities from 1.5 to 4.6 km/s," *Int. J. Impact Engng*., **19**(1): 1-13 (1997).

Failure Front

- *Reverse ballistic experiments of borosilicate glass into a long, gold rod*

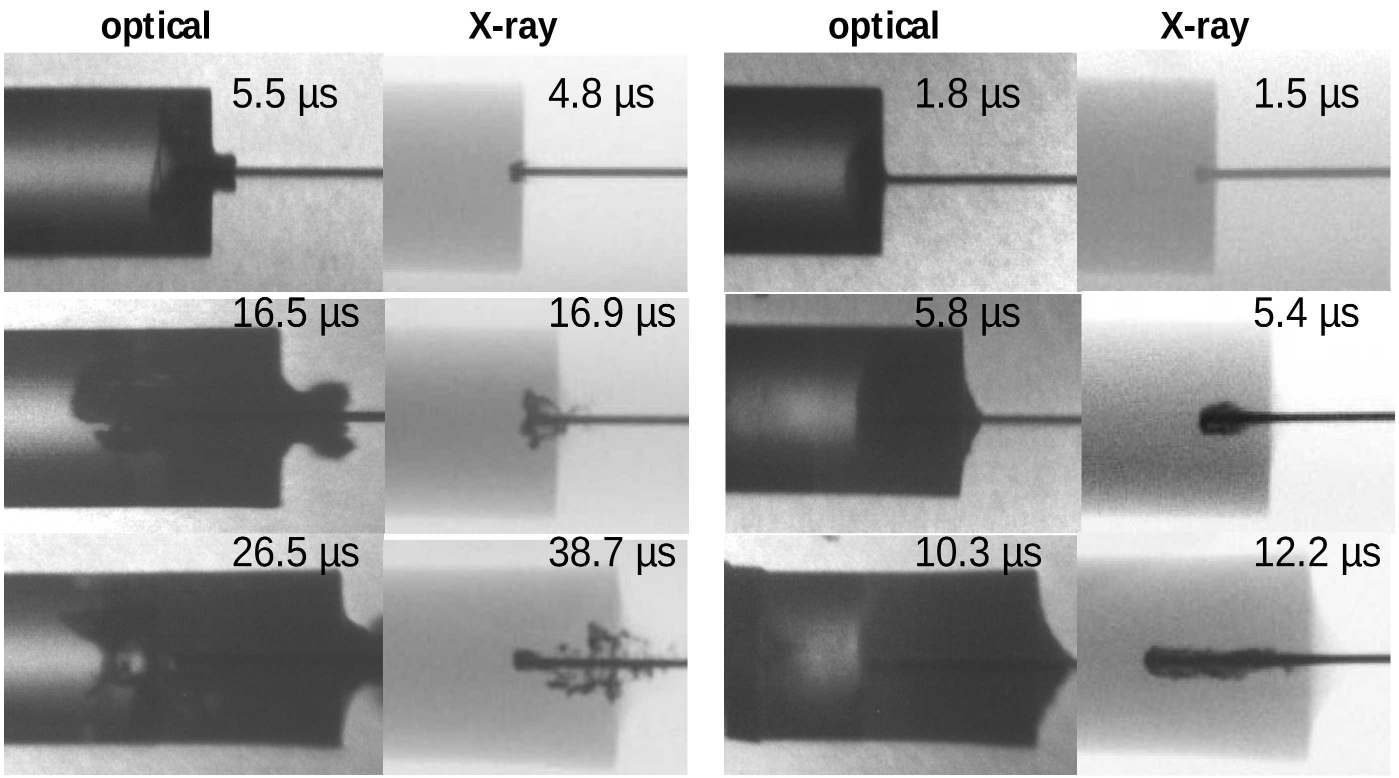

Exp. 10557, v_P = 786 m/s **Exp. 10585, v_P = 2328 m/s**

T. Behner, C. E. Anderson, Jr., D. L. Orphal, V. Hohler, M. Moll, and D. W. Templeton, "Penetration and failure of lead and borosilicate glass against rod impact," *Int. J. Impact Engng*., **35**(6): 447-456 (2008).

CEA Consulting

Position of Failure Front wrt Rod Tip

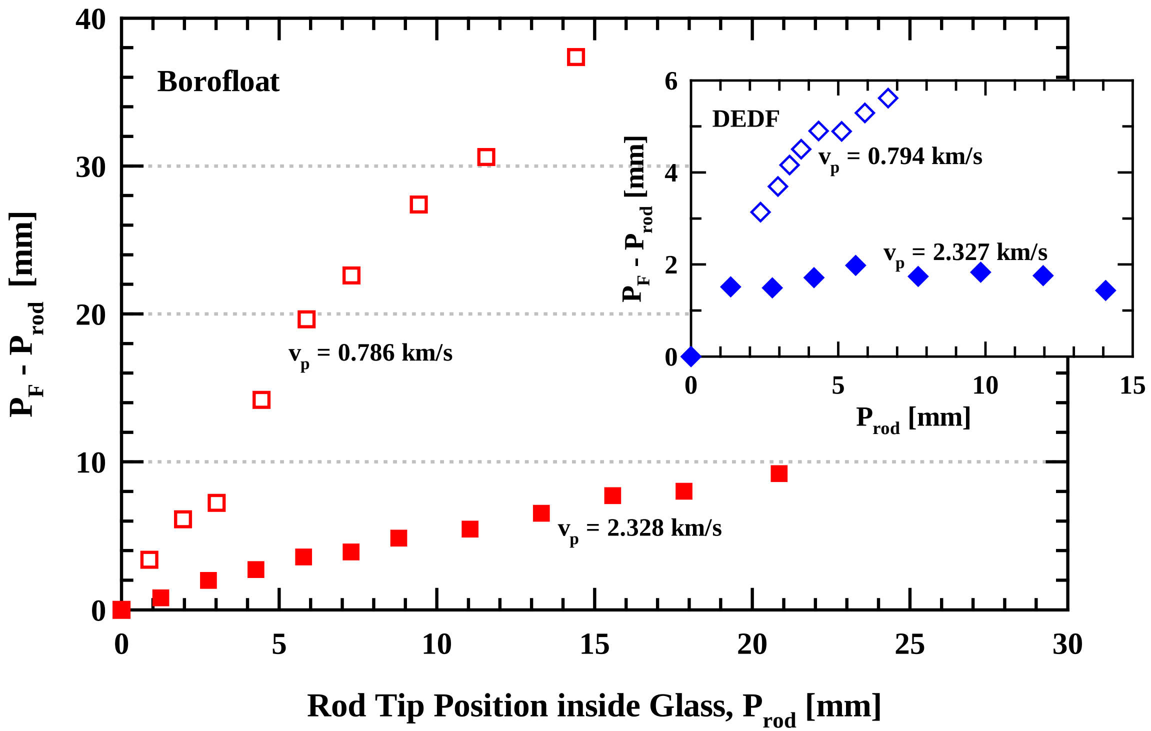

- *Failure front moves faster than penetrating projectile → projectile penetrating failed material*

Yarn Impact

Yarn Impact

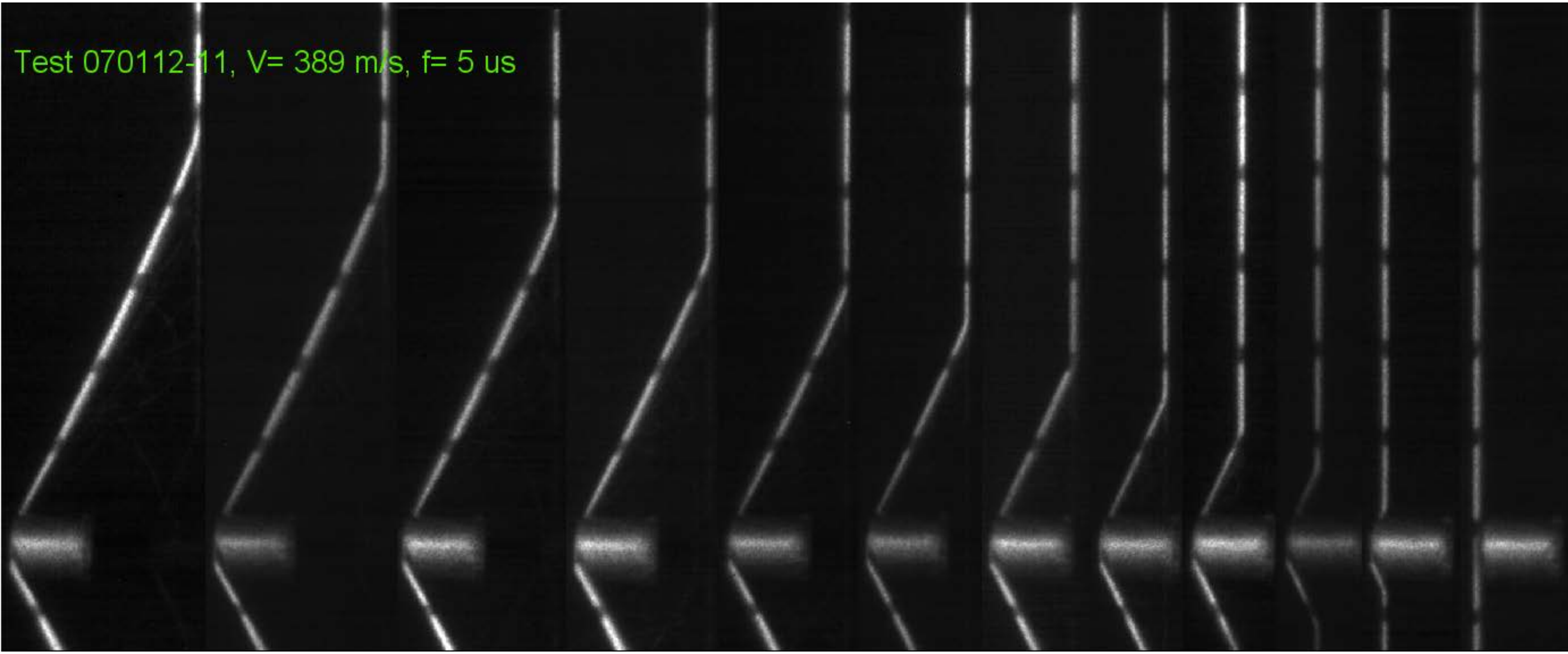

Courtesy of S. Chocron

Wave Propagation in Yarns

- *Longitudinal wave travels at speed of sound c*
- *Transverse wave travels slower at a speed U*
- *Wave reflects on boundary and impact point increasing by $\Delta\varepsilon$ at each reflection until yarn breaks.*

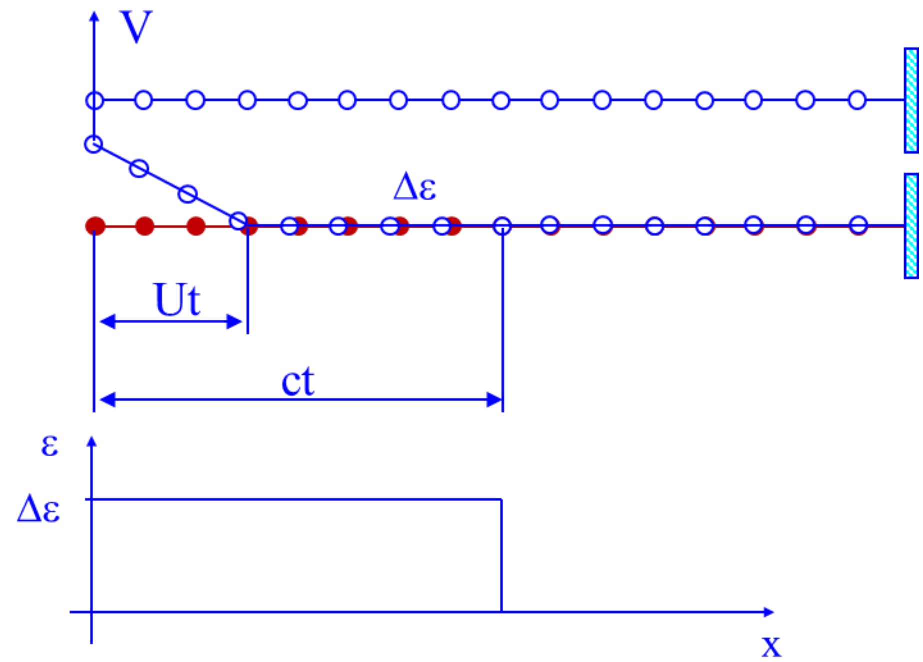

J. C. Smith, F. L. McCrackin, and H. F. Schiefer, **“**Stress-strain relationships in yarns subjected to rapid impact loading: Part V: Wave propagation in long textile yarns impacted transversely,” *Textile Res. Journal*, **28:** 288-302, 1958.

Wave Propagation in Yarns

- *Given impact velocity and sound speed in the yarn, can determine the strain and the transverse wave velocity:*

$$V = c\sqrt{\varepsilon\left(2\sqrt{\varepsilon(1+\varepsilon)} - \varepsilon\right)}$$

$$U = c\left(\sqrt{\varepsilon(1+\varepsilon)} - \varepsilon\right)$$

- *When* $\sum \Delta\varepsilon \geq \varepsilon_f$ *yarn breaks*

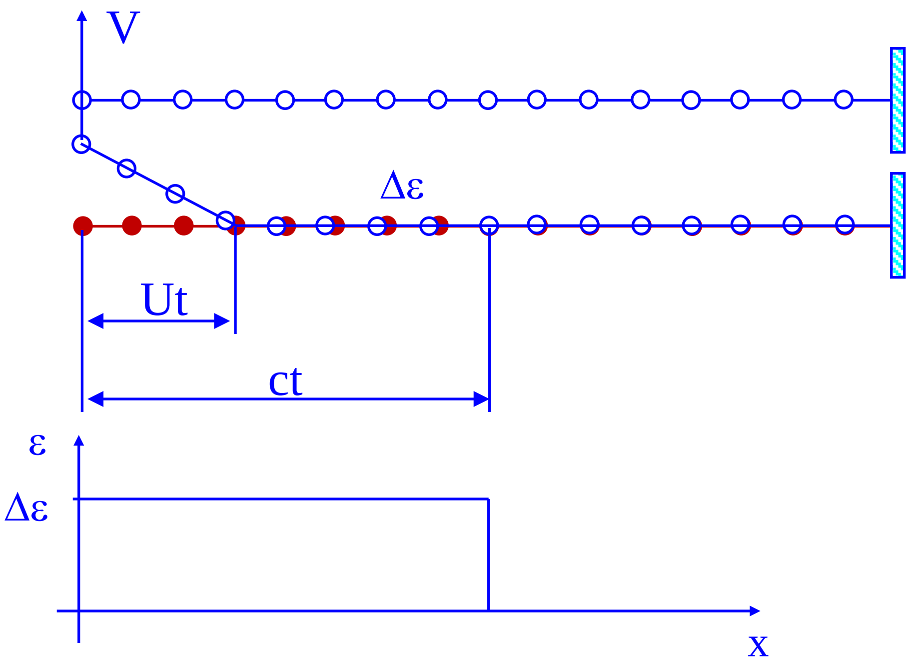

J. C. Smith, F. L. McCrackin, and H. F. Schiefer, "Stress-strain relationships in yarns subjected to rapid impact loading: Part V: Wave propagation in long textile yarns impacted transversely," *Textile Res. Journal*, **28:** 288-302, 1958.

Critical Velocity

- *Critical velocity, V_{br}, is the impact velocity where the induced strain is ε_f*
- *However, using FSP's, the critical velocity is generally less than that predicted by the classical Smith theory, e.g., ~627 m/s instead of 945 m/s for KM2 (ε_f = 4.25%)*
- *An analytical model was developed that incorporates the wave interactions from the sides of the flat projectile, plus any "bounce" of the yarn, reduces the critical velocity*

$$V_{br} = c\sqrt{\varepsilon_f\left(2\sqrt{\varepsilon_f(1+\varepsilon_f)} - \varepsilon_f\right)}$$

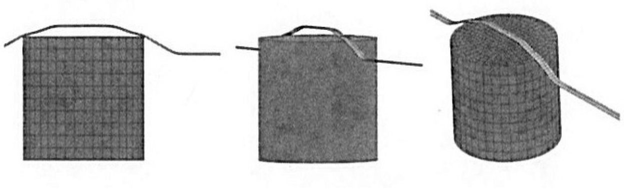

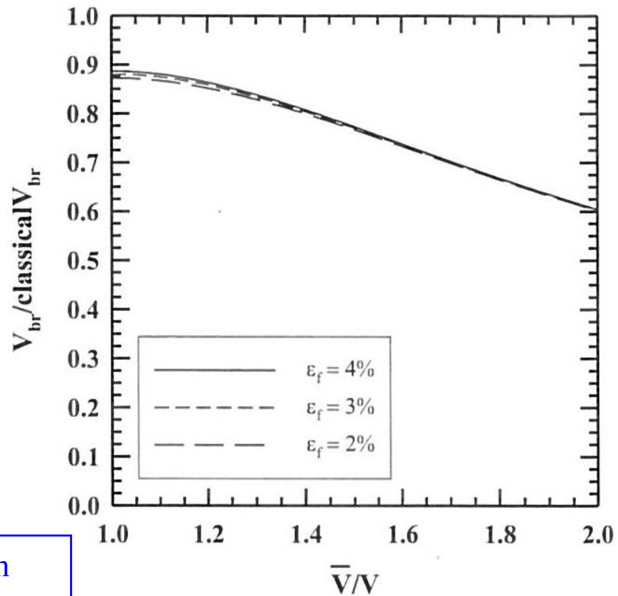

J. D. Walker and S. Chocron, "Why impacted yarns break at lower speed than classical theory predicts," *J. Appl. Mech.*, **78**: 051021-1/7, 2011.

Fabric Response & Resin-Impregnated Fabrics

CEA Consulting

Response of Fabrics

- *Like to plot V_{50} as some function that accounts for different fabric materials, different number of plies, and different projectile masses*
- *Defined a non-dimensional abscissa:*
- *A_d = areal density of fabric (accounts for different number of plies and fabric density)*
- *m_p/A_p = areal density of projectile (accounts for different projectile cross-sectional areas and projectile masses)*

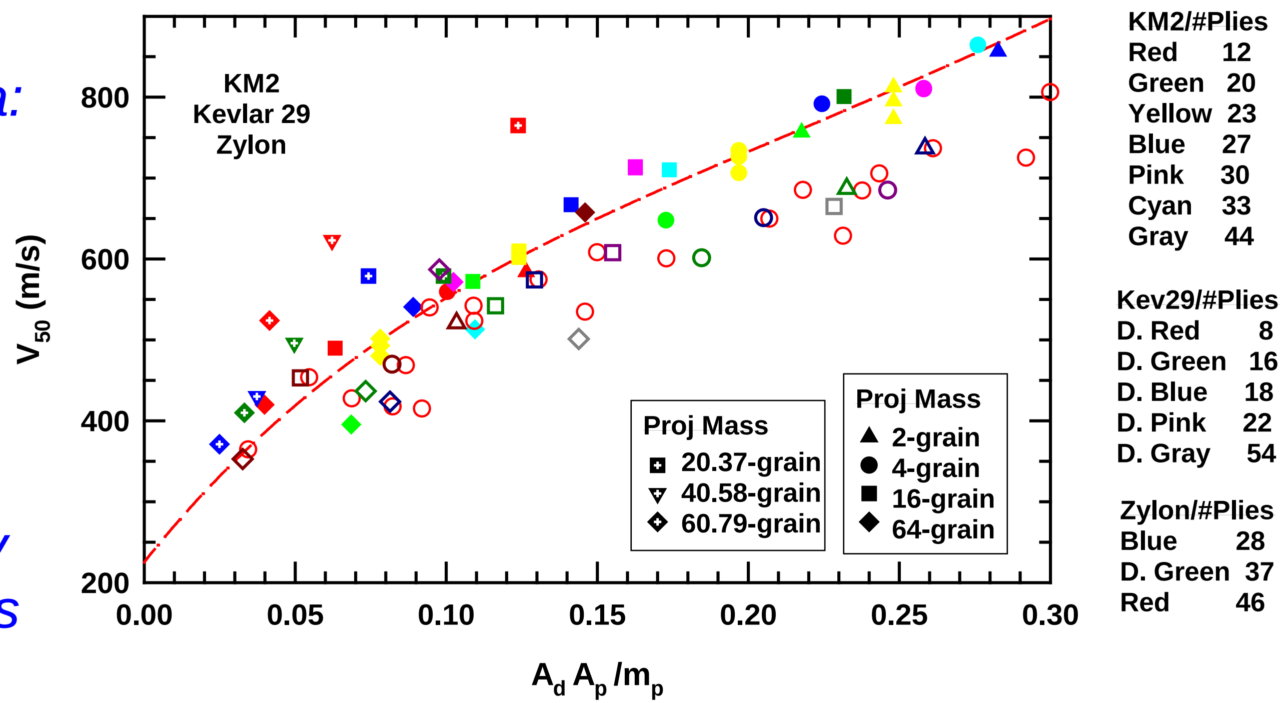

P. M. Cunniff, "Dimensionless parameters for optimization of textile-based body armor systems," *Proc. 18th Symp. Ballistics*, **2**: 1303-1310, Technomic Publishing Co, Lancaster, PA, 1999.

Fabric Response

- Couple fabric response to properties of the yarns
- Typically, yarns are linearly elastic until failure
- Strain energy per volume:

$$U = \frac{1}{\rho}\int \sigma d\varepsilon = \frac{1}{2}\frac{\sigma_u}{\varepsilon_f}$$

- Cunniff defined a new variable
- $U^* = Uc = U\sqrt{E/\rho}$ [m³/s³]
- $V^* = \left(U^*\right)^{1/3}$

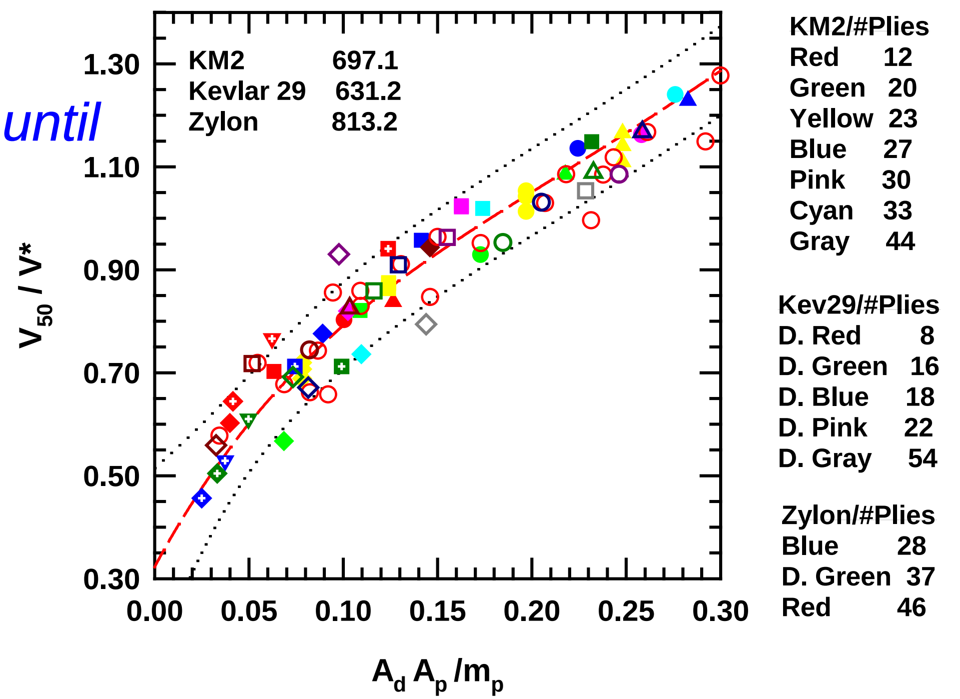

P. M. Cunniff, "Dimensionless parameters for optimization of textile-based body armor systems," *Proc. 18th Symp. Ballistics*, **2**: 1303-1310, Technomic Publishing Co, Lancaster, PA, 1999.

Fabric Modeling

- Deformation of fabrics results in a definitive pyramidal shape
- Modeling this response analytically was a challenge

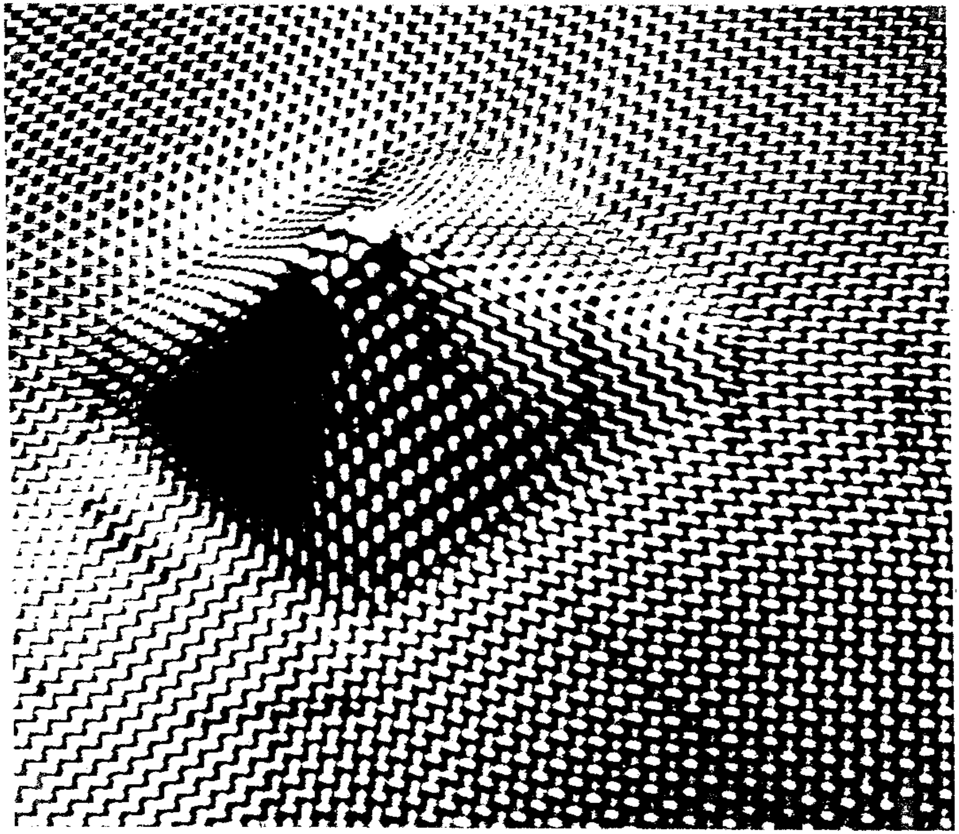

Fabric Modeling

- Fabric a limiting case of a spring system
  - Solution to static deflection of fabric sheet
  - Determine strains from sheet deflection
  - Use the strain to determine force versus deflection
  - Use Piola-Kirhhoff stress (stress with respect to the initial configuration)

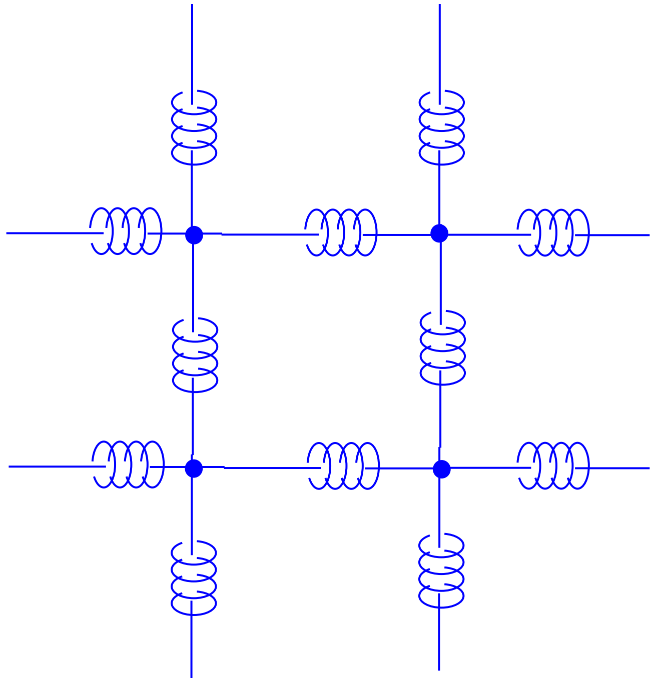

J. D. Walker, "Constitutive model for fabrics with explicit static solution and ballistic limit," *Proc. 18th Int. Symp. Ballistics*, **2**: 1231-1238, Technomic Publishing Co., Lancaster, PA, 1999.

Out-of-Plane Solution

- *Develop solution for out-of-plane deformation*

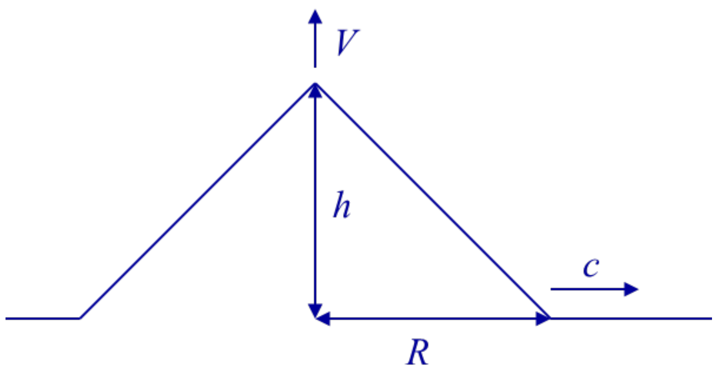

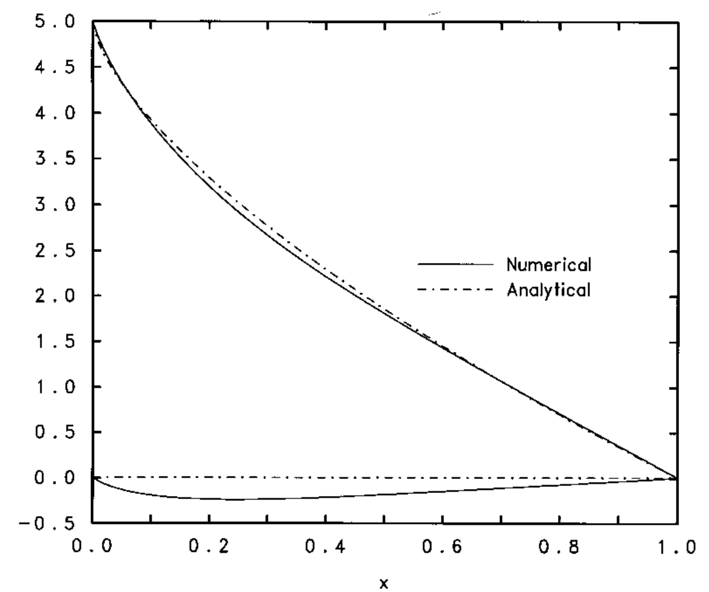

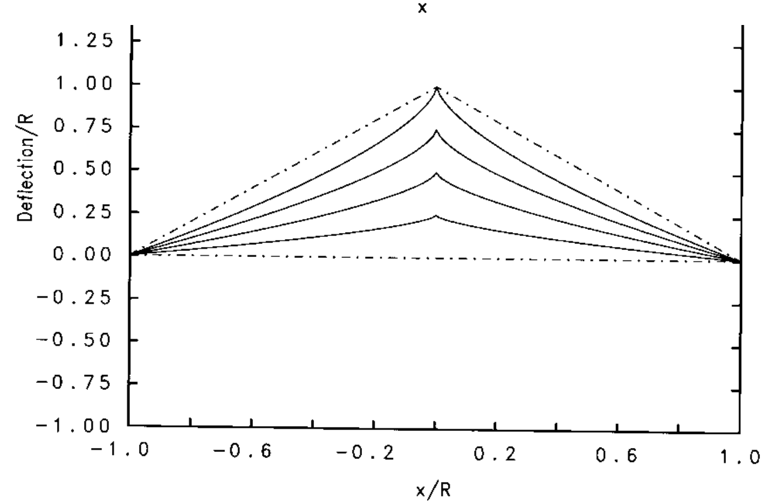

$$u_z = h\left\{1-\sqrt{(x/R)^{4/3}+(y/R)^{4/3}}\right\}$$

$$h\left\{1-(y/R)^{2/3}\right\}$$

$$\varepsilon_x = \frac{2}{9}(h/R)^2 (R/x)^{2/3}$$

Yarn Impact (Jameson, 1957)

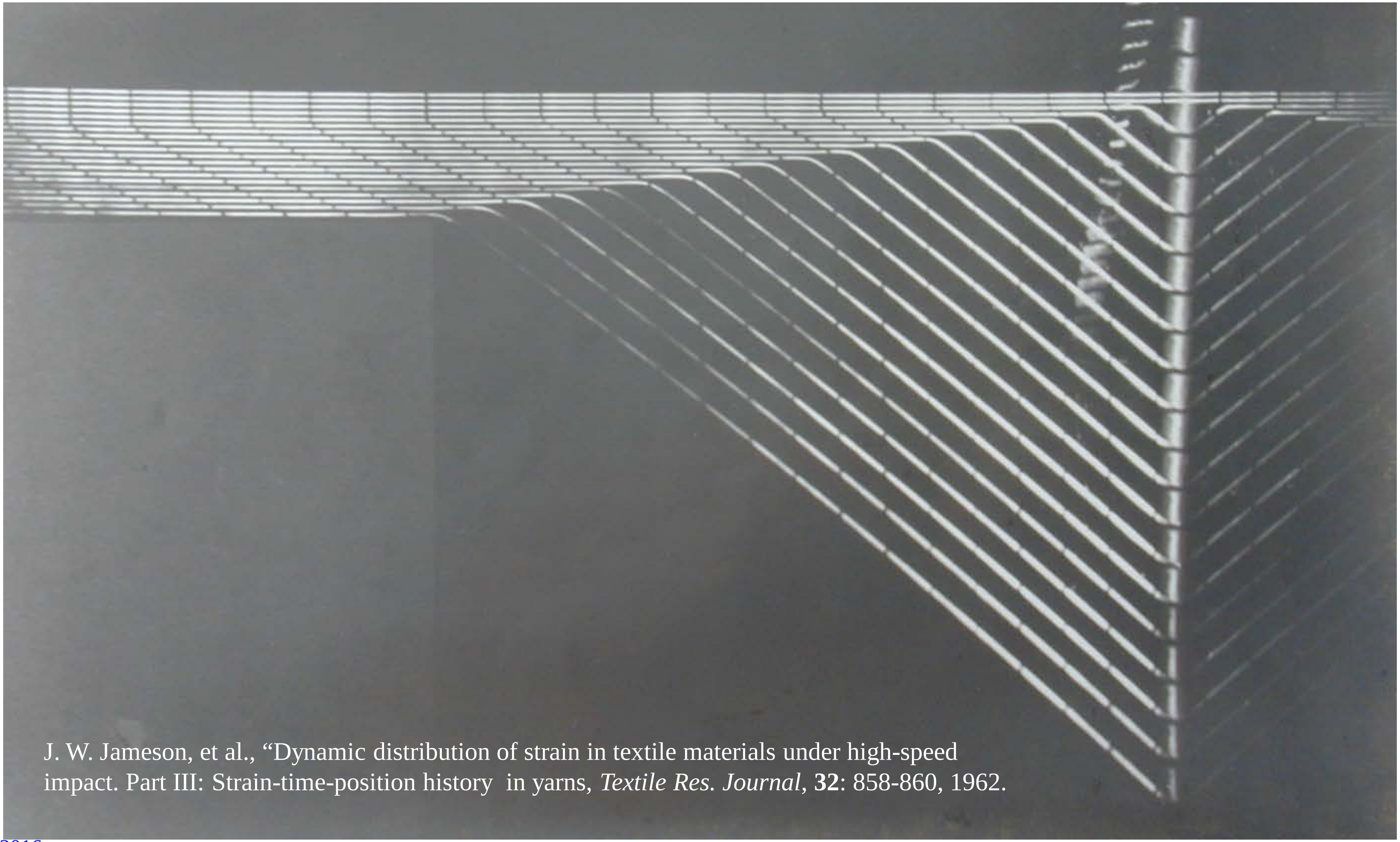

J. W. Jameson, et al., “Dynamic distribution of strain in textile materials under high-speed impact. Part III: Strain-time-position history in yarns, *Textile Res. Journal*, **32**: 858-860, 1962.

CEA Consulting

In-Plane Motion

- *Developed an equation for in-plane motion*

$$u_x(x,y) = -\frac{2}{3}\frac{h^2}{R}\left\{1-(y/r)^{4/3}\right\}^{1/4}$$
$$\left\{\left(1-(y/R)^{2/3}\right)\left[1-\frac{x/R}{\left\{1-(y/R)^{2/3}\right\}^{3/4}}\right]-\left(1-\sqrt{(x/R)^{4/3}+(y/R)^{4/3}}\right)\right\}$$

$$u_x = -\frac{2}{3}\frac{h^2}{R}\left\{\left(\frac{x}{R}\right)^{2/3}-\frac{x}{R}\right\}$$

J. D. Walker, "Constitutive model for fabrics with explicit static solution and ballistic limit," *Proc. 18th Int. Symp. Ballistics*, **2**: 1231-1238, Technomic Publishing Co., Lancaster, PA, 1999.

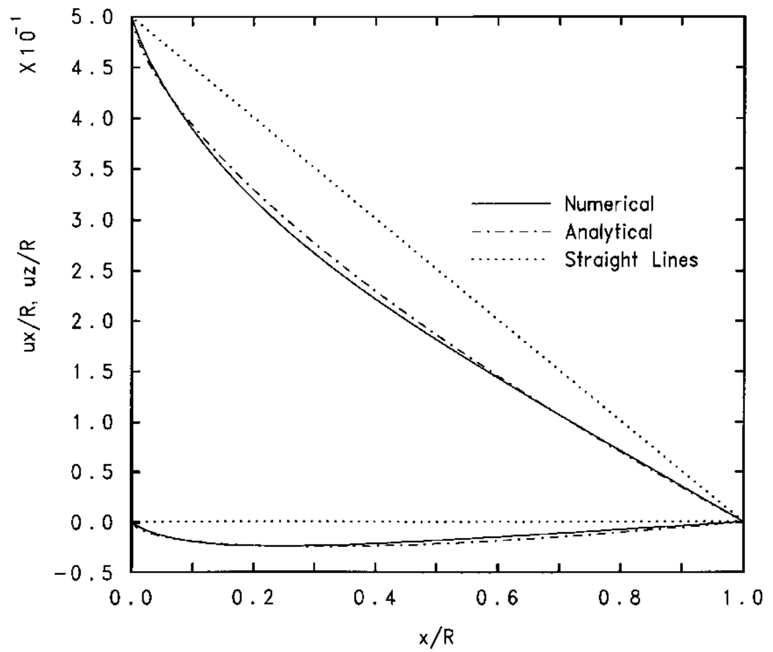

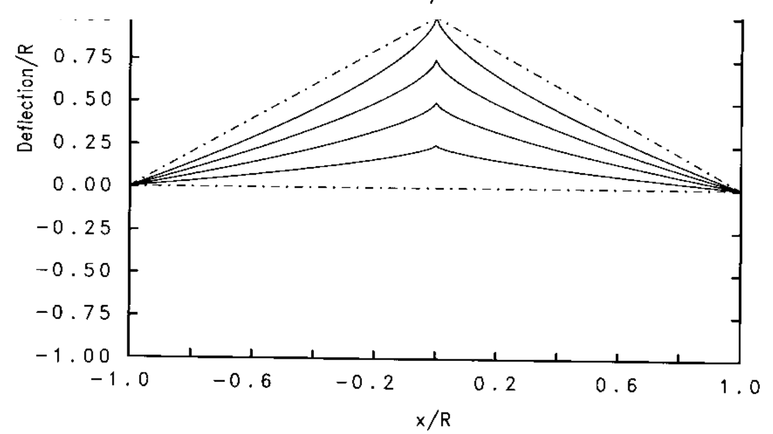

Strain Along Edge

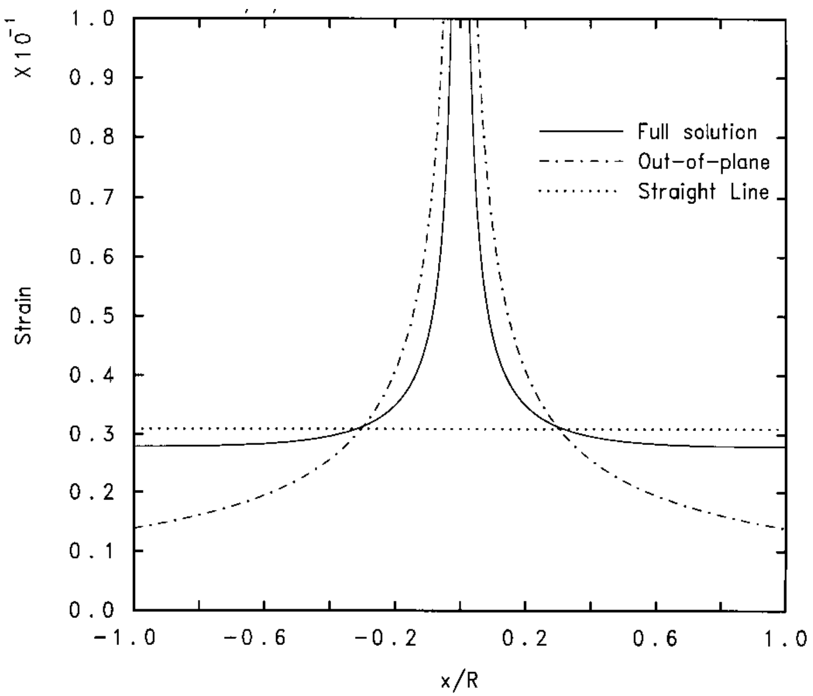

- *Analytic solution allows calculation of strain*
- *Strain along edge*

$$\varepsilon_x \approx \frac{2}{9}\left(\frac{h}{R}\right)^2\left\{\left(\frac{R}{x}\right)^{2/3} - 2\left(\frac{R}{x}\right)^{1/3} + 3\right\}$$

- *Strains from out of plane solution differ from total solution*

Calculate V_{50}

- *Need to know how fast the tent is expanding under the impact (how much fabric is involved in the impact)*
- *Set deceleration of projectile and fabric equal to the force*

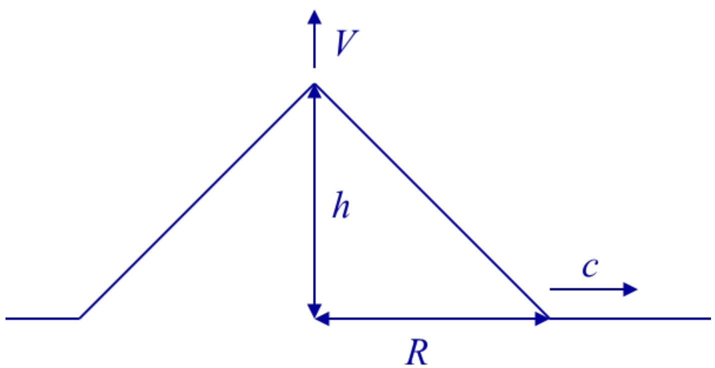

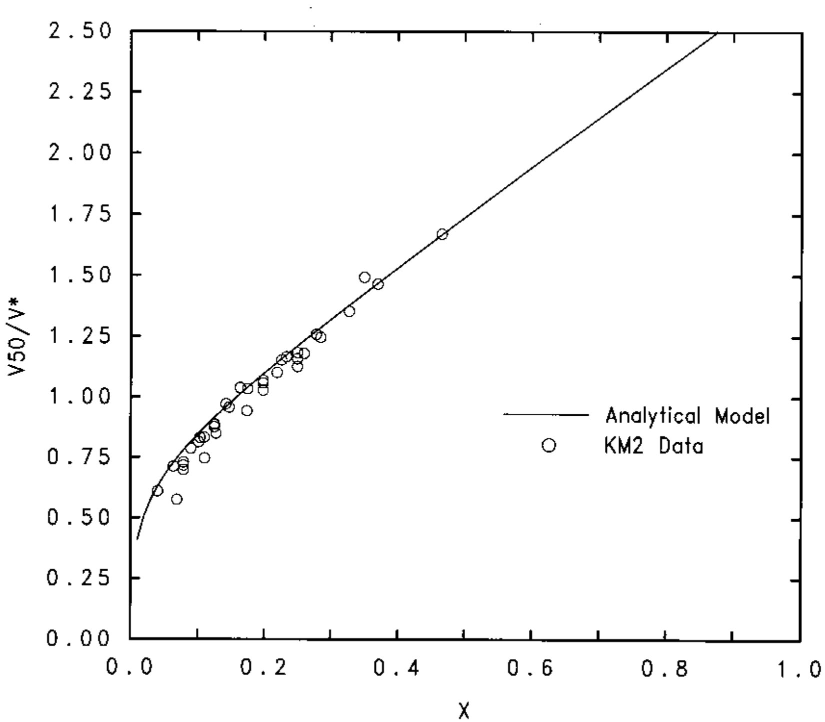

J. D. Walker, "Constitutive model for fabrics with explicit static solution and ballistic limit," *Proc. 18th Int. Symp. Ballistics*, **2**: 1231-1238, Technomic Publishing Co., Lancaster, PA, 1999.

CEA
Consulting

Fabric Model

Addition of Resin to Fabrics

- For same areal density, addition of resin means removal of fabric (loss of tensile strength)
- Resin adds bending moment to response, thus increasing strength
- Addition of resin increases shear wave speed, thus reducing the strain
- Harder composite deforms projectile
- Fabrics held in resin may now shear

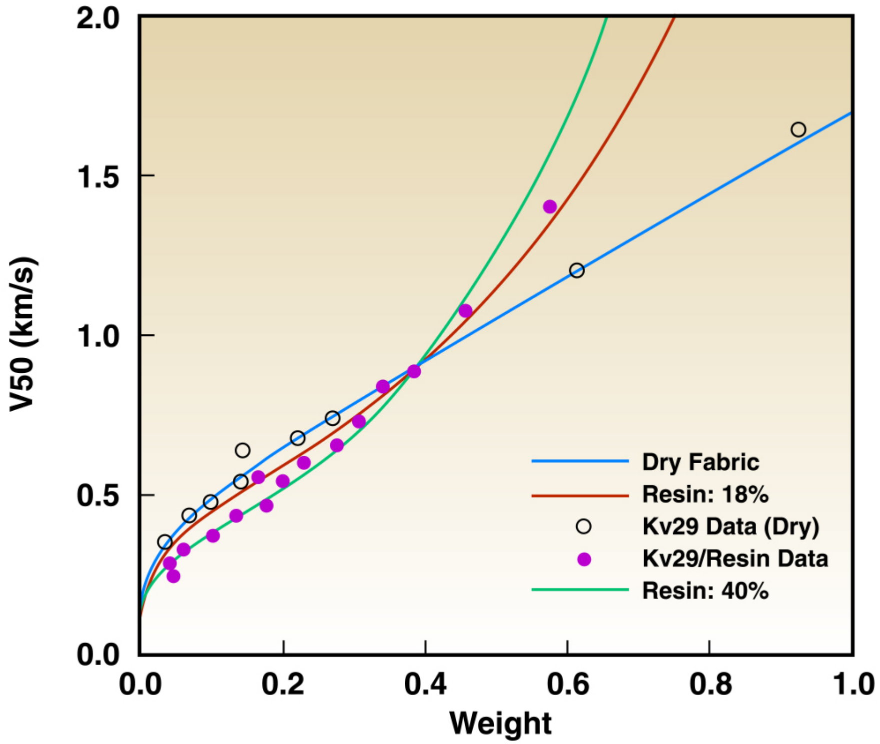

J. D. Walker, “Ballistic limit of fabrics with resin,” *Proc. 19th Int. Symp. Ballistics*, **3**: 1409-1414, Interlaken, Switzerland, 2001.

Dwell and Dwell-Penetration Transition

An Analytic Model for Dwell

$$\rho_p \ell \frac{d\mathrm{v}}{dt} = -Y_p$$

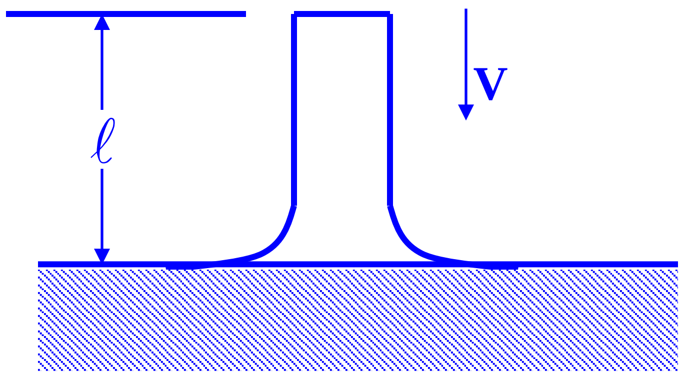

$$\frac{d\ell}{dt} = -(\mathrm{v} - u)$$

for dwell $u = 0$

C. E. Anderson, Jr. and J. D. Walker, "An analytic model for dwell and interface defeat," *Int. J. Impact Engng.*, **31**(9): 1119-1132 (2005)

Analytic Dwell Model-1

$$\rho_p \ell \frac{d\mathrm{v}}{dt} = -Y_p, \qquad \frac{d\ell}{dt} = -\mathrm{v}$$

Can be solved simultaneously and integrated:

$$\frac{1}{2}\rho_p\left(\mathrm{v}^2 - \mathrm{v_o}^2\right) = Y_p \ln\left(\ell/\ell_o\right)$$

After some rearranging

$$KE \equiv \frac{1}{2}\rho_p \ell \mathrm{v}^2 = \frac{1}{2}\rho_p\left(\ell - \ell_0\right)\mathrm{v}_0^2 + Y_p \ell \ln\left(\ell/\ell_0\right) + KE_0$$

CEA Consulting

Analytic Dwell Model-2

$$\frac{1}{KE_0}\frac{d\,KE}{dt} = -\frac{\mathrm{v}}{\ell_0}\left\{\underbrace{1+\frac{Y_p}{\frac{1}{2}\rho_p \mathrm{v}_0^2}\ln\left(\ell/\ell_0\right)}_{\text{erosion}}+\underbrace{\frac{Y_p}{\frac{1}{2}\rho_p \mathrm{v}_0^2}}_{\text{deceleration}}\right\}.$$

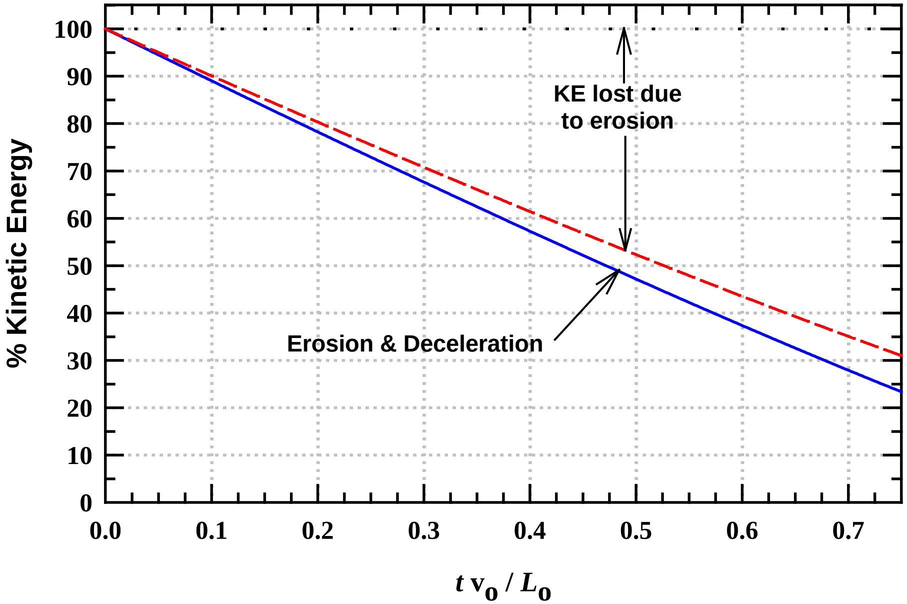

Long Rod

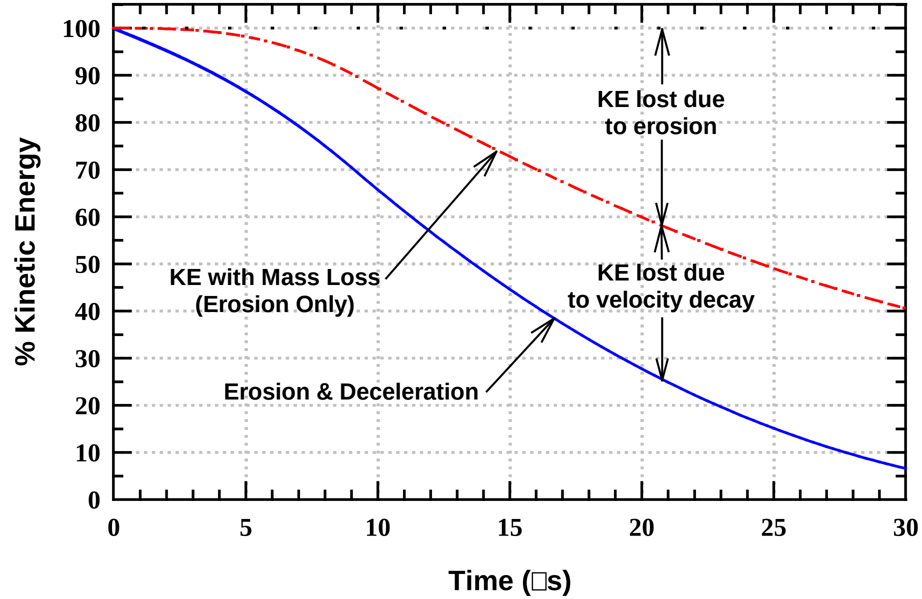

Armor Piercing

CEA Consulting

Dwell-Penetration Transition

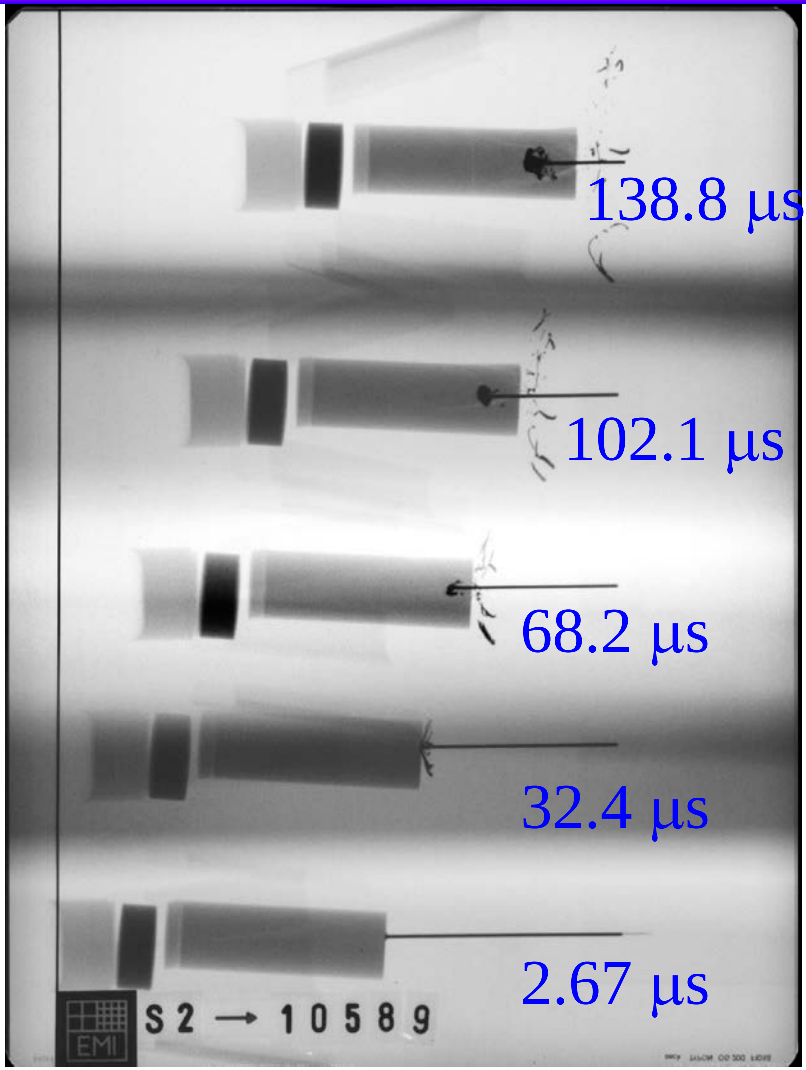

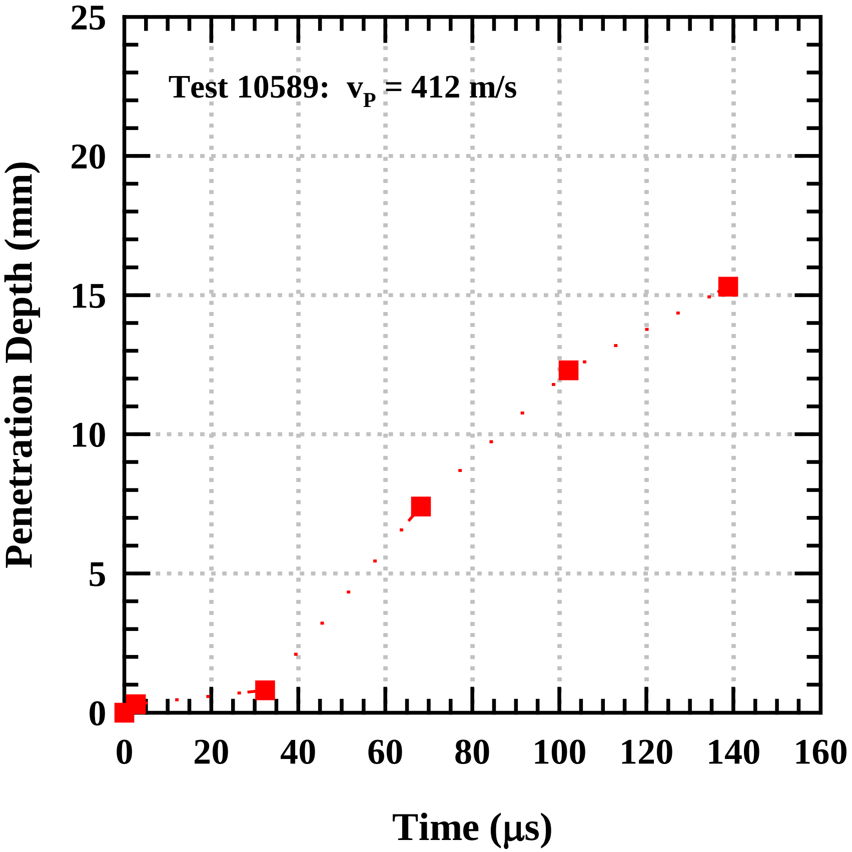

Borosilicate glass

Confined B_4C Experiments

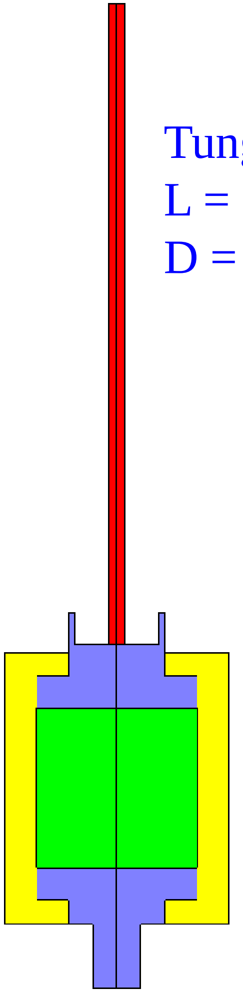

Tungsten projectile
L = 80 mm
D = 2 mm

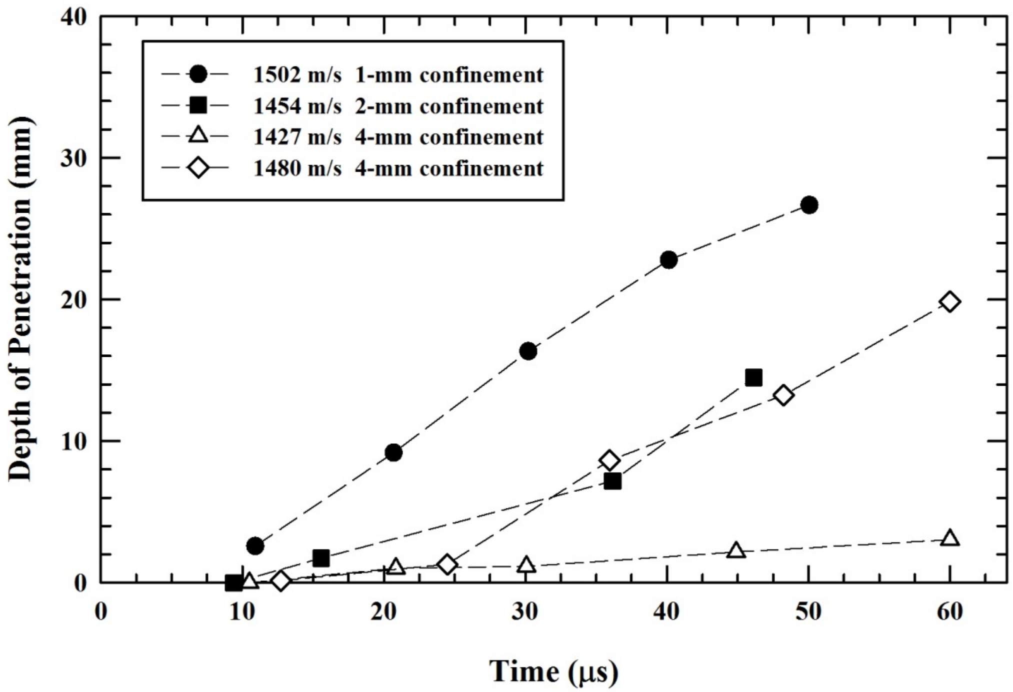

L. Westerling, P. Lundberg, and B. Lundberg, "Tungsten long-rod penetration into confined cylinders of boron carbide at and above ordnance velocity," *Int. J. Impact Engng.*, **25**(7): 703-714, 2001.

Transition from Interface Defeat

- *Lundberg and colleagues have been studying interface defeat for a number of years (1998-present)*
- *Modeled the pressure distribution, P, of the projectile on the surface*
  - *Radial distribution from low-velocity water jet results*
  - α *<< 1; ratio of elastic to inertial effects*
  - β *<< 1; ratio of plastic to inertial effects*
  - K_p *= bulk modulus;* q_p *= Bernoulli pressure;* V_o *= impact speed*

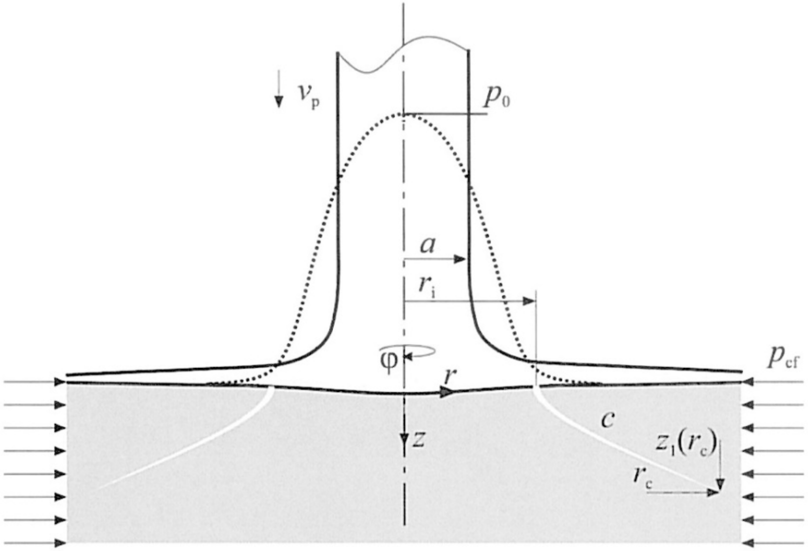

$$P(r,\alpha,\beta) = q(r)\left[1 + \frac{1}{2\alpha} + 3.0\beta - 1.6\beta^2\right]$$

$$\alpha = \frac{K_p}{q_p} \quad \beta = \frac{\sigma_{yp}}{q_\rho} \quad q_p = q(0) = \frac{1}{2}\rho_p V_o^2$$

P. Lundberg, R. Renström, and O. Andersson, "Influence of length scale on the transition from interface defeat to penetration in unconfined ceramic targets," *J. Appl. Mech.*, **80**: 031801-1/9, 2013.

Transition from Interface Defeat

- *First estimated transition velocity by equating the maximum load per unit area with the shear yield strength of the ceramic material*
- *Subsequent work used fracture mechanics to estimate the critical stress, P^*_0 to drive a crack, first for an unconfined target, then a target with applied prestress, P_{cf}*

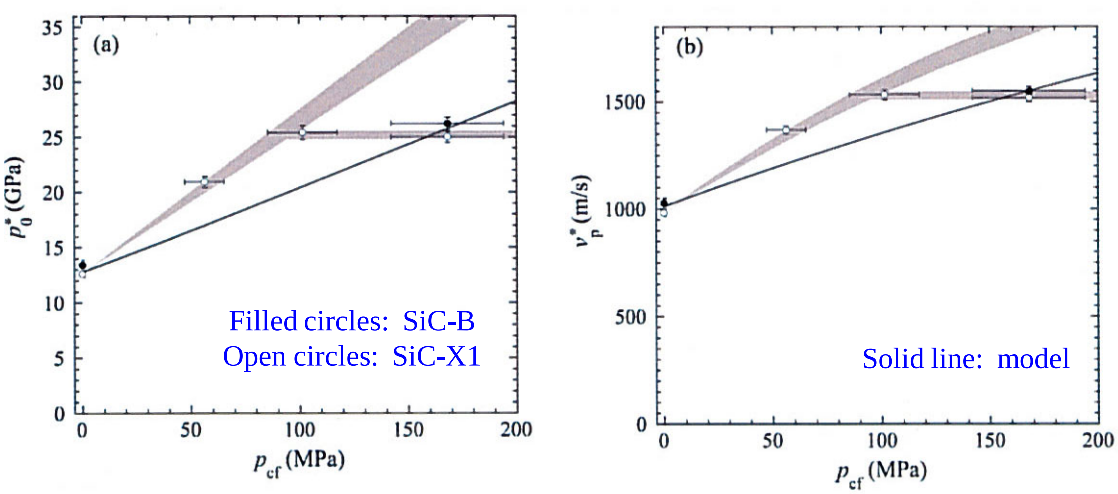

Solid line: model estimate
Gray shading: possible two-mode behavior

P. Lundberg, R. Renström, and O. Andersson, "Influence of confining prestress on the transition from interface defeat to penetration in ceramic targets," *Defence Technology*, in press, 2016.

Three Regimes of Penetration

- *Case 1. $V_o < V_T$: Interface defeat*
- *Case 2. $V_o > V_T$: Dwell followed by penetration*
- *Case 3. $V_o >> V_T$: Short dwell followed by penetration*

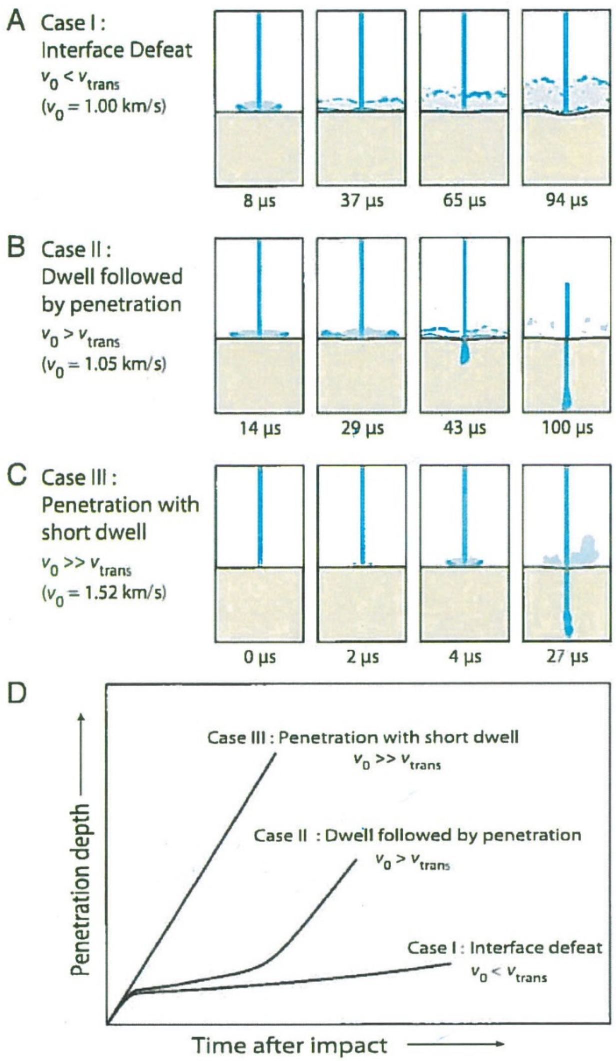

T. Uth and V. S. Deshpande, "Unsteady penetration of a target by a liquid jet," *PNAS*, **110**(50): 20028-33, 2013

CEA Consulting

Fluid-Structure Interaction Model

- *Unsteady penetration rate due to impact of a fluid jet with velocity V_o*
- *During initial stages of jet impact, the target surface is flat and the fluid spreads horizontally*
- *As the jet deforms the target and penetrates at depth δ, it creates a dimple at the impact site*
- *Flow pattern changes, resulting in backflow of the fluid with a velocity V and a consequent increase in the penetration pressure*

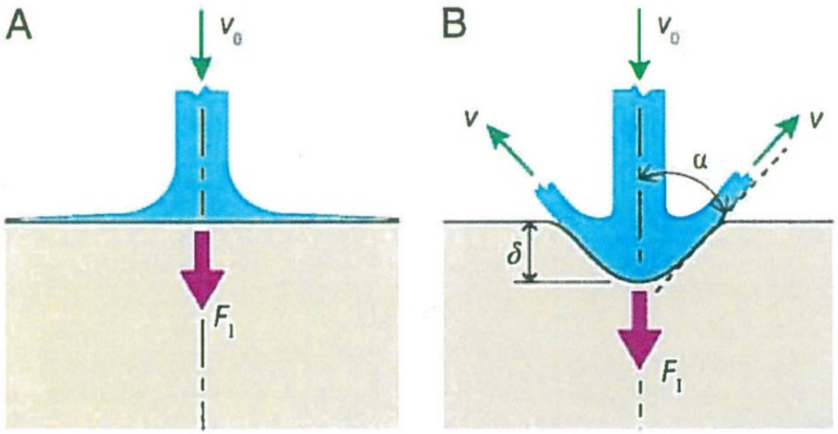

$$P = \frac{F_I}{A_{jet}} = (1 + \cos\alpha)\rho_{jet} V_o^2$$

T. Uth and V. S. Deshpande, "Unsteady penetration of a target by a liquid jet," *PNAS*, **110**(50): 20028-33, 2013

CEA Consulting

Experiments: 2-mm-diameter Water Jet on Vacuum Grease

- *Provided experimental evidence*
  - *Case 1. $V_o < V_T$: Pressure remains constant; radially flow of jet*
  - *Case 2. $V_o > V_T$: Pressure increases sharply at t ~ 500 µs; $\delta \approx r_{jet}$ penetration rate increases rapidly*
  - *Case 3. $V_o >> V_T$: Measurements and observations closely resemble those of Case 2, but with no discernible dwell phase*

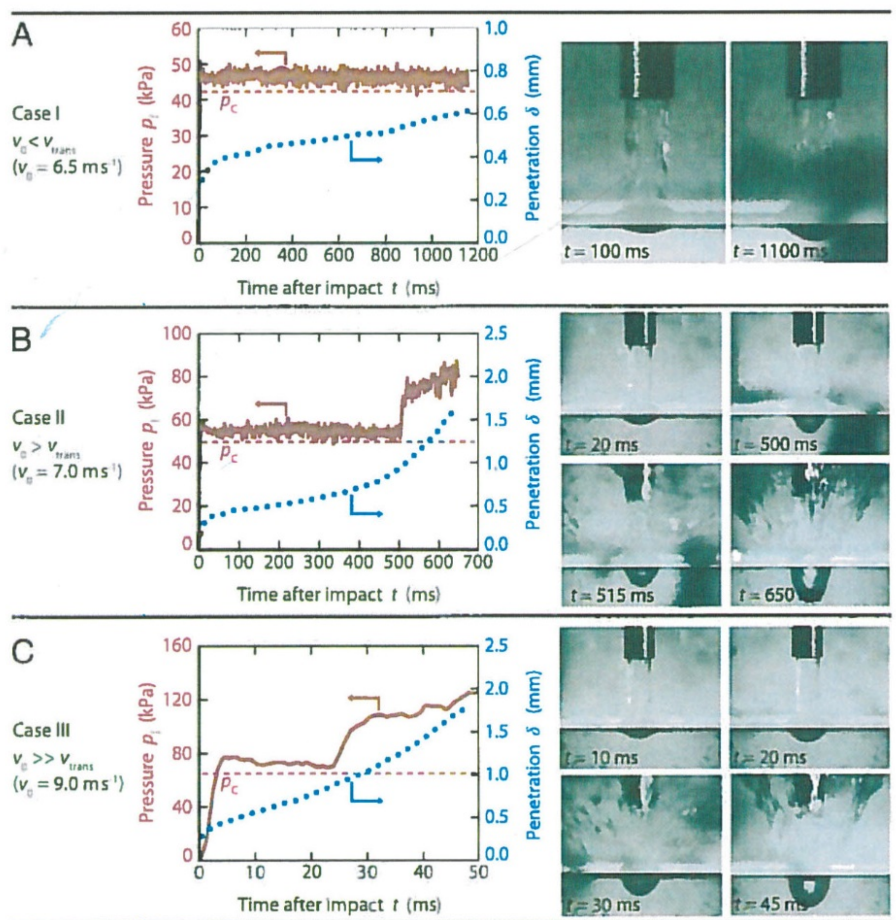

T. Uth and V. S. Deshpande, "Unsteady penetration of a target by a liquid jet," *PNAS*, **110**(50): 20028-33, 2013

$$P = \frac{F_I}{A_{jet}} = (1 + \cos\alpha)\rho_{jet} V_o^2$$

Jet vs. Creep Penetration

- $$P_{creep} = \rho_{jet} V_o^2$$
- $$P = \frac{F_I}{A_{jet}} = (1+\cos\alpha)\rho_{jet} V_o^2$$
- *Case 1: 2 experiments give similar response creep*
- *Case 2: Penetration rate for creep case remains steady; sharp increase in jet penetration rate*
- *Case 3: Backflow sets in early and penetration rate is higher for the jet compared to creep experiment*

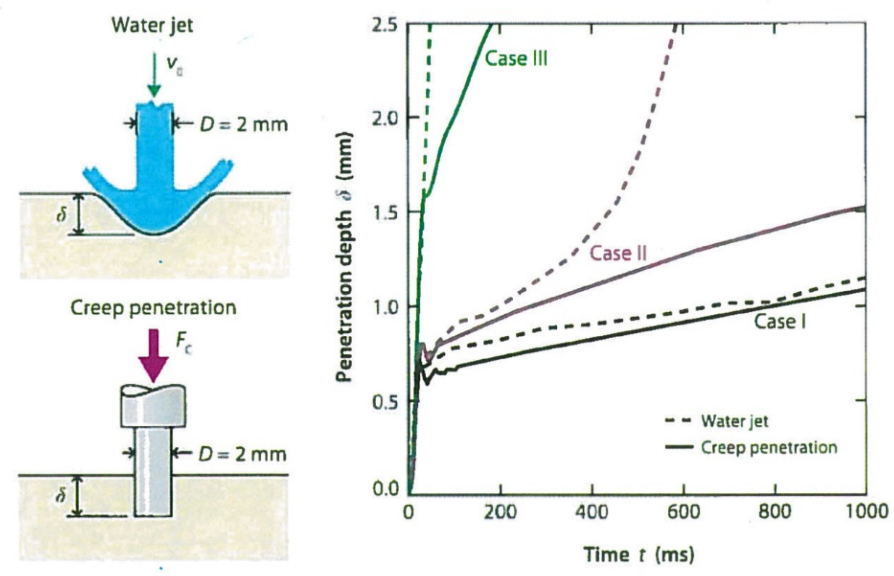

T. Uth and V. S. Deshpande, "Unsteady penetration of a target by a liquid jet," *PNAS*, **110**(50): 20028-33, 2013

Fluid-Structure Interaction and Dwell-Penetration Transition

- *Demonstrated that backflow of impacting jet, rather than any damage to the target material, can cause unsteady penetration*
- *Experimentally, damage observed in ceramics that show interface defeat*
- *Damage and backflow are not mutually exclusive*
- *Impacting jet needs to penetrate to a depth of approximately the jet radius before backflow can be established*
- *Brittle targets such as ceramics must have some damage to permit penetration to half of the projectile radius*
- *Backflow then acts like a switch, doubling the pressure, and amplifying the penetration rate*

Summary

Modeling

- *Understanding is displayed by how well we can model*
- *Accuracy versus trends:*
  - *many difficult problems, accuracy is subjective*
  - *but if cannot get trends right, then do not understand*
- *Modeling*
  - *materials response (constitutive) models*
  - *numerical simulations*
  - *analytical models*

Modeling

- *If you can model the phenomenology, it demonstrates a certain level of understanding*
- *Of course, we have to be careful that we are truly modeling, and not simply curve fitting (adjusting parameters)*
- *That's why in penetration mechanics modeling, need to verify the ability to predict at different velocities, different geometries, and different materials*

If have numerical simulations, why the need for analytical models?

Analytical Modeling

- *If we can develop an analytical model that captures the essence of the phenomenology:*
  - *Not only demonstrated that we understand*
  - *Also demonstrates that we have grasped the essential and relevant mechanics of the phenomenology*
- *Now have a tool for predictions, design studies, optimization, etc., that is fast running compared to numerical simulations*

THE END